

Deliverable D1 (D1.1)

Guidelines, datasets of non-regulated pollutants incl.
metadata, methods.



RI-URBANS

**Research Infrastructures Services Reinforcing Air
Quality Monitoring Capacities in European Urban &
Industrial AreaS (GA n. 101036245)**

By

CSIC, IMT, PSI, NILU & UHEL



UNIVERSITY OF HELSINKI

30th September 2022

Deliverable D1 (D1.1): Guidelines, datasets of non-regulated pollutants incl. metadata, methods

Authors: Andrés Alastuey (CSIC), Xavier Querol (CSIC), Meri García (CSIC), Pedro Trechera (CSIC), Marjan Savadkoohi (CSIC), Angeliki Karanasiou (CSIC), María Cruz Minguillón (CSIC), Markus Fiebig (NILU), Kaspar R. Dallénbach (PSI), Thérèse Salameh (IMT), Stephane Sauvage (IMT), Tuukka Petäjä (UHEL)

Work package (WP)	WP1 Guidelines, datasets of non-regulated pollutants incl. metadata, methods,
Deliverable	D1 (D1.1)
Lead beneficiary	CSIC
Deliverable type	<input checked="" type="checkbox"/> R (document, report) <input type="checkbox"/> DEC (websites, patent filings, videos...) <input checked="" type="checkbox"/> Other: ORDP (open research data pilot)
Dissemination level	<input checked="" type="checkbox"/> PU (public) <input type="checkbox"/> CO (confidential, only members of consortium and European Commission))
Estimated delivery deadline	M12 (30/09/2022)
Actual delivery deadline	30/09/2022
Version	Final
Reviewed by	WP1 leader
Accepted by	RI-URBANS Project Coordination Team
Comments	This report presents basic information, describes the data treatment, and provides links to datasets and guidelines. We must recognize and thank the essential contribution of the providers of the data, indicated in the document but not included in the list of authors.

Table of Contents

1	ABOUT THIS DOCUMENT	1
2	PARTICLE NUMBER CONCENTRATION (PNC) AND PARTICLE NUMBER SIZE DISTRIBUTION (PNSD)	2
2.1	PNC AND PNSD DATASETS	2
2.2	PNC AND PNSD GUIDELINES METHODS	10
2.2.1	<i>PNC and PNSD CEN /ACTRIS</i>	10
2.2.2	<i>RI-URBANS recommendations</i>	12
2.3	DETERMINATION OF LUNG DEPOSITED SURFACE AREA (LDSA) LEVELS	13
2.3.1	<i>Calculation of the size-fractionated lung-deposited surface area (LDSA)</i>	13
2.3.2	<i>LDSA Datasets</i>	14
2.3.3	<i>General characteristics of LDSA at different measurement sites</i>	14
2.4	ANNEX / FILES DATASETS	17
2.4.1	<i>PNC/PNSD</i>	17
2.4.2	<i>LDSA</i>	17
2.5	REFERENCES	17
3	EQUIVALENT BLACK CARBON	19
3.1	EBC DATASETS	19
3.2	EBC GUIDELINES/METHODS	31
3.2.1	<i>MAAP</i>	31
3.2.2	<i>AE33</i>	31
	<i>ACTRIS In Situ Aerosol: Guidelines for Manual QC of AE33 absorption photometer data</i>	31
3.2.3	<i>RI-URBANS recommendations</i>	31
3.3	ANNEX / FILES DATASETS	36
3.4	REFERENCES	36
4	OFFLINE PM CHEMICAL COMPOSITION	38
4.1	DATASETS	38
4.1.1	<i>Data treatment</i>	42
4.2	GUIDELINES	45
4.2.1	<i>Sampling</i>	45
4.2.2	<i>Analysis of organic carbon (OC) and elemental carbon (EC)</i>	46
4.2.3	<i>Analysis of ions</i>	47
4.2.4	<i>Analysis of Organic Tracers</i>	47
4.2.5	<i>Elemental analysis</i>	47
4.2.6	<i>Ri-URBANS recommendations</i>	48
4.3	ANNEX / FILES DATASETS	49
4.4	REFERENCES	49
5	ONLINE PM CHEMICAL COMPOSITION	52
5.1	DATASETS	52
5.2	GUIDELINES	56
5.3	ANNEX / FILES DATASETS	56
5.4	REFERENCES	57
6	VOLATILE ORGANIC COMPOUNDS (VOCS)	60
6.1	DATASETS	60
6.2	GUIDELINES	63
6.2.1	<i>Sampling</i>	64

6.2.2	Analysis.....	65
6.3	RI-URBANS RECOMMENDATIONS.....	65
6.4	ANNEX / FILES DATASETS	66
6.5	REFERENCES:	66
7	AMMONIA (NH₃).....	67
7.1	DATASETS	67
7.2	GUIDELINES	68
7.3	RI-URBANS RECOMMENDATION	69
7.4	ANNEX / FILES DATASETS	69
8	DATA MANAGEMENT	70

1 About this document

WP1 evaluates the European added value of the use of the novel metrics and tools for better assessment of AQ and AQ-health. It evaluates the potential of nanoparticles, PM speciation, BC and VOCs metrics and 3D measurements and develops Service Tools (STs) for their accurate source contributions using interoperable advanced instrumentation implemented by RIs-AQMNs. Based on available online and off-line high-quality data collection from ACTRIS and IAGOS, and supersites from AQMNs, advanced instrumental and source apportionment will be developed and applied to datasets from up to 15 supersites.

WP1 is organized in three major tasks:

- T1.1. Data survey and compilation of non-regulated pollutants
- T1.2. Developing and implementing advanced source apportionment STs
- T1.3. Developing products and methods for AQ from profiling observations

One major WP1 outcomes (in Task 1.1) is the **Compilation of existing datasets and coordination of RIs-AQMNs for interoperable services**. To Interaction with AQ Reference Laboratories in Europe (AQUILA network), existing urban AQ supersites from AQMNs and RIs will provide data on the aforementioned novel AQ metrics for new service development. **The data will be gathered (D.1.1) and made accessible** for the source apportionment (T1.2), health effect assessment (WP2), and improved emission inventories and modelling evaluation (WP3). For each variable, **the measurement requirements** (instrumental and operational conditions) will be evaluated **according to existing guidelines and protocols**, e.g., those from the European Committee for Standardization (CEN) for nanoparticles, ACTRIS, and data management from ACTRIS Data Centre (ACTRIS DC) complying with the FAIR principles. Based on these existing protocols, RI URBANS will produce Guidelines for measurement and data treatment, to be provided for pilots (WP4).

Thus, D1.1, consists of:

- **Data sets, including meta data**, of novel AQ metrics including nanoparticle PNSD, BC, PM chemical composition with high or low time resolution including major and trace elements, ions, organic species and organic mass spectra (for OA source apportionment); VOC species; and NH₃. **Datasets** have been made available to the other WPs in the RI Urbans Intranet ([RI-URBANS D1 \(D1.1\) DATASETS](#)).
- **Guidelines** for measurement and data management of the selected novel metrics. Links to guidelines are included in the text.

The document is organised in sections covering the considered variables. For each variable, information is given on the number of datasets, data providers, periods, instrumentation, QA/QC links to datasets and metadata, guidelines, methods, among others.

In this report we present basic information, we describe the data treatment and provide links to datasets and guidelines.

This is a public document that will be distributed to all RI-URBANS partners for their use and submitted to European Commission as a RI-URBANS deliverable D1 (D1.1). This document can be downloaded at <https://riurbans.eu/work-package-1/#deliverables-wp1>

2 Particle number concentration (PNC) and particle number size distribution (PNSD)

Particle number concentration (PNC) and particle number size distribution (PNSD) data have been collected from open databases (mainly from ACTRIS Data Centre-EBAS), or directly provided by Air Quality Monitoring Networks and other research stations. Data has been checked out and harmonized following ACTRIS recommendations. In order to provide input information for health studies (WP2) and modelling (WP3), specific parameters, such as concentrations of the Nucleation mode (N_{10-25}), Aitken mode (N_{25-100}), Accumulation mode (N_{10-800}), N_{25-800} and PNC (N_{10-800}), all in $\# \text{ cm}^{-3}$ have been calculated. These are available at the archived datasets (https://riurbans-my.sharepoint.com/personal/csic_riurbans_onmicrosoft_com/_layouts/15/onedrive.aspx?ga=1&id=%2Fpersonal%2Fcsic%5Friurbans%5Fonmicrosoft%5Fcom%2FDocuments%2FCSIC%20Scientific%20Data%2FPNSD).

Additionally, due to the high interest in the determination of the lung deposited surface area (LDSA) for exposure assessment, the LDSA was estimated based on the compiled PNSD data. This information is summarized at the end of this section.

2.1 PNC and PNSD Datasets

This project has a total of twenty-six European sites providing hourly 2017-2019 data of UFP-PSD (ultrafine particles-particle size distribution) by air quality monitoring networks and research supersites to RI-URBANS, including:

- fifteen urban background (UB) sites covering most Europe: Athens, Barcelona, Birmingham, Budapest, Dresden, Granada, Helsinki, Langen, Leipzig, two in London, Madrid, Marseille, Zurich and Rochester (in New York state in US).
- six traffic (TR) sites in Central, West and North Europe: Dresden, Helsinki, two in Leipzig, London and Stockholm.
- four suburban background (SUB) sites: Athens, Lille, Paris and Prague.
- one regional background (RB) site in the Po Valley in Ispra (Italy), which was included because no datasets could be obtained from urban areas in the Po Valley, and this is a pollution hotspot in Europe, where most of the PM pollution has a regional origin.

From the twenty-six sites, twelve already report data to the ACTRIS data Centre, but fourteen stations do not. Data of co-measured pollutants and meteorological parameters were also collected, when available, from the same sites, or nearby air quality monitoring sites (see Table 2.1 and Figure 2.1).

In addition, these hourly datasets are going to be interpreted with a focus on source apportionment distribution analyses and epidemiological studies. To assess short-term health associations with Particle Number Concentration (PNC)s, size modes (Nucleation, Aitken or Accumulation) and source contributions, the range of datasets was extended to 2009-2019, or to the largest datasets available during this period. However, the compilation of all datasets and their proper organisation is still incomplete. Anyway, the type of instruments used for the UFP-PSD measurements is well explained for each station.

In addition, Table 2.2 provides the exact dataset periods for 2017-2019 and the link to each Excel file station, where the first sheet of these Excel files provides more detailed information on the UFP-PSD instrumentation, including various details of the measurements.

The data treatment was as follows; first, the required data for the period 2017-2019 was accessed/consulted/searched for the chosen stations. Then, data processing and statistical analysis was performed

using R statistical software (v4.1.3) and the Openair package (Carslaw and Ropkins, 2012). Finally, an Excel template, see table 2.2, was produced where the hourly datasets for 2017-2019 were organised.

In the Excel files there are two sheets, the first one contains all the information on the instrumentation used for each parameter during the sampling period 2017-2019. The second sheet is sorted hourly, starting at 00:00 h UTC on 01/01/2017 and ending at 23:00 h UTC on 31/12/2019. There, the columns follow the subsequent order, BC (in ng m^{-3}), PM_x (PM_{10} , $\text{PM}_{2.5}$, PM_1 , in $\mu\text{g m}^{-3}$), gaseous pollutants (SO_2 , NO, NO_2 and O_3 , in $\mu\text{g m}^{-3}$ and CO in mg m^{-3}) and meteorological parameters (Temperature, $^{\circ}\text{C}$; Relative humidity, %; Pressure, hPa; Solar Radiation, W m^{-2} ; Wind speed, m s^{-1} ; Wind direction, $^{\circ}$; and Rainfall, mm). Then, there are the UFP-PSD datasets for each measured bin, in dN/dlogDp , ending with the concentrations of the Nucleation mode (N_{10-25}), Aitken mode (N_{25-100}), Accumulation mode ($\text{N}_{100-800}$) and PNC (N_{10-800}), all in $\# \text{cm}^{-3}$.

Table 2.2 shows averaged 2017-2019 PNCs for each site, including Nucleation, Aitken and Accumulation concentrations. In addition, Figure 2.2 shows the averaged 2017-2019 PNCs across Europe and Figure 2.3 shows the 2017-2019 UFP-PSD.

Comparing levels of the compiled PNC datasets from the finest size detected is difficult due to their different lower detection limits. Furthermore, measurement errors in the finest size fractions were detected, probably due to lower detection efficiencies at these sizes, the use of CPCs with not fast enough response times, and uncertainties related to diffusion correction of measurements, among others. In order to avoid these errors, the concentration values of some size bins were deleted ('corrected range' for BCN_UB, LIL_SUB, MAR_UB, PAR_SUB and ZUR_UB). Thus, the minimum detection size of all the twenty-six sites ranged from 3 to 20 nm, and the maximum size from 410 to 1000 nm. The coarser size detection limit has a lower influence on the total PNC, in general. However, the finer size detection limit has a considerable impact, especially in the Nucleation mode (N_{x-25}). For this reason, PNC (N_{10-800}) and N_{25-800} concentrations were analysed to reduce this effect. In any case, when comparing PNC, one should consider the site-specific lower detection size.

There are currently two publications in progress, focusing on the 2017-2019 period. One on the description of the concentrations of UFP-PSD across urban Europe, and one on the determination of lung deposited surface area (LDSA) levels in urban Europe. In addition, UFP-PSD ranges from 2009-2019 will also be evaluated in the future to link source apportionment analyses with epidemiological studies looking for short-term associations with PNCs, size modes and source contributions.

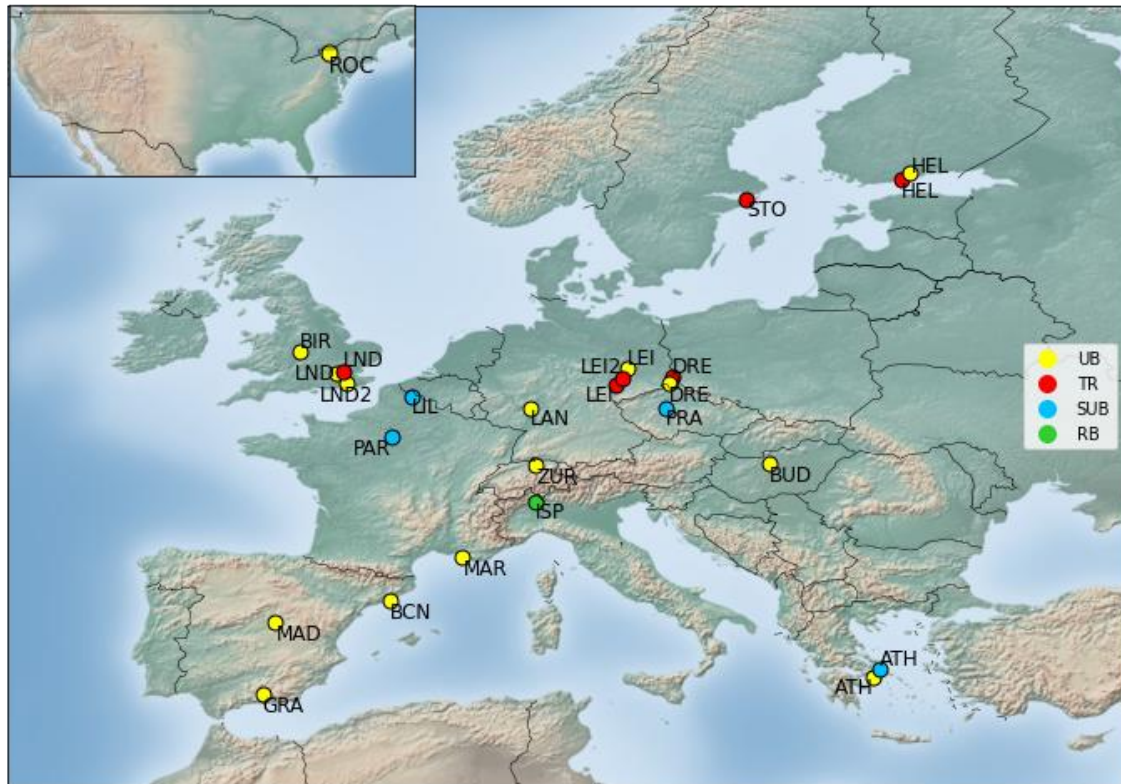


Figure 2.1.: Map with sites and type of station.

Table 2.1.: List of air quality sites supplying UFP-PSD datasets, location, type of environment and data provider, names, contact, EBAS access and UFP-PSD equipment. SMPS, Scanning Mobility Particle Sizer; CPC, Condensation Particle Counter; DMPS, Differential Mobility Particle Sizer; TSMPS, Twin Scanning Mobility Particle Sizer; DMA, Differential Mobility Analyser; TDMPS, Twin Differential Mobility Particle Sizer; UCPC, Ultrafine Condensation Particle Counter; OPC, Optical Particle Counter.

City (Country)	Station Name	Station type	Acronym	Coord.; (Alt., m a.s.l.)	Data provider	Names	Contact	EBAS	UFP-PSD Equipment
Athens (GR)	Thissio	UB	ATH_UB	38.00 N, 23.72 E; (110)	NOA	Nikos Mihalopoulos	nmihalo@noa.gr ;	NO	SMPS TSI 3080L + CPC TSI 3772
Barcelona (ES)	Palau Reial	UB	BCN_UB	41.39 N, 2.13E; (80)	IDAEA-CSIC	Noemi Pérez	noemi.perez@idaea.csic.es	NO	SMPS TSI 3080 + CPC TSI 3772
Birmingham (GB)	BAQS	UB	BIR_UB	52.46 N, 1.93 W; (140)	NCAS	David Beddows	d.c.beddows@bham.ac.uk	NO	SMPS TSI 3082 + CPC TSI 3750
Budapest (HU)	CAAG	UB	BUD_UB	47.48 N, 19.06 E; (115)	ELTE	Imre Salma	salma.imre@ttk.elte.hu	NO	DMPS + CPC TSI 3775
Dresden (DE)	Winckelmannstraße	UB	DRE_UB	51.04 N, 13.73 E; (120)	TROPOS	Alfred Wiedensohler	ali@tropos.de ;	YES	TROPOS-TSMPS uses a Vienna-type DMA 28 cm + CPC TSI 3010/3772
Granada (ES)	UGR	UB	GRA_UB	31.18 N, 3.58 W; (680)	IISTA-CEAMA	Juan Andrés Casquero-Vera	casquero@ugr.es	YES	SMPS TSI 3080 + CPC TSI 3772
Helsinki (FI)	Kumpula Campus	UB	HEL_UB	60.12 N, 24.58 E; (26)	INAR	Tuukka Petäjä	tuukka.petaja@helsinki.fi janne.lampilahti@helsinki.fi	YES	TDMPS Hauke-type DMA 10.9 cm + CPC TSI 3025
Langen (DE)	UBA	UB	LAN_UB	50.00 N, 8.39 E; (130)	UBA	Susanne Bastian	Susanne.Bastian@smekul.sachsen.de	NO	SMPS TSI 3936 + UCPC TSI 3776
Leipzig (DE)	TROPOS	UB	LEI_UB	51.35 N, 12.43 E; (113)	TROPOS	Alfred Wiedensohler	ali@tropos.de	YES	TROPOS-TDMPS uses a Vienna-type DMA 11 cm + UCPC TSI 3025
London (GB)	North Kensington	UB	LND_UB	51.52 N, 0.21 W; (27)	Environmental Research Group, Imperial College London	Anja H. Tremper	anja.tremper@imperial.ac.uk	NO	SMPS TSI 3080 + CPC TSI 3775 with long DMA
London (GB)	Honor Oak Park	UB	LND2_UB	51.45 N, 0.04 W; (31)	Environmental Research Group, Imperial College London	Anja H. Tremper	anja.tremper@imperial.ac.uk	NO	SMPS TSI 3080 + CPC TSI 3775 with long DMA
Madrid (ES)	CIEMAT-Moncloa	UB	MAD_UB	40.45 N, 3.73 W; (669)	CIEMAT	Begoña Artiñano	b.artinano@ciemat.es	YES	SMPS TSI 3080L + CPC TSI 3775
Marseille (FR)	Longchamp	UB	MAR_UB	43.31 N, 5.39 E; (71)	CNRS	Nicolas Marchand	nicolas.marchand@univ-amu.fr	NO	SMPS TSI long DMA 3081A + CPC TSI 3752
Rochester NY (US)	NYS DEC	UB	ROC_UB	43.15 N, 77.55 W; (137)	PHS	Philip K. Hopke	phopke@clarkson.edu	NO	SMPS TSI 3071 + CPC TSI 3010
Zurich (CH)	Kaserne	UB	ZUR_UB	47.38 N, 8.53 E; (410)	Empa	Christoph Hüglin	Christoph.Hueglin@empa.ch	NO	SMPS TSI 3034 + Nafion aerosol dryer
Dresden (DE)	North	TR	DRE_TR	51.09 N, 13.76 E; (116)	TROPOS	Alfred Wiedensohler	ali@tropos.de	YES	TROPOS-SMPS uses a Vienna-type DMA 28 cm + CPC TSI 3772
Helsinki (FI)	Mäkelänkatu	TR	HEL_TR	60.19 N, 24.95 E; (26)	HSY	Jarkko V. Niemi	jarkko.niemi@hsy.fi	NO	UHEL DMPS Vienna-type DMA + CPC Airmodus A20

Leipzig (DE)	Mitte	TR	LEI_TR	51.34 N, 12.38 E; (111)	TROPOS	Alfred Wiedensohler	ali@tropos.de	YES	TROPOS-TDMPS uses a Vienna-type DMA 11 cm + UCPC TSI 3025
Leipzig (DE)	Eisenbahnstraße	TR	LEI2_TR	51.35 N, 12.41 E; (120)	TROPOS	Alfred Wiedensohler	ali@tropos.de	YES	TROPOS-TDMPS uses a Vienna-type DMA 11 cm + UCPC TSI 3025
London (GB)	Marylebone Road	TR	LND_TR	51.52 N, 0.15 W; (27)	Environmental Research Group, Imperial College London	David C. Green	d.green@imperial.ac.uk	NO	SMPS TSI 3080 + CPC TSI 3775 with long DMA
Stockholm (SE)	Hornsgatan	TR	STO_TR	59.32 N, 18.05 E; (20)	SLB-analys	Michael Norman	michael.norman@slb.nu	NO	SMPS TSI 3071 + CPC TSI 3775
Athens (GR)	Demokritos	SUB	ATH_SUB	37.99 N, 23.82 E; (270)	ENRACT	Konstantinos Eleftheriadis	elefther@ipta.demokritos.gr	YES	SMPS TSI 3034 + CPC TSI 3010
Lille (FR)	Villeneuve d'Ascq	SUB	LIL_SUB	50.61 N, 3.14 E; (70)	LOA	Suzanne Crumeyrolle	suzanne.crumeyrolle@univ-lille.fr	NO	SMPS TSI 3082
Paris (FR)	SIRTA	SUB	PAR_SUB	48.71 N, 2.16 E; (162)	INERIS	Olivier Favez; Jean-Eudes	Olivier.FAVEZ@ineris.fr	YES	SMPS GRIMM 5416 + OPC GRIMM
Prague (CZ)	Schudol	SUB	PRA_SUB	50.13 N, 14.38 E; (277)	DACP	Jakub Ondracek	Ondracek@icpf.cas.cz	YES	SMPS TSI 3034 rebuilt at TROPOS
Ispra (IT)	JRC	RG	ISP_RB	45.80 N, 8.63 E; (209)	JRC	Jean Putaud	Jean.PUTAUD@ec.europa.eu	YES	DMPS Vienna-type, home-made + CPC TSI 3010/3772

Table 2.2.: Data coverage of UFP-PSD, ranges, EBAS code and dataset file name in RI-Urbans Intranet. Datasets can found in [PNSD Final Data 2017_2019](#)

Site	Period	Range available (nm)	Range corrected (nm)	% of data	EBAS code	File name	N ₁₀₋₈₀₀	N ₂₅₋₈₀₀	Nucleation	Aitken	Accumulation
ATH_UB	07/02/2017 – 30/12/2019	10.4-469.8	ü	63.7	x	ATHENS Thissio PNSD 2017_2019	8552	7049	1503	5338	1711
BCN_UB	01/01/2017 – 31/12/2019	10.9-478.3	12.2-478.3	76.8	x	Barcelona PNSD 2017_2019	11186	6940	4245	5560	1380
BIR_UB	08/07/2019 – 31/12/2019	11.8-552.3	12.6-552.3	14.5	x	Birmingham PNSD 2019	3532	2871	661	2197	673
BUD_UB	28/01/2017 – 31/12/2019	6-994.2	10.8-816.2	92.7	x	Budapest PNSD 2017-2019	10837	7146	3691	4973	2173
DRE_UB	01/01/2017 – 31/12/2019	10-800	ü	72.3	DE0064B	Dresden Winckelmannstrasse PNSD 2017_2019	6215	4280	1935	3038	1242
GRA_UB	01/01/2017 – 31/12/2019	10.9-495.8	ü	81.5	ES0020U	Granada PNSD 2017-2019	10535	7406	3129	5629	1776
HEL_UB	01/01/2017 – 30/12/2019	2.8-891	10-794	99.9	FI0038U	Helsinki KC PNSD 2017-2019	4208	2789	1419	2144	644
LAN_UB	16/01/2017 – 31/12/2019	10-543.7	ü	82.8	x	Langen PNSD 2017_2019	9956	5328	4628	4074	1254
LEI_UB	10/01/2017 – 30/12/2019	10-800	ü	89.3	DE0055B	Leipzig TROPOS PNSD 2017_2019	8163	4928	3236	3524	1403
LND_UB	01/01/2017 – 31/12/2018	16.6-604.3	ü	52.1	x	London NK PNSD 2017_2019	4489	3874	614	2983	891
LND2_UB	28/11/2018 – 19/12/2019	16.6-604.3	ü	20.9	x	London HP PNSD 2017_2019	4415	3875	540	2912	964
MAD_UB	01/01/2017 – 31/12/2019	10.2-661.2	15.1-661.2	42.9	ES0021U	Madrid PNSD 2017_2019	7937	5940	1997	4806	1134
MAR_UB	13/11/2018 – 31/05/2019	14.6-661.2	15.1-661.2	17.4	x	Marseille PNSD 2017_2019	10297	7618	2679	5894	1723
ROC_UB	06/01/2017 – 31/12/2019	11.1-469.8	ü	90.4	x	Rochester NY PNSD 2017_2019	4407	2973	1434	2370	602
ZUR_UB	01/01/2017 – 13/11/2019	11.3-478.3	16.8-478.3	34.3	x	Zurich PNSD 2017_2019	4201	3905	296	2845	1061
DRE_TR	18/01/2017 – 31/12/2019	5.1-800	10-800	77.7	DE0063K	Dresden Nord PNSD 2017_2019	8791	5144	3647	3892	1252
HEL_TR	01/01/2017 – 05/06/2019	6-800	11-800	70.9	x	Helsinki MK PNSD 2017-2019	10457	4366	6091	3357	1009
LEI_TR	22/11/2017 – 31/12/2019	10-800	ü	69.1	DE0067K	Leipzig Mitte PNSD 2017_2019	13563	6852	6711	5272	1580
LEI2_TR	01/01/2017 – 31/12/2019	10-800	ü	97.9	DE0066K	Leipzig Eisenbahnstrasse PNSD 2017_2019	12023	6774	5249	5075	1699

LND_TR	01/01/2017 – 14/05/2019	16.6-604.3	ü	46.5	x	London MY PNSD 2017 2019	10614	8653	1961	6753	1900
STO_TR	01/01/2017 – 17/09/2018	10-410	ü	47.2	x	Stockholm PNSD 2017 2019	5056	3409	1646	2756	653
ATH_SUB	02/01/2017 – 31/12/2019	10-550	ü	74.3	GR0100B	Athens Demokritos PNSD 2017 2019	6103	4449	1654	3245	1203
LIL_SUB	04/07/2017 – 31/12/2019	15.7-593.5	20.2-593.5	50.6	x	Lille PNSD 2017 2019	6129	5569	560	4148	1421
PAR_SUB	01/01/2017 – 31/12/2019	10.6-791.5	10.9-791.5	91.8	FR0020R	Paris PNSD 2017 2019	4465	3443	1022	2567	876
PRA_SUB	01/01/2017 – 31/12/2019	9.5-519.4	10.3-519.4	86	CZ0004B	Praga PNSD 2017 2019	7893	5378	2515	3823	1555
ISP_RB	01/01/2017 – 31/12/2019	10-800	ü	95.2	IT0004R	Ispra PNSD 2017 2019	7373	6377	996	4058	2319

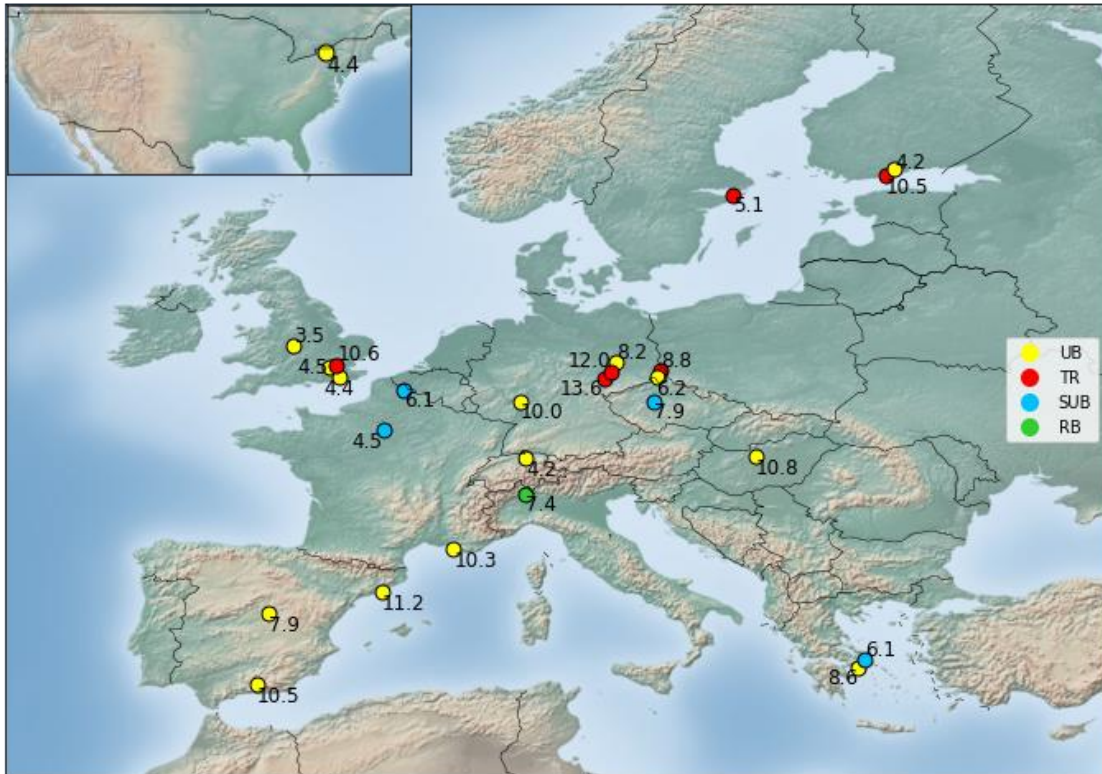


Figure 2.2.: Map with averaged 2017-2019 PNCs of the sites (in # cm⁻³ 10³).

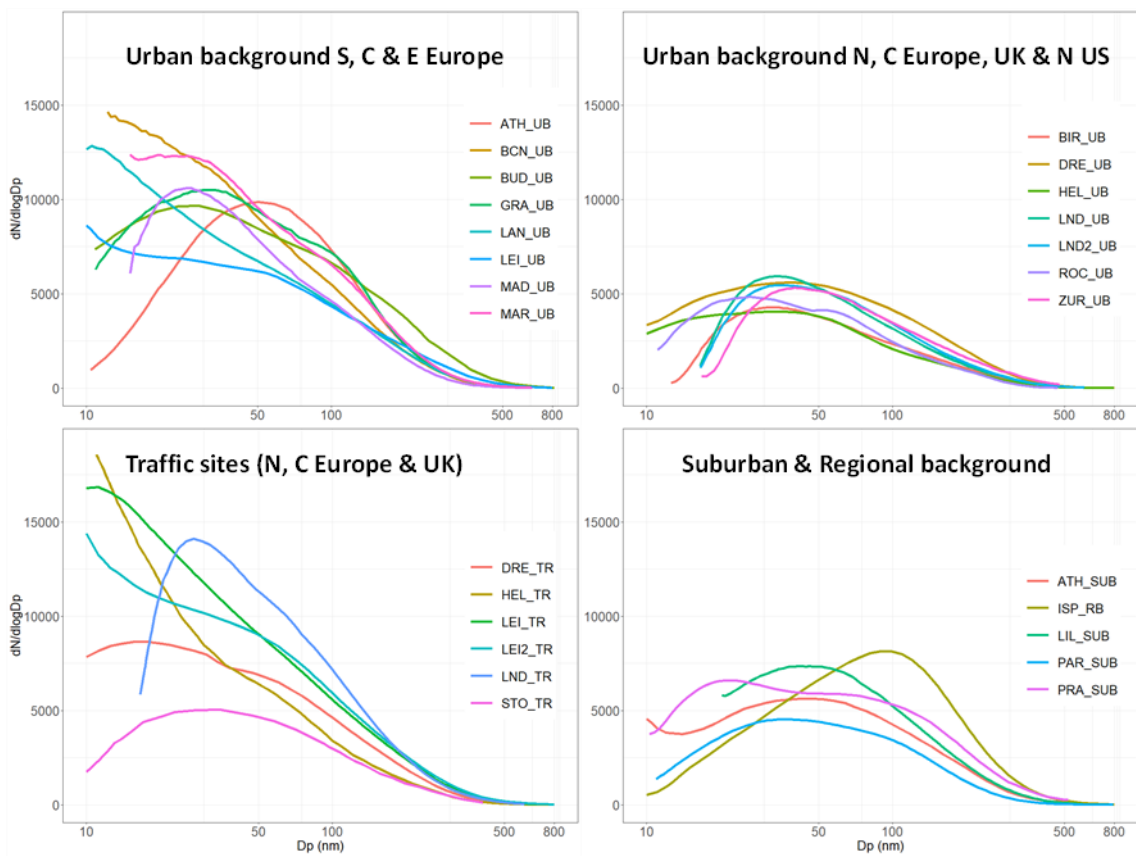


Figure 2.3.: Averaged 2017-2019 particle size distributions.

2.2 PNC and PNSD Guidelines Methods

Online measurements of UFP-PSD are complex, and these are usually carried out by means of electrical mobility analysers (Flagan, 1998) in which the particles are neutralised in charge and separated in sizes by applying an electrical field and counted with a condensation particle counter (CPC). This electrical field can be stepped or scanned, although scanning is the most used. These measurements yield to datasets of PNC for multiple size bins. Using these systems, the range of particle sizes covered from 3 to 15 nm (as finer detection size limit) up to 400 to 1000 nm (as coarser one). Since neither total PNC nor UFP-PSD are included in the current air quality standards, there are not reference methods for these measurements in the context of air quality monitoring.

2.2.1 PNC and PNSD CEN /ACTRIS

CEN has recently developed the following legislations:

- CEN/TS 17434:2020 - Ambient air - Determination of the particle number size distribution of atmospheric aerosol using a Mobility Particle Size Spectrometer (MPSS) for UFP-PSD measurements from 10 to 800 nm.
- CEN/TS 16976:2016 - Ambient air - Determination of the particle number concentration of atmospheric aerosol for total PNC measurements.

These documents describe the performance characteristics and minimum requirements of the instruments and equipment to be used, and describe sampling, operation, data processing and QA/QC procedures, including calibration. The CEN/TS 16976 is however currently in the transition phase to become a EU-Norm, in which the CEN working group decided to change the lower detection efficiency diameter (DP50) from 7 to 10 nm for the EU-Norm to harmonize the lower end of the size range with the CEN/TS 17434 for MPSS measurements. This norm will probably not be in place before 2023.

Furthermore, ACTRIS (2021) provides a set of recommendations to be followed to measure both UFP-PSD and PNC for outdoor air measurements, which are close to the CEN standards, but go below 10 nm if required. The fact is that the prior lack of harmonization of these measurements (both instrumentation and measurement conditions) makes difficult the direct comparison of data from different cities (i.e., a large difference in the fine detection limit might account for a significant difference in total PNC or in the Nucleation mode, <25 nm).

Measurement guidelines provided by ACTRIS (<http://www.actris-ecac.eu/measurement-guidelines.html>) summarise the following recommendations for ultrafine particle sampling:

- Inlets: for ultrafine particles, it is necessary to minimise the effects of diffusional losses in the inlets. For this, the individual pipes to the instruments should be kept as short as possible and the Reynolds number should be around 2000 (<https://www.actris-ecac.eu/aerosol-inlets-and-conditioning.html>). A low flow PM2.5 impactor or cyclone is recommended in the front of these instruments at observatories with a significant fraction of coarse particles. This is important to avoid multiple charged particles of the coarse mode in the MPSS measurements. In the case of nano-particle measurements, they should be preferably done at a separate inlet with minimized diffusional losses.
- Drying: ultrafine particle measurements shall be performed at RH < 40%. This is necessary to obtain comparable data, independently of the hygroscopic behaviour of the aerosol particles. Note the exception for nano-particle measurements going down to 1-3 nm sizes. Existing guidelines & publications can be found under <https://www.actris-ecac.eu/aerosol-inlets-and-conditioning.html>.
 - The recommended method to achieve a relative humidity (RH) below 40% is the Nafion dryer (only using a single Nafion tube). The Nafion membrane must be replaced based on the performance, keeping the RH below 40%.

- Dilution with dry particle-free air behind the inlet head can be employed in tropical and subtropical regions with high dew point temperatures ($T_{dew} > 20^{\circ}\text{C}$). The dilution by dry air should be done according to the description of Annex E in the CEN/TS17434 document.
- Heating of the sampling pipe must not be used. However, a moderate heating of the inlet head is allowed for stations at low ambient temperatures to avoid freezing or to evaporate droplets in a whole air inlet.
- In addition, for each instrument:
 - The volumetric aerosol flow rate should be determined at the inlet of the instrument.
 - The actual pressure should be measured with a high time resolution at a central point, such as at the aerosol splitter inside of the measurement room.
 - The actual relative humidity and temperature should be determined also with a high time resolution at the inlet of each individual instrument. The pressure and temperature are needed for the calculation of the concentration at “Standard Temperature & Pressure” (STP).

Moreover, for the measurement of PNC, different recommendations are provided according to the size range measured. For PNC > 10 nm, ACTRIS recommends following the CEN/TS 16976 for particle number concentration measurements. The EU-Norm to harmonize the lower end of the size range with the CEN/TS 17434 for MPSS measurements will probably not be in place before 2023. However, it is recommended the use a CPC with the coming up 50 % lower detection efficiency diameter of 10 nm. The change of the 50 % lower detection efficiency diameter from 7 to 10 nm of a CEN/TS 16976 compatible CPC must be done by an ECAC-CAIS unit.

In addition:

- CPCs must be traceable, meaning that the PNC reading of an ethernet/USB/serial port must be identical to the calculated PNC from the primary output of the photodetector. A “pulse output” port is therefore obligatory. For PNCs below 5000 cm^{-3} (insignificant coincidence), the internally calculated PNC read from the USB/ethernet/serial port must be within 2 % to PNC calculated from the “pulse out” port. This will be part of the ACTRIS compatibility test at the WCCAP or PACC.
- The provision of following diagnostic parameters of the CPC is obligatory in ACTRIS: Volumetric aerosol flow rate, RH, T, p at inlet of the instrument, Saturator T, Condenser T, Optics T.
- The provision of following diagnostic parameters of the CPC is useful as additional information to monitor the condition of the instrument: nozzle pressure at the inlet to optical cell, critical orifice pressure (if the CPC flow is controlled using critical orifice), laser current, liquid level

For PNSD, ACTRIS recommends following the CEN/TS 17434 for MPSS, where general information is provided by Wiedensohler et al. (2018, 2012). In addition, several aerosol in-situ instrumentation are well recommended by ACTRIS in a list for each specific measurement (<http://www.actris-ecac.eu/actris-gaw-recommendation-documents.html>). Summarized recommendations for PNSD measurements are:

- Particle size range is defined as 10 – 800 nm (the size range could be extended to larger particle sizes, if the MPSS allows this).
- Aerosols to sheath flow ratios between 1:10 and 1:5 are allowed.
- Krypton 85, Nickel 63, and Americium 241 are preferable nuclides for the bipolar chargers. Bipolar chargers based on X-ray, corona discharge, or plasma are not recommended yet (lacking knowledge of long-term stability). MPSS based on unipolar charging are not qualified for these measurements due to increased and unknown uncertainties in the inversion matrix.
- Makeup/bypass flows before or after the DMA are not recommended (CPC aerosol flow is the DMA aerosol inlet and sample flow).

- The CPC should follow the CEN/TS 16976 (or later the corresponding EU norm). The 50 % lower detection efficiency diameter should be set to 10 nm, and the provision of diagnostic parameters of the CPC is obligatory.
- The recommended particle size resolution is 16 to 32 bins/decade. A higher particle size resolution is not recommended due to the poor counting statistics for atmospheric measurements.
- The provision of the following additional diagnostic parameters is obligatory in ACTRIS: Volumetric aerosol inlet flow rate, volumetric sheath air flow rate, aerosol inlet flow RH, T, p, sheath flow RH, T
- All MPSS must be traceable and must fulfil the target uncertainties. All data inversions (incl. multiple charge and internal diffusion loss corrections) for MPSS measurements will be done centrally in the future. Therefore, all manufacturers will have to bring their instrument (following the above criteria) to the WCCAP or PACC for an ACTRIS compatibility test.
- In addition, another CPC (CEN/TS 16976) must be operated in parallel for online QC. This CPC must not be used for other purposes such as the calibration of other instrumentation to avoid contamination.

Nano PNC measurements for the size range below 10 nm can be done with an additional CPC such as an Ultrafine CPC or PSM. In addition, Nano PNSD measurements from 1 to 10 nm can be done with a second Nano-MPSS (see below). Nano particle measurements are not obligatory in ACTRIS.

2.2.2 RI-URBANS recommendations

The first recommendation from RI-URBANS is that data from urban monitoring sites should be uploaded to the EBAS database because only eight sites are already reporting data, from the twenty-one urban sites (UB+TR) evaluated in this project. It is also important to note that only fourteen out of all datasets have data availability >70 % in the study period, and seven have availabilities <50 %. This reflects the complexity of the UFP-PSD measurements and the need for detailed supervision and frequent maintenance of the instrumentation.

Only ten of the twenty-six sites measure UFP-PSD between the size ranges recommended by ACTRIS (2021) and CEN (10-800 nm). Most sites start with size measurements from 11 to 20 nm and/or end from 410 to 661 nm. These differences make very difficult to compare UFP concentrations from different cities, given that a larger size detection limit could drastically reduce PNC. Accordingly, an effort should be made to implement the ACTRIS's and CEN's recommendations. Furthermore, in five datasets measurement errors were detected in the finest size bins, pointing to the need for good equipment maintenance and quality control.

The main recommendations from RI-Urbans are:

- (i) Implementation of CEN and ACTRIS guidelines recommendations for the accurate measurement of UFP-PSD concentrations ranging 10-800 nm in urban areas, to obtain a representable database and to reduce the effects of missing concentrations in the comparison between different areas, especially regarding the smaller size fractions
- (ii) The use of the correct instrumentation to measure UFP-PSD following ACTRIS recommendations (<https://www.actris-ecac.eu/actris-gaw-recommendation-documents.html>)
- (iii) Finally, it is important to cover large periods of measurements rather than the short periods currently available for many of the urban datasets. This is important to be able to detect seasonal and temporal trends.
- (iv) Easy accessibility to the datasets (data upload to the EBAS database is recommended)
- (v) Operation of another CPC (CEN/TS 16976) in parallel for quality control of the data

- (vi) Consideration of appropriate measurements of nanoparticle (<10 nm) concentrations and size distributions in line with ACTRIS recommendations would improve information on the nucleation mode and finer range of UFP, which are related to health effects. There is currently a considerable lack of studies on the relationship between nanoparticle concentrations (<10 nm) and the effects they may have on human health

2.3 Determination of lung deposited surface area (LDSA) levels

The determination of the concentrations of lung deposited surface area (LDSA) is of high interest for exposure assessment, since it captures the toxicologists' idea that particle surface area available in the lung is a relevant to exposure metric. Based on International Commission on Radiological Protection (ICRP 1994), the head/throat (HA), the tracheobronchial (TB) and alveolar (ALV) region deposition efficiencies are used to define LDSA as function of the particle size. Therefore, LDSA has been proposed as a critical predictor for health outcomes from aerosol exposure, as it appears to be one of the most relevant physical metrics for evaluating exposure to particles (Chang et al. 2022; Schmid and Stoeger 2016).

Based on the compiled 2017-2019 hourly particle number size distributions (PNSD), the LDSA deposited in HA, TB, and ALV regions of the human respiratory system was estimated. This information can be used for the purpose of epidemiological studies and urban planning. Further studies will focus on evaluating the short-term health effects of LDSA using a selection of the analysed time series.

2.3.1 Calculation of the size-fractionated lung-deposited surface area (LDSA)

Measuring the LDSA in principle requires a measurement of the entire particle size distribution, followed by a summation of particle surface in each size bin weighted by its lung-deposition probability. Todea et al. (2015) conducted extensive measurements for several LDSA sensors and instruments and concluded that, for particle sizes of 20–400 nm, the LDSA measurement accuracy of all devices is >30%. Furthermore, Asbach et al. (2009) reported that LDSA concentrations are mainly driven by the number of particles <400 nm. The finer and coarser size detection limit of most sites were 10 and 800 nm, but varied considerably among the sites (3-17 nm, and 400-1000 nm, respectively). Thus, to comparing LDSA from all sites, the PNSD data was selected by comparing the PNC in the size range of 20-400 nm (N_{20-400}).

In case of spherical particles, the PNSD can be easily transferred into surface area size distributions (SASD) by means of the known relationship between a sphere's surface area and its diameter. These distributions can be integrated over the wanted size range to obtain the total surface area concentrations. To obtain LDSA concentrations, the SASDs can be weighted with lung deposition curves (Hussein et al. 2013) and integrated over the size range of interest. In this study, a model was applied to divide the respiratory tract into three main regions, including HA, TB, and ALV regions, based on the International Commission on Radiological Protection (ICRP) and multiple path particle dosimetry (MPPD) models (Hussein et al. 2013). In our calculations we used size-dependent regional deposition fraction (DF) curves obtained from a combination of experimental estimation reported by (Löndahl et al. 2007). The deposition efficiencies of size-fractionated PNCs in the HA ($DF_{HA,i}$), TB ($DF_{TB,i}$), and ALV ($DF_{ALV,i}$) were calculated according to ICRP model (ICRP 1994) (Eqs. 1-3):

$$DF_{HA,i} = \left(0.5 + \frac{0.5}{1+0.00076 \times D_{p,i}^{2.8}} \right) \times \left(\frac{1}{1+\exp(6.84+1.183 \ln D_{p,i})} + \frac{1}{1+\exp(0.924-1.885 \ln D_{p,i})} \right), \text{ (Eq.1);}$$

$$DF_{TB,i} = \frac{0.00352}{D_{p,i}} \times \left(\exp \left(-0.234 (\ln D_{p,i} + 3.40)^2 \right) + 63.9 \exp \left(-0.819 (\ln D_{p,i} - 1.61)^2 \right) \right), \text{ (Eq.2);}$$

$$DF_{ALV,i} = \frac{0.0155}{D_{p,i}} \times \left(\exp\left(-0.416(\ln D_{p,i} + 2.84)^2\right) + 19.11 \exp\left(-0.482(\ln D_{p,i} - 1.362)^2\right) \right), \text{ (Eq.3)}$$

The LDSA values were calculated by first counting the number of particles in each size bin and then multiplying the PNC with the specific alveolar deposition fraction of the given particle size. The total surface area of the deposited particles was then calculated accordingly (Eqs. 4-5).

$$dLDSA/d\log D_p = \pi \cdot D_p^2 \cdot dN/d\log D_p \quad \text{(Eq.4)}$$

$$LDSA = \int_{D_{p1}}^{D_{p2}} dLDSA/d\log D_p \quad \text{(Eq.5)}$$

2.3.2 LDSA Datasets

Following the PNSD dataset and the above formula, we calculate the LDSA. In the Excel file (LDSA-data) there are four sheets. There, the sheets follow the subsequent order, total LDSA ($\mu\text{m}^2/\text{cm}^3$), HA-LDSA ($\mu\text{m}^2/\text{cm}^3$), TB-LDSA ($\mu\text{m}^2/\text{cm}^3$), ALV-LDSA ($\mu\text{m}^2/\text{cm}^3$). For each sheet, it is sorted hourly, starting at 00:00 h UTC on 01/01/2017 and ending at 23:59 h UTC on 31/12/2019 for all monitoring stations.

2.3.3 General characteristics of LDSA at different measurement sites

We analysed the annual average LDSA concentrations during the past three years (2017-2019) (Figure 2.4a). Significant spatial differences ($p < 0.01$) in LDSA concentrations among twenty-six European sites and the site of USA were observed, ranging from 15 to 52 $\mu\text{m}^2/\text{cm}^3$ (Table 2.3). The annual average concentrations of total LDSA in all sites were higher than 15 $\mu\text{m}^2/\text{cm}^3$, indicating potential health risk at each monitoring site. Comparing all monitoring sites, for UB areas, the highest annual average LDSA concentration was found in BUD_UB (52±32 $\mu\text{m}^2/\text{cm}^3$), followed by MAR_UB (39±28 $\mu\text{m}^2/\text{cm}^3$), while the lower was in ROC_UB (15±9.4 $\mu\text{m}^2/\text{cm}^3$) and HEL_UB (15±9.6 $\mu\text{m}^2/\text{cm}^3$). For TR site, the highest annual average LDSA was found in LDN_TR (42±25 $\mu\text{m}^2/\text{cm}^3$), followed by LEI2_TR (40±24 $\mu\text{m}^2/\text{cm}^3$), while the lowest was in STO_TR (19±9.7 $\mu\text{m}^2/\text{cm}^3$) and HEL_TR (26±18 $\mu\text{m}^2/\text{cm}^3$). For SUB/RB areas, the highest annual average LDSA was found in PRA_SUB (34±54 $\mu\text{m}^2/\text{cm}^3$), followed by LIL_SUB (30±20 $\mu\text{m}^2/\text{cm}^3$), while the lowest was in ATH_SUB (26±15 $\mu\text{m}^2/\text{cm}^3$) and PAR_SUB (18±13 $\mu\text{m}^2/\text{cm}^3$). Interestingly, ISP_RB, located in a pollution hotspot region in Europe (the PO Valley) also had the second highest LDSA concentration (43±32 $\mu\text{m}^2/\text{cm}^3$) of all monitoring sites. Overall, the highest concentration of LDSA was found in UB (BUD_UB) and the lowest was also found in UB (HEL_UB) (Figure 2.4 & Table 2.3).

Moreover, particles are deposited in the respiratory tract depending on their sizes, densities, shapes, charges, surface properties, and the breathing patterns of the individuals (Heyder 2004). Therefore, the contributions to deposition of annual average LDSA in different regions of the respiratory tract, including HA, TB, and ALV, were estimated in all research sites during observed period (Figure 2.4.b, Table 2.3). The results showed that the LDSA concentration was majorly accumulated in ALV, which was considered to bring the most harm to human lungs (Fung et al. 2022; Salo et al. 2021), but low contributions were obtained for HA and TB deposition, indicating the strong size-dependence of deposition (Kumar et al. 2014).

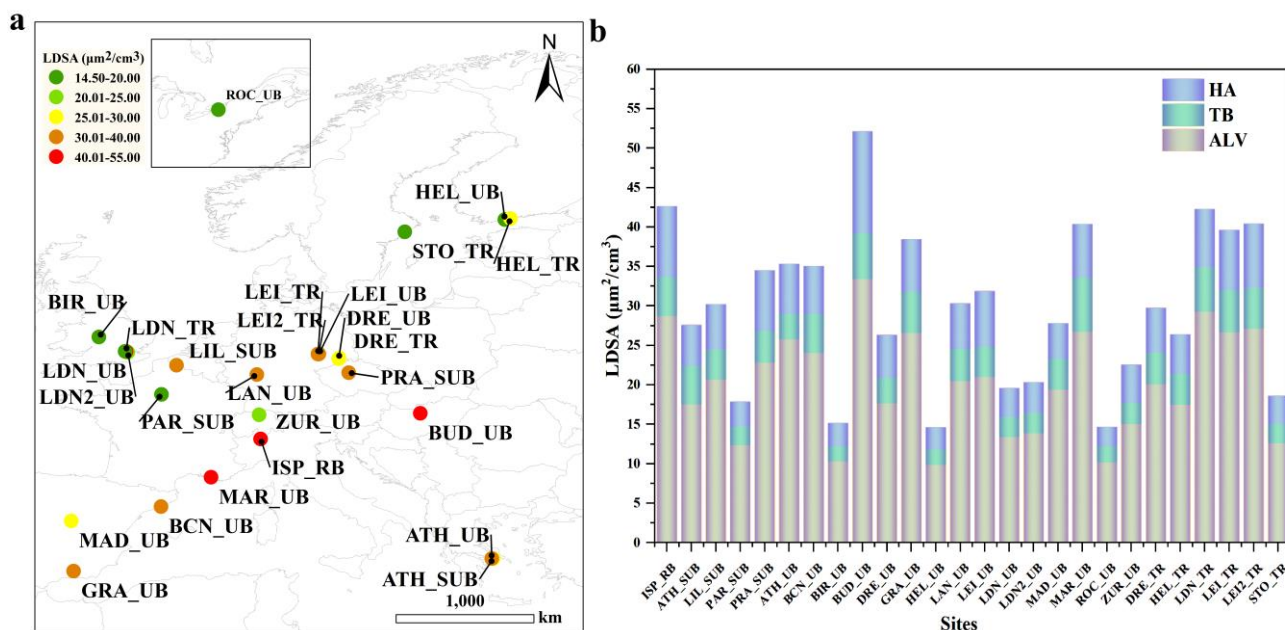


Figure 2.4.: (a), 2017-2019 average concentrations of total LDSA in twenty-five European sites and one in USA and (b), the contribution of annual average LDSA in different regions of the respiratory tract, including head (HA), tracheobronchial (TB), and alveolar (ALV).

Table 2.3.: 2017-2019 averaged LDSA of total, head (HA), tracheobronchial (TB), and alveolar (ALV) (in $\mu\text{m}^2/\text{cm}^3$).

Site	Total-LDSA	HA-LDSA	TB-LDSA	ALV-LDSA
ATH_SUB	25.91	5.09	3.23	17.59
ATH_UB	36.97	6.26	4.89	25.82
BCN_UB	35.02	5.95	4.94	24.13
BIR_UB	15.12	2.83	1.93	10.36
BUD_UB	52.33	12.81	5.84	33.67
DRE_TR	29.94	5.60	4.05	20.30
DRE_UB	26.29	5.32	3.24	17.73
GRA_UB	38.42	6.56	5.20	26.66
HEL_UB	14.79	2.71	1.95	9.93
HEL_TR	26.35	4.86	3.91	17.57
ISP_RB	42.59	8.86	4.92	28.81
LAN_UB	30.29	5.70	4.07	20.53
LEI_TR	39.61	7.53	5.35	26.74
LEI2_TR	40.39	8.01	5.21	27.17
LEI_UB	31.86	6.95	3.83	21.08
LIL_SUB	30.16	5.60	3.81	20.75
LDN_UB	19.55	3.55	2.53	13.47
LDN_TR	42.25	7.25	5.67	29.33
LDN2_UB	20.39	3.78	2.57	13.96
MAD_UB	27.79	4.43	3.93	19.44
MAR_UB	38.74	6.71	6.81	26.81
PAR_SUB	17.84	3.08	2.36	12.40
PARA_SUB	34.46	7.55	4.02	22.89
ROC_UB	14.65	2.35	2.06	10.23
STO_TR	18.57	3.46	2.43	12.68
ZUR_UB	22.53	4.73	2.65	15.14

2.4 Annex / Files Datasets

2.4.1 PNC/PNSD

The PNC/PNSD datasets are fully available at RI-URBANS intranet ([PNSD Final Data 2017 2019](#)). The data is presented in an excel file for each site, organized in two excel sheets:

Sheet 1: Site-instrumentation information. This sheet provides information about the site measured; location, type of station, coordinates, altitude, measurement period and other possible important observations of the site of AQ monitoring station.

Sheet 2: Hourly Dataset. This sheet provides an hourly dataset of BC (ng m^{-3}), PM_x (PM_{10} , $\text{PM}_{2.5}$, PM_1 , in $\mu\text{g m}^{-3}$), Gaseous pollutants (SO_2 , NO, NO_2 , O_3 in $\mu\text{g m}^{-3}$ and CO in mg m^{-3}), metadata (Temperature, $^{\circ}\text{C}$; Relative Humidity, %; Pressure, mbar; Solar Radiation, W m^{-2} ; wind speed, m sec^{-1} ; wind direction $^{\circ}$; Rain, mm), PNSD concentrations in dN/dlogDp and Nucleation, Aitken, Accumulation mode, N_{25-800} and PNC (N_{10-800}), all in $\# \text{cm}^{-3}$.

2.4.2 LDSA

The PNC/PNSD datasets are fully available at RI-URBANS intranet ([LDSA](#)). The data is presented in an excel file for each site, organized in four excel sheets:

Data presented in four sheets; for each sheet, it is sorted hourly, starting at 00:00 h UTC on 01/01/2017 and ending at 23:59 h UTC on 31/12/2019 for all monitoring stations.

Sheet 1: total LDSA ($\mu\text{m}^2/\text{cm}^3$),

Sheet 2: HA-LDSA ($\mu\text{m}^2/\text{cm}^3$),

Sheet 3: TB-LDSA ($\mu\text{m}^2/\text{cm}^3$)

Sheet 4: ALV-LDSA ($\mu\text{m}^2/\text{cm}^3$)

2.5 References

- Asbach C, Fissan H, Stahlmecke B, Kuhlbusch T, Pui D. 2009. Conceptual limitations and extensions of lung-deposited Nanoparticle Surface Area Monitor (NSAM). *Journal of Nanoparticle Research* 11(1):101-109.
- ACTRIS, C. for A.I.-S.M., Preliminary, 2021. Preliminary ACTRIS recommendation for aerosol in-situ sampling , measurements, and analysis. <https://www.actris.eu/sites/default/files/2021-06/Preliminary%20ACTRIS%20recommendations%20for%20aerosol%20in-situ%20measurements%20June%202021.pdf>
- Carslaw, D.C., Ropkins, K., 2012. openair — An R package for air quality data analysis. *Environ. Model. Softw.* 27-28, 52–61. <https://doi.org/10.1016/j.envsoft.2011.09.008>
- CEN/TS 16976:2016 - Ambient air - Determination of the particle number concentration of atmospheric aerosol [WWW Document], 2016. URL <https://standards.iteh.ai/catalog/standards/cen/91f1ac67-f6d6-408c-af89-e81763194fd3/cen-ts-16976-2016> (accessed 6.20.22).
- CEN/TS 17434:2020 - Ambient air - Determination of the particle number size distribution of atmospheric aerosol using a Mobility Particle Size Spectrometer (MPSS) [WWW Document], 2020. URL <https://standards.iteh.ai/catalog/standards/cen/a841bc08-ed34-4fa8-94ca-8c5e07b99db9/cen-ts-17434-2020> (accessed 6.20.22).
- Chang P, Griffith SM, Chuang H, Chuang K, Wang Y, Chang K, Hsiao T. 2022. Particulate matter in a motorcycle-dominated urban area: Source apportionment and cancer risk of lung deposited surface area (LDSA) concentrations. *Journal of Hazardous Materials* 427:128188.

- Flagan, R.C., 1998. History of Electrical Aerosol Measurements. *Aerosol Sci. Technol.* 28, 301–380. <https://doi.org/10.1080/02786829808965530>
- Fung PL, Zaidan MA, Niemi JV, Saukko E, Timonen H, Kousa A, Kuula J, Rönkkö T, Karppinen A, Tarkoma S. 2022. Input-adaptive linear mixed-effects model for estimating alveolar lung-deposited surface area (LDSA) using multipollutant datasets. *Atmospheric Chemistry and Physics* 22(3):1861-1882.
- Heyder J. 2004. Deposition of inhaled particles in the human respiratory tract and consequences for regional targeting in respiratory drug delivery. *Proceedings of the American Thoracic Society* 1(4):315.
- Hussein T, Löndahl J, Paasonen P, Koivisto AJ, Petäjä T, Hämeri K, Kulmala M. 2013. Modeling regional deposited dose of submicron aerosol particles. *Science of The Total Environment* 458-460:140-149.
- ICRP. 1994. ICRP: Published for the International Commission on Radiological Protection [By 1-3 p.
- Kumar P, Morawska L, Birmili W, Paasonen P, Hu M, Kulmala M, Harrison RM, Norford L, Britter R. 2014. Ultrafine particles in cities. *Environment international* 66:1-10.
- Löndahl J, Massling A, Pagels J, Swietlicki E, Vaclavik E, Loft S. 2007. Size-resolved respiratory-tract deposition of fine and ultrafine hydrophobic and hygroscopic aerosol particles during rest and exercise. *Inhalation toxicology* 19(2):109-116.
- Salo L, Rönkkö T, Saarikoski S, Teinilä K, Kuula J, Alanen J, Arffman A, Timonen H, Keskinen J. 2021. Concentrations and Size Distributions of Particle Lung-deposited Surface Area (LDSA) in an Underground Mine. *Aerosol and Air Quality Research* 21(8):200660.
- Schmid O, Stoeger T. 2016. Surface area is the biologically most effective dose metric for acute nanoparticle toxicity in the lung. *Journal of Aerosol Science* 99:133-143.
- Todea AM, Beckmann S, Kaminski H, Asbach C. 2015. Accuracy of electrical aerosol sensors measuring lung deposited surface area concentrations. *Journal of Aerosol Science* 89:96-109.
- Wiedensohler, A., Birmili, W., Nowak, A., Sonntag, A., Weinhold, K., Merkel, M., Wehner, B., Tuch, T., Pfeifer, S., Fiebig, M., Fjåraa, A.M., Asmi, E., Sellegri, K., Depuy, R., Venzac, H., Villani, P., Laj, P., Aalto, P., Ogren, J.A., Swietlicki, E., Williams, P., Roldin, P., Quincey, P., Hüglin, C., Fierz-Schmidhauser, R., Gysel, M., Weingartner, E., Riccobono, F., Santos, S., Grüning, C., Faloon, K., Beddows, D., Harrison, R., Monahan, C., Jennings, S.G., O’Dowd, C.D., Marinoni, A., Horn, H.G., Keck, L., Jiang, J., Scheckman, J., McMurry, P.H., Deng, Z., Zhao, C.S., Moerman, M., Henzing, B., De Leeuw, G., Löschau, G., Bastian, S., 2012. Mobility particle size spectrometers: Harmonization of technical standards and data structure to facilitate high quality long-term observations of atmospheric particle number size distributions. *Atmos. Meas. Tech.* 5, 657–685. <https://doi.org/10.5194/amt-5-657-2012>
- Wiedensohler, A., Wiesner, A., Weinhold, K., Birmili, W., Hermann, M., Merkel, M., Müller, T., Pfeifer, S., Schmidt, A., Tuch, T., Velarde, F., Quincey, P., Seeger, S., Nowak, A., 2018. Mobility particle size spectrometers: Calibration procedures and measurement uncertainties. *Aerosol Sci. Technol.* 52, 146–164. <https://doi.org/10.1080/02786826.2017.1387229>

3 Equivalent Black Carbon

One specific objective of the RI-URBANS project is to interpret and reveal the benefits of obtaining datasets from urban sites on novel air quality metrics as Black Carbon (BC) and their source contribution to provide guidelines. In this section, we describe compiled datasets of ambient Black Carbon (BC) measurements with instrumental and operational settings to determine the source contributions from biomass burning and traffic.

3.1 eBC datasets

This section includes information regarding the number of datasets, data providers, data coverage, types of instruments, data QA/QC, data utilization, and information about the final dataset's organization. This will be presented in the context of the report or in the tables in the following sections.

In the RI-URBANS project, a long-term database of concentrations of eBC measured at 53 sites/stations in 31 European cities, and 14 European countries, was used to evaluate the use of BC as a measurement parameter in pollution control networks (see Figure 3.1). The database was collected using data available in the EBAS Network (5 sites) and several European cities where data were unavailable in EBAS. Mainly data was provided by RI-URBANS partners and the collaboration of some institutions which are not involved in the project. As shown in Figure 3.1, the distribution of the site which provided BC data is not homogeneous. Countries like Finland and Netherlands from Northern Europe have more share of BC measurements unlike other countries such as Italy. In addition, long-time series measurements of Elemental Carbon (EC) and Black Carbon were provided by Rochester, New York from the US. These cities are characterized by different meteorological conditions and emissions. BC particle concentrations are commonly obtained from filter-based photometers such as the Aethalometers. These instruments convert the measured light attenuation into BC concentrations (*called equivalent BC, eBC*) using defined mass absorption cross sections (MAC) for freshly emitted BC particles. Available eBC concentrations were measured with Aethalometers (AE33-31-22-21) and multi-angle absorption photometers (MAAP) in the selected urban environments (see Figure 3.2). Figure 3.2 shows the instrumental distribution to measure BC concentrations in countries that collaborated in RI-URBANS. The viability and quality of data have been checked by data providers and the responsible in charge of data compilation in the phase of the data analysis and interpretation. In the present study, continuous measurements over multi-year periods have been done in European cities. Different periods were investigated in each city. Mainly datasets cover years between 2017-2019. This period has been selected because of the Covid-19 lockdown's significant effects on air quality from March 2020. In this case, this period is considered as a reference measurement period of the study to be consistent in all sites for further health studies and trend analysis. However, the minimum start of datasets was observed from 31/05/2006 in the SMEAR II, Hyytiälä, Finland, to the maximum date 23/02/2022 in Birmingham, UK.

It should be highlighted that the main objective of RI-URBANS is to evaluate the interest in using BC measurements for Air Quality. The measurements obtained in various sites and by different instruments must be comparable. This will be needed for health studies and potentially establishing a limit value. To this aim, recommendations for reporting "black carbon" in situ measurements of MAAP and Aethalometers have been provided by the ACTRIS guidelines, manuals, and other related publications (Müller *et al.*, 2011; Petzold *et al.*, 2013; Drinovec *et al.*, 2015; Tuch and Wiedensohler, 2018b, 2018a).

To ensure quality assurance and quality control of datasets, the instructions to prepare the datasets on template have been sent to partners to be consistent in different sites. Further, received datasets have been pre-processed for possible errors, detection limits, flags, peaks, and negative values. In the case of EBAS, datasets were available in level 2 format, including physical parameters, aggregated to hourly averages, information on recommended variability, and quality assured by human inspection. Regarding the datasets provided directly by partners, they have been received in different types of processing and quality levels. For instance, from Level 0, raw data was obtained from the instrument with original time resolution to completely harmonized and analyzed datasets used

for scientific publications (K Grange *et al.*, 2020). These compiled datasets will be used for project-related tasks (e.g., trend analysis, source apportionment, health effects, etc.) and further publications considering that some of them have already been used for previous scientific studies (Helin *et al.*, 2018). Data from Leipzig, Granada, and Ispra were obtained from EBAS, which is available online (i.e., [EBAS \(nilu.no\)](http://ebas.nilu.no)). Therefore, it has been observed that there is still a critical need to expand the collaboration of data providers to associate more data submissions to EBAS.

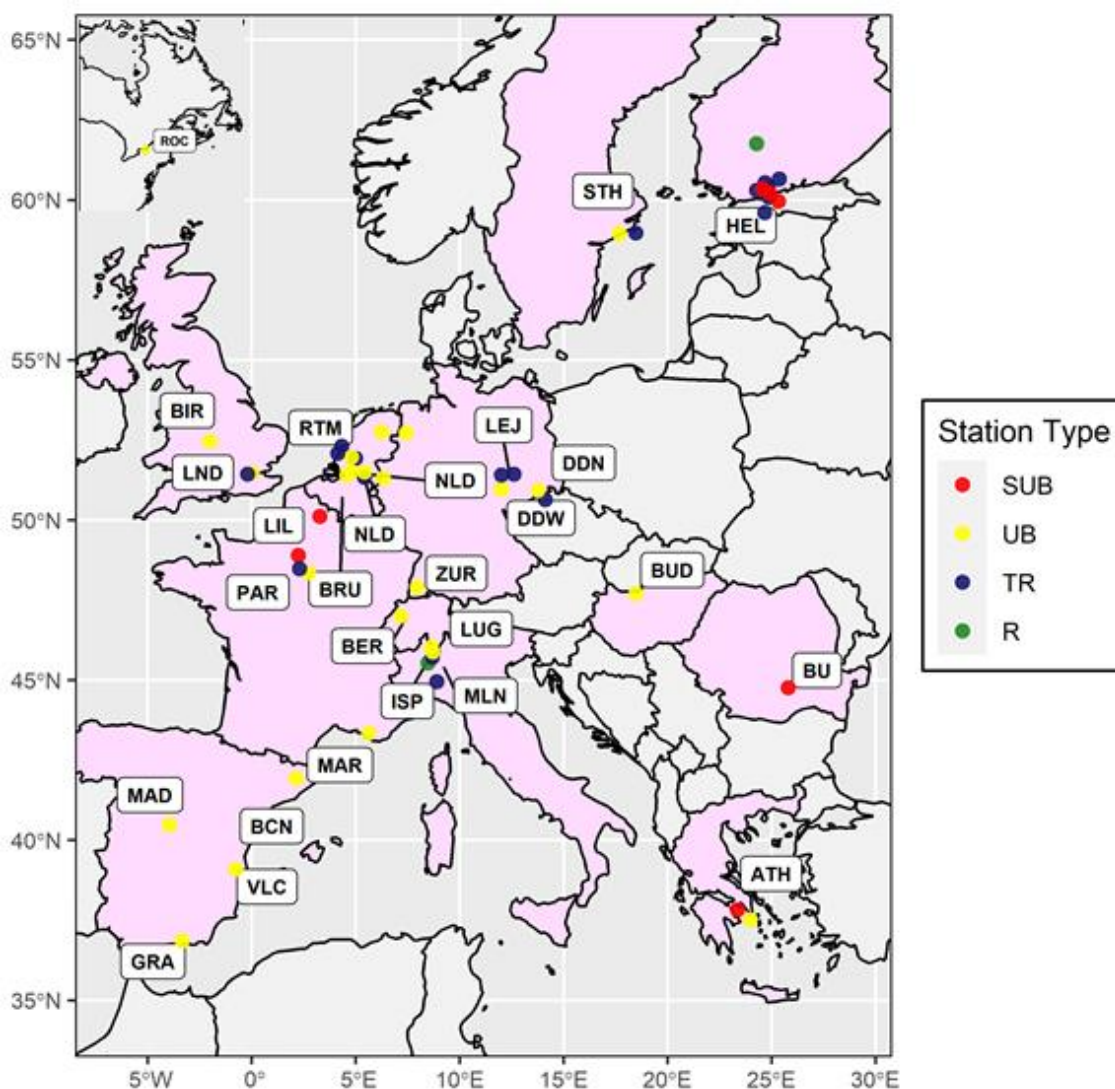


Figure 3.1. Distribution of the sites involved in RI-URBANS

Following is the list of sites/stations from European cities collaborating in the RI-URBANS project. The type of sites, instruments, and information about data providers are listed in detail (see Table. 3.1). In total, eBC data from 53 sites have been collected. It should also be noted that among 53 sites/stations, Elemental Carbon (EC) measurements were available only in 20 sites which were not primarily sufficient for further analysis as harmonization of eBC measurements. Among them, 13 sites have been selected to harmonize eBC measurements. Unlike the continuous observations of the Aethalometers, EC concentrations were available as daily samples and ranged from being sampled with different time resolutions (every 4 to 12 days). The EC and OC mass concentrations were measured mainly using a semi-continuous thermal-optical organic/elemental carbon analyzer in European monitoring sites. These measurements should follow the general ACTRIS and GAW guidelines and

recommendations for aerosol in-situ sampling (<https://www.actris-ecac.eu/measurement-guidelines.html>, no date). Further, with the aim of data analysis, using eBC and EC data together, the eBC observations were aggregated to daily resolutions. Only days with both EC and eBC observations were used for harmonization of eBC measurements because the interpolation of the less frequent EC data was not attempted.

Final processed eBC datasets are available online in the RI-URBANS server among the partners. It consists of different folders based on the type of instruments (i.e., AE33, MAAP, AE31-21-22). Overall, 25 datasets are processed with data from the AE33, an online measurement technique of aerosol light absorption with the reference MAC [$7.77 \text{ m}^2\text{g}^{-1}$] at 880nm. Each dataset contains three data sheets. The first sheet describes Metadata as information about the measurement site, instrument, and technical operation details. The second sheet contains data/time (UTC), hourly averaged reference eBC at 880 nm, and absorption at seven wavelengths for long-term measurements. Available EC data to calculate the experimental MAC and rolling MAC is also provided in the third sheet of excel files with daily resolution. The third sheet (EC-MAC) contains eBC recalculation results from a rolling regression technique, where the measured Babs (880nm channel for AE33 and 637 nm for MAAP) is aggregated to daily values and regressed against EC with a window width of 14 days and right alignment.

This organization of the excel file is also considered for the eBC measurements from AE31 (7 wavelengths), AE21, and AE22 (2-Wavelength). The Aethalometer, model AE-22, measures the light transmission at 370 and 880 nm. Regarding the multi-angle absorption photometer (MAAP), 31 sites/locations BC datasets were obtained and processed. It follows the same structure, including eBC at reference MAC [$6.6 \text{ m}^2\text{g}^{-1}$], Reference eBC wavelength [637 nm], and recalculation of the eBC measurements applying Median RI-URBANS MAC and site-specific MAC.

In addition, eBC concentrations measured by a multi-wavelength Aethalometer33 used for source apportionment based on the Sandradewi et al. (Sandradewi *et al.*, 2008) model. Briefly, the method is based on the dependence of aerosol absorption on the wavelength (470 and 950 nm $\text{AAE}_{470} = 1$ and $\text{AAE}_{950} = 2$) of light used to investigate the sample, parameterized by the source-specific absorption Ångström exponent (α). Since fossil fuel and biomass contributions to aerosol absorption feature specific values of the absorption Ångström exponent, it is possible to construct a source-specific two-component model. It should be mentioned that the Sandradewi model was not applied for the source apportionment of AE31-21-22 discontinued models. Furthermore, the temporal variability of the MAC is studied by comparing absorption measurements from AE33 and MAAP and EC concentrations performed at the selected cities. Then the reference eBC at 880 nm is recalculated applying RI-URBANS median mass absorption cross-section ($\text{MAC} = 10.57 \text{ m}^2\text{g}^{-1}$) and the site-specific (Local MAC: Absorption/EC). In detail, this method will be further explained in the eBC Guidelines/recommendation section.

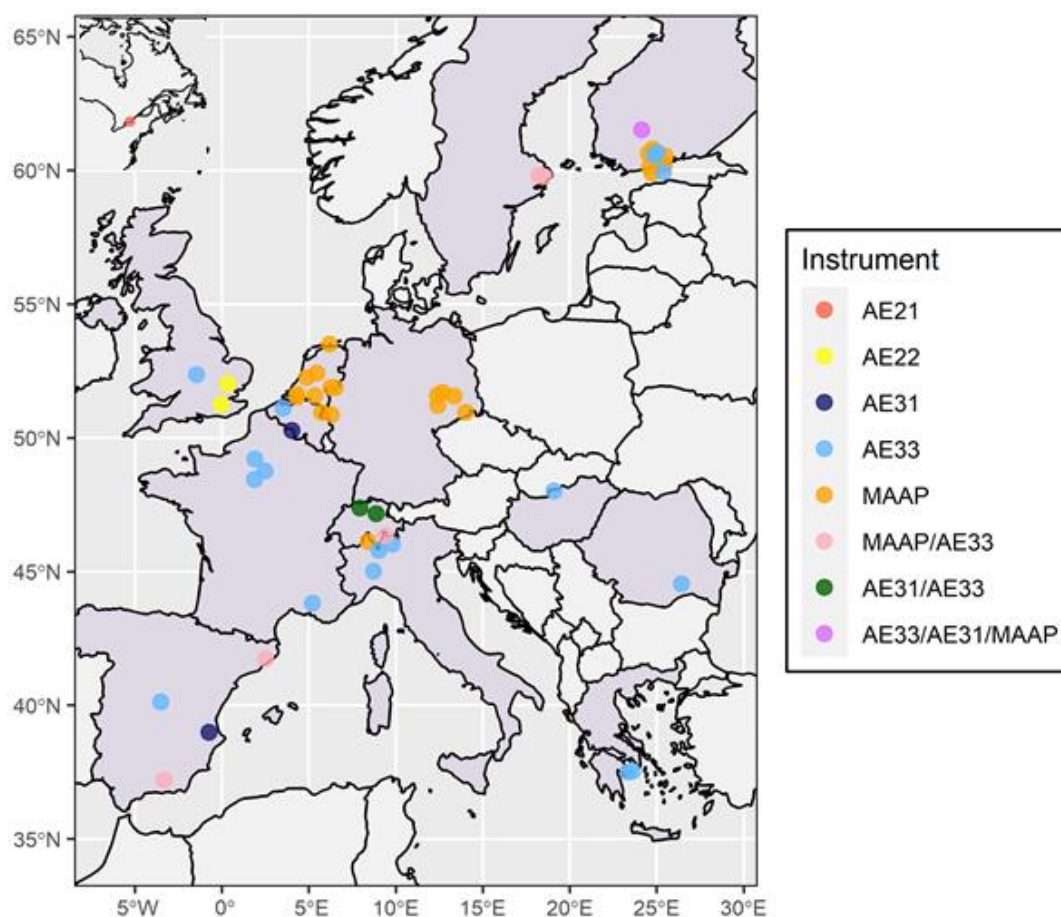


Figure 3.2. Distribution of the instruments used to measure eBC concentrations

- **Data treatment, pre-processing**

After compiling datasets, further analysis was performed considering the absorption coefficients provided by the MAAP or Aethalometers depending on time resolution and coverage or the measurement availability at several wavelengths. The AE33 and MAAP data (supplied with a high temporal resolution) were used to study the seasonal variations. Data treatment and statistical analysis were carried out using R statistical computing software (R-4.2.1) and the Openair package (Tools for the Analysis of Air Pollution Data) (Carslaw and Ropkins, 2012). First, data was synchronized into hourly median time resolution (UTC). Subsequently, data were converted into the same unit for all 53 sites for better comparison. We identified and eliminated the outliers, including negative values, to follow a normal data distribution. We examined this by plotting histograms for each variable. A few datasets were already received corrected with a threshold and values below the detection limit (DL). For further analysis, missing data were not gap-filled. Based on the length and the extent of the missing gap in datasets, it was eliminated. Data sets received by partners with some differences. In some cases, seven different wavelengths with the absorption coefficient received or 7 eBC concentrations to retrieve absorption considering the filter tapes. There were some challenges in recovering the information about when filter-tapes changed during the measurements period due to the lack of information from data providers. According to confirmation of Magee Scientific Co., the approximate dates are as follows:

The first filter (M8020) was used approximately between 2011 and February 2016. Filter M8050 between February 2016 and October 2017, and M8060 from October 2017 until now. Thus, it was decided to retrieve the absorption coefficient from AE33 based on the default C & Z depending on the station and filter tape considered. Therefore,

for further analysis, it was necessary to follow a fixed standardized method for a good estimation of absorption and eBC concentrations. Following are the equations used for retrieving MAC calculated from EC and Absorption data:

Absorption:

$$\text{Abs (MAAP) [637 nm]} = [\text{BC}] * 6.6 * 1.05$$

$$\text{Abs (AE33; M8060) [880 nm]} = [\text{BC}] * \text{MAC} / \text{H1} \text{ (H harmonization factor = 0.57)}$$

$$\text{Abs (AE33; M8020) [880 nm]} = [\text{BC}] * \text{MAC} / \text{H2} \text{ (H harmonization factor = 2.21)}$$

$$\text{Abs (AE31-21-22) [880 nm]} = [\text{BC}] * \text{MAC} / \text{H3} \text{ (H harmonization factor = 3.5)}$$

MAC:

$$\text{MAC} (\lambda) = \text{Abs} (\lambda) / \text{EC} (\lambda = 637 \text{ nm and } 880 \text{ nm})$$

$$\text{MAC [637 nm]} = \text{MAC [880]} * 880 / 637 \text{ (AAE = 1)}$$

The harmonization factor will change due to filters. So, absorption is well calculated. Finally, the mean of eBC concentrations is calculated for selected sites, as shown in Figure 3.3.

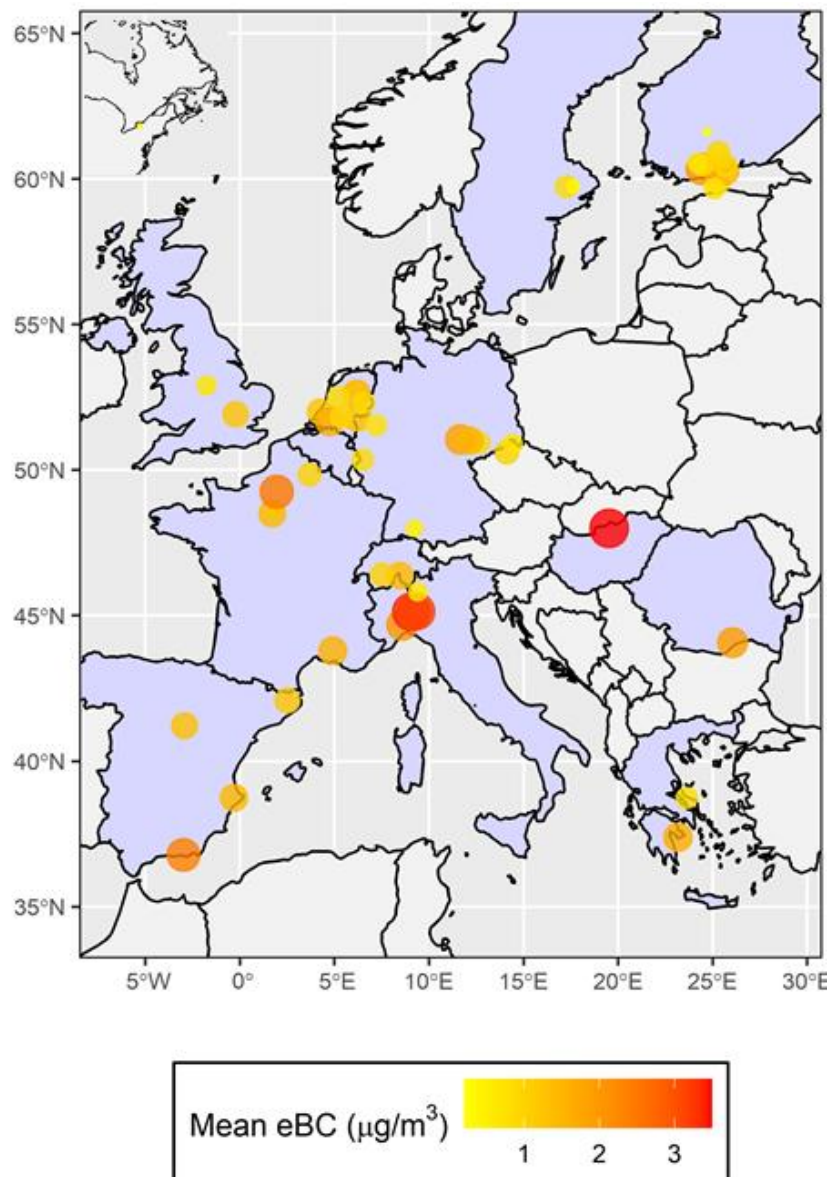


Figure 3.3. Mean eBC concentration in RI-URBANS sites

It is vital to have a reliable and quantitative data on BC pollution sources to implement effective air quality policies. From the result, we do not observe a clear gradient at the urban level in European cities. Based on the preliminary results of Sandradewi model for source apportionment of BC of fossil and non-fossil, on average, traffic is the primary source of BC (see Table 3.2). Some interesting features will be explored to understand which sources contribute to the peaks in the future. Among the 53 sites/locations, the highest mean value is from Milan-Marche and Pascal (3.20 $\mu\text{g m}^{-3}$ and 3.14) between the 2018-2021 measured by AE33, considering all data. The lowest mean eBC concentrations reported in SMEAR II Hyytiälä were measured by an AE33, 0.28 $\mu\text{g m}^{-3}$ between the 2018-2021. The lowest mean concentration value measured by a MAAP is also reported in SMEAR II Hyytiälä between the years 2013-2021 in 0.209 $\mu\text{g m}^{-3}$ and the highest value reported from Milan Pascal between years 2013-2021 respectively 2.65 $\mu\text{g m}^{-3}$.

Following is the list of the measurement sites and data providers supplying eBC data to this project. UB, Urban Background; TR, Traffic; SUB, Suburban Background; RG, Regional Background (Table 3.1). Table 3.2 describes data coverage, data availability%, PM size, mean eBC concentrations, and it's apportioned to two major BC sources: fossil fuel and biomass burning applied by the Sandradewi AETH model. These preliminary results of source apportionment have been provided to perform preliminary assessment regarding the identification of different BC sources.

Table 3.1. List of air quality sites supplying BC/EC datasets by location, type, instruments and data provider

No	Site	City_Country	Station Type	Acronym	Coordinates	Data provider_Institution	Available on EBAS?	eBC_Instrument	EC Available?
1	Thissio	Athens-Greece	UB	ATH_UB	37.973, 23.718	National Observatory of Athens (NOA)	No	AE33	Yes
2	Palau Reial	Barcelona-Spain	UB	BCN_UB	41.387, 2.115	IDAEA-CSIC	Yes	AE33 & MAAP	Yes
3	UGR	Granada-Spain	UB	GRA_UB	37.18, -3.58	University of Granada & http://ebas-data.nilu.no/	Yes	AE33 & MAAP	Yes
4	CIEMAT	Madrid-Spain	UB	MAD_UB	40.456, -3.725	IISTA-CEAMA (University of Granada)	No	AE33	No
5	Burjassot	Valencia-Spain	UB	VLC_UB	39.51, - 0.42	CIEMAT	No	AE31	No
6	Uccle	Brussels-Belgium	UB	BRU_UB	50.7977, 4.362	IRM-KMI	No	AE31	No
7	Longchamp	Marseille-France	UB	MAR_UB	43.305, 5.394	AtmoSud-LCE	No	AE33	Yes
8	Paris-13	Paris-France	UB	PAR_UB	48.864, 2.349	LSCE-INERIS	No	AE33	No
9	Winckelmannstrasse	Dresden-Germany	UB	DDW_UB	51.036, 13.730	Saxon state office for environment, agriculture and geology	No	MAAP	Yes
10	Tropos	Leipzig-Germany	UB	LEJ_UB	51.352, 12.434	Leibniz Institute for Tropospheric Research, TROPOS	Yes	MAAP	No
11	BpART Lab	Budapest-Hungary	UB	BUD_UB	47.475, 19.0625	Eötvös Loránd University	No	AE33	Yes
12	Kallio (UB1)	Helsinki-Finland	UB	HEL_UB1	60.1872, 24.950	HSY	No	MAAP	No
13	Winkelhorst (UB1)	Enschede-NLD	UB	NLD_UB1	52.234, 6.919	National Institute for Public Health and the Environment- RIVM	No	MAAP	No
14	Nijensteinheerd (UB2)	Groningen-NLD	UB	NLD_UB2	53.246, 53.246	RIVM	No	MAAP	No
15	Jamboreepad (UB3)	Heerlen-NLD	UB	NLD_UB3	50.900, 5.986	RIVM	No	MAAP	No
16	Ruyterstraat (UB4)	Nijmegen-NLD	UB	NLD_UB4	51.838, 5.856	RIVM	No	MAAP	No
17	NL01488 (RZW)	Rotterdam-NLD	UB	RZW_UB	51.894, 4.4876	DCMR	No	MAAP	No
18	Europalaan (UB5)	Veldhoven-NLD	UB	NLD_UB5	51.407, 5.393	RIVM	No	MAAP	No
19	Torkel Knutssonsgatan	Stockholm-Sweden	UB	STH_UB	59.316, 18.057	Stockholm Environment and Health Administration	No	AE33 & MAAP	Yes
20	Bollwerk	Bern-Switzerland	UB	BER_UB	46.951, 7.440	EMPA	No	AE33	Yes
21	Università	Lugano-Switzerland	UB	LUG_UB	46.011, 8.9572	EMPA	No	AE33 & MAAP	Yes
22	Kaserne	Zurich-Switzerland	UB	ZUR_UB	47.3775, 8.5305	EMPA	No	AE33	Yes
23	BAQS	Birmingham-UK	UB	BIR_UB	52.455, -1.928	University of Birmingham	No	AE33	No
24	North Kensington	London-UK	UB	LND_UB	51.521, -0.213	Imperial College London	No	AE22-AE33	Yes
25	ROC	Rochester-USA	UB	ROC_UB	43.146, -77.542	New York State Dept of Environmental Conservation, Division of Air	No	AE21	Yes
26	Pascal	Milan-Italy	UB	MLN_RB	45.464, 9.188	ARPA Lombardia	No	AE33 & MAAP	No

27	Nord	Dresden-Germany	TR	DDN_TR	51.087, 13.7630	Saxon state office for environment, agriculture and geology	No	MAAP	Yes
28	Mannerheimintie (TR1)	Helsinki-Finland	TR	HEL_TR1	60.1697, 24.939	HSY	No	MAAP	No
29	Mäkelänkatu (TR2)	Helsinki-Finland	TR	HEL_TR2	60.196, 24.952	HSY	No	MAAP	Yes
30	Töölöntulli (TR3)	Helsinki-Finland	TR	HEL_TR3	60.190, 24.916	HSY	No	MAAP	No
31	Kehä I (TR4)	Helsinki-Finland	TR	HEL_TR4	60.241, 25.025	HSY	No	MAAP	
32	Tikkurila (TR5)	Helsinki-Finland	TR	HEL_TR5	60.289, 25.039	HSY	No	MAAP	No
33	Leppävaara (TR6)	Helsinki-Finland	TR	HEL_TR6	60.220, 24.811	HSY	No	MAAP	No
34	Haussmann	Paris-France	TR	PAR_TR	48.874, 2.323	LSCE-INERIS	No	AE33	No
35	Mitte (TR1)	Leipzig-Germany	TR	LEJ_TR1	51.344, 12.377	Leibniz Institute for Tropospheric Research, TROPOS	Yes	MAAP	Yes
36	Eisenbahnstrasse (TR2)	Leipzig-Germany	TR	LEJ_TR2	51.345, 12.406	Leibniz Institute for Tropospheric Research, TROPOS	Yes	MAAP	No
37	Senato (TR1)	Milan-Italy	TR	MLN_TR1	45.464, 9.188	ARPA Lombardia	No	AE33	No
38	Marche (TR2)	Milan-Italy	TR	MLN_TR2	45.464, 9.188	ARPA Lombardia	No	AE33	No
39	Noordbrabantlaan (TR1)	Eindhoven- NLD	TR	NLD_TR1	51.444, 5.444	RIVM	No	MAAP	No
40	NLO1492 (RDM)	Rotterdam- NLD	TR	RDM_TR	51.914, 4.48	DCMR	No	MAAP	No
41	Graafseweg (TR2)	Nijmegen- NLD	TR	NLD_TR2	51.841, 5.857	RIVM	No	MAAP	No
42	NLO1487 (RPW)	Rotterdam- NLD	TR	RPW_TR	51.891, 4.481	DCMR	No	MAAP	No
43	Hornsgatan 108	Stockholm-Sweden	TR	STH_TR	59.3171, 18.048	Stockholm Environment and Health Administration	No	AE33 & MAAP	No
44	Marylebone Road	London-UK	TR	LND_TR	51.522, -0.1546	Imperial College London	No	AE22-AE33	Yes
45	Demokritos	Athens-Greece	SUB	ATH_SUB	37.99, 23.82	NCSR Demokritos	Yes	AE33	Yes
46	INO	Bucharest-Romania	SUB	BU_SUB	44.348, 26.029	INOE	No	AE33	No
47	Rekola (DH4)	Helsinki-Finland	SUB	HEL_DH4	60.331, 25.075	HSY	No	AE33	No
48	Itä-Hakkila (DH5)	Helsinki-Finland	SUB	HEL_DH5	60.291, 25.112	HSY	No	AE33	No
49	Pirkkola (DH6)	Helsinki-Finland	SUB	HEL_DH6	60.234, 24.922	HSY	No	AE33	No
50	Villeneuve d'Ascq	Lille-France	SUB	LIL_SUB	50.611, 3.1403	IMT, Departement Sciences de l'Atmosphere et Genie de l'Environnement, Lille Douai	No	AE33	No
51	SIRTA	Paris-France	SUB	PAR_SUB	48.7086, 2.1588	LSCE / INERIS	Yes	AE33	Yes
52	Ispra	IPR	RB	ISP_RB	45.8, 8.633	EC-JRC-IES, Institute for Environment and Sustainability	Yes	MAAP	Yes
53	SMEAR II	Juupajoki (Hyytiälä)-Finland	RB	HYT_RB	61.847, 24.295	HSY	No	AE33- AE31 & MAAP	Yes

Table 3.2 eBC datasets compiled with supplementary information

No	Station Name	PM size	Data availability%	Data coverage	All eBC data			eBC data 2017-2019			File name
					Average eBC	%BC _{ff}	%BC _{wb}	Average eBC	%BC _{ff}	%BC _{wb}	
1	ATH_UB	PM10	24.4	2017-12/31/2019	1.66	68.9	31	1.75	69.1	30.8	Athens_NOA_AE33_2017-2019.xlsx
2	BCN_UB	PM10	AE33: 34.7 MAAP: 77.6	AE33: 4/3/2015-9/20/2020 MAAP: 1/13/2009- 3/31/2021	AE33: 1.66 MAAP: 1.45	84.3	15.6	AE33: 1.51 MAAP: 1.20	84	15.9	Barcelona_Palau Reial_AE33_2015-2020.xlsx BCN_Palau Reial_MAAP_2009-2021.xlsx
3	GRA_UB	Total	AE33: 25.2 MAAP: 87.6	AE33: 1/1/2014-12/31/2019 MAAP: 01/01/2006-31/12/2020	AE33: 2.28 MAAP: 2.28	77.5	22.4	AE33: 2.0 MAAP: 1.94	70.1	29.8	Granada_MAAP_2006-2020.xlsx Granada_UGR_AE33_2014-2019.xlsx
4	MAD_UB	PM10	30.5	14/01/2013-31/12/2019	1.70	86.5	13.4	1.34	83.22	16.77	Madrid_CIAMAT_AE33_2015-2020.xlsx
5	VLC_UB	ND	12	1/9/2017-12/7/2020	1.37	*	*	1.48	*	*	Valencia_Burjassot_AE31_2017-2019.xlsx
6	BRU_UB	Total	48.9	12/1/2013-12/31/2021	*	*	*	*	*	*	Brussels_Uccle_AE31_2014-2021.xlsx
7	MAR_UB	PM2.5	18.2	1/1/2017-12/31/2019	1.60	80.2	19.7	1.60	80.2	19.7	Marseille_Longchamp_AE33_2017-2019.xlsx
8	PAR_UB	ND	23.7	1/1/2016-12/31/2019	1.55	71.4	28.5	1.45	71.1	28.8	Paris_PA13_AE33_2016-2019.xlsx
9	DDW_UB	PM1	19	1/1/2017-12/31/2019	0.67	*	*	0.67	*	*	DDW_Winckel_MAAP_2017-2019.xlsx
10	LEJ_UB	PM10	73.5	1/1/2009-12/31/2020	1.07	*	*	0.91	*	*	Leipzig_Tropos_MAAP_2009-2020.xlsx
11	BUD_UB	PM2.5	6.6	2/24/2014-3/11/2014	3.49	68.9	31	*	*	*	Budapest_BpART_AE33_2014.xlsx
12	HEL_UB1	PM1	50	1/4/2012-12/31/2019	0.51	*	*	0.44	*	*	Helsinki_Kallio(UB1)_2012-2019.xlsx
13	NLD_UB1	Aerosol	41.7	4/29/2015-12/31/2021	0.70	*	*	0.73	*	*	NLD_RIVM_Enschede_2015-2021.xlsx
14	NLD_UB2	Aerosol	41.4	5/4/2015-12/31/2021	0.52	*	*	0.57	*	*	NLD_RIVM_Groningen_2015-2021.xlsx
15	NLD_UB3	Aerosol	42.5	4/9/2015- 12/31/2021	0.80	*	*	0.84	*	*	NLD_RIVM_Heerlen_2015-2021.xlsx

16	NLD_UB4	Aerosol	41.9	4/30/2015- 12/31/2021	0.85	*	*	0.87	*	*	NLD_RIVM_Nijmegen-Ruyterstraat_2015-2021.xlsx
17	RZW_UB	Total	74.9	1/1/2010- 12/31/2021	1.07	*	*	0.90	*	*	Rotterdam(RZW)_MAAP_2010-2021.xlsx
18	NLD_UB5	Aerosol	41.6	5/21/2015- 12/31/2021	0.91	*	*	0.95	*	*	NLD_RIVM_Veldhoven_2015-2021.xlsx
19	STH_UB	MAAP: PM2.5 AE33: PM1	MAAP: 6.9 AE33: 29.2	AE33: 10/14/2014 -12/31/2019 MAAP: 10/2/2014- 11/3/2015	MAAP: 0.39 AE33: 0.33	75.1	24.8	AE33: 0.30	75.4	24.5	Stockholm_TorkeI_MAAP_2014-2015.xlsx Stockholm_TorkeI_AE33_2014-2019.xlsx
20	BER_UB	PM2.5	42.95	1/1/2015- 12/31/2021	1.0633	71.1	28.6	1.0	74.4	25.5	Bern_Bollwerk_AE33_2015-2021.xlsx
21	LUG_UB	PM2.5	MAAP: 62.3 AE33: 1	MAAP: 1/1/2012- 11/3/2021 AE33: 11/3/2021- 12/31/2021	MAAP: 0.72 AE33: 0.85	*	*	0.59	*	*	Lugano_Università_AE33_2021.xlsx Lugano_MAAP_2012-2021.xlsx
22	ZUR_UB	PM2.5	63.2	1/1/2012- 12/31/2021	0.5801	74.6	25.3	0.48	75.3	24.6	Zurich_Bollwerk_AE33_2012-2021.xlsx
23	BIR_UB	PM2.5	18.1	3/19/2019- 2/23/2022	0.67	72.6	27.3	*	*	*	Birmingham_BAQS_AE33_2019-2022.xlsx
24	LND_UB	PM2.5	AE22: 65.6 AE33: 25.2	AE22: 1/1/2009- 11/7/2019 AE33: 01/01/2020- 01/01/2022	AE33: 0.75	75	24.9	*	*	*	London_NK_AE22_2009-2020.xlsx London_N. Kensington_AE33_2020-2021.xlsx
25	ROC_UB	PM2.5	83.8	6/23/2008- 12/9/2021	0.41	*	*	0.33	*	*	Rochester_ROC_AE21_2008-2021.xlsx
26	MLN_UB	ND	12.5	AE33: 06/08/2018-11/04/2019 MAAP: 06/02/2013-21/11/2021	3.14	74.3	25.6	3.14	74.3	25.6	Milan_Pascal_AE33_2018-2019.xlsx Milan_Pascal_MAAP_2013-2021.xlsx
27	DDN_TR	PM1	19	01/01/2017-31/12/2019	1.04	*	*	1.04	*	*	DDN_Nord_MAAP_2017-2019.xlsx
28	HEL_(TR1)	PM1	49.9	1/1/2011- 12/31/2019	0.81	*	*	0.67	*	*	Helsinki_Mannerheimintie (TR1)_2011-2019.xlsx
29	HEL_(TR2)	PM1	30.7	1/30/2015- 12/31/2019	1.09	*	*	0.96	*	*	Helsinki_Mäkelänkatu (TR2)_2015-2019.xlsx
30	HEL_(TR3)	PM1	12.2	11/1/2010- 30/12/2015	2.08	*	*	*	*	*	Helsinki_Töölöntulli (TR3)_2010,2015.xlsx
31	HEL_(TR4)	PM1	6.1	1/1/2012- 12/28/2012	1.57	*	*	*	*	*	Helsinki_Kehä I (TR4)-2012.xlsx

32	HEL_(TR5)	PM1	19	Years 2014, 2016 & 2018	0.83	*	*	0.80	*	*	Helsinki_Tikkurila (TR5)_2014,2016,2018.xlsx
33	HEL_(TR6)	PM1	12.3	Years 2015 & 2017	0.77	*	*	0.66	*	*	Helsinki_Leppävaara (TR6)_2015,2017.xlsx
34	PAR_TR	ND	24.5	1/1/2016- 12/29/2019	2.61	88.3	11.6	2.48	87.7	12.2	Paris_Boulevard Haussmann_AE33_2016-2019.xlsx
35	LEJ_TR1	PM10	56.2	04/01/2017-26/12/2019	2.34	*	*	1.81	*	*	Leipzig_Mitte_MAAP_2010-2019.xlsx
36	LEJ_TR2	PM10	62.3	17/01/2009-31/12/2020	1.80	*	*	1.52	*	*	Leipzig_Eisenbahnstrasse_MAAP_2009-2020.xlsx
37	MLN_TR1	ND	13	12/06/2019-22/11/2021	2.04	76.0	23.9	*	77.5	22.4	Milan_Senato_AE33_2019-2021.xlsx
38	MLN_TR2	ND	12.5	23/05/2019-15/11/2021	3.20	78.2	21.7	*	*	*	Milan_Marche_AE33_2019-2021.xlsx
39	NLD_TR1	Aerosol	42	28/04/2015-31/12/2021	1.33	*	*	1.37	*	*	NLD_RIVM_Eindhoven_2015-2021.xlsx
40	RDM_TR	Total	90.1	01/07/2007-31/12/2021	1.65	*	*	1.26	*	*	Rotterdam(RDM)_MAAP_2007-2021.xlsx
41	NLD_TR2	Aerosol	41.4	26/05/2015-31/12/2021	1.48	*	*	1.52	*	*	NLD_RIVM_Nijmegen-Graafseweg_2015-2021.xlsx
42	RPW_TR	Total	74.7	01/01/2010-31/12/2021	2.16	*	*	1.66	*	*	Rotterdam(RPW)_MAAP_2010-2021.xlsx
43	STH_TR	MAAP: PM2.5 AE33:PM1	MAAP: 6.9 AE33: 30.1	MAAP: 04/11/2015-05/12/2016 AE33: 14/10/2014-31/12/2019	MAAP: 0.94 AE33: 1.02	88.3	11.6	0.87	86.6	13.3	Stockholm_Hornsgatan_MAAP_2015-2016.xlsx Stockholm_Hornsgatan_AE33_2014-2019.xlsx
44	LND_TR	PM2.5	AE22: 66.2 AE33: 25.2	AE22: 16/03/2009-31/12/2019 AE33: 1/24/2020- 1/1/2022	AE33: 1.33	77	22.9	*	*	*	London_MY_AE22_2009-2020.xlsx London_Marylebone Road_AE33_2020-2021.xlsx
45	ATH_SUB	PM10	15.8	11/01/2017-31/12/2019	0.82	75.7	24.2	0.82	75.7	24.2	Athens_Demokritos_AE33_2017-2019.xlsx
46	BU_SUB	PM10	26.3	27/02/2014-11/01/2022	1.92	63.7	36.2	2.12	61.4	38.5	Bucharest_INO_AE33_2014-2021.xlsx
47	HEL_DH4	PM1	2.4	05/01/2017-31/05/2017	0.95	69.4	30.4	*	*	*	Helsinki_Rekola (DH4)_AE33_2017.xlsx
48	HEL_DH5	PM1	5.1	03/01/2018-23/10/2018	0.95	65.6	34.3	*	*	*	Helsinki_Itä-Hakkila (DH5)_AE33_2018.xlsx
49	HEL_DH6	PM1	6.3	31/12/2018-31/12/2019	0.73	68.6	31.3	*	*	*	Helsinki_Pirkkola (DH6)_AE33_2019.xlsx

50	LIL_SUB	PM1	11.9	01/01/2017-31/12/2019	1.01	69.3	30.6	1.01	69.3	30.6	Lille_Villeneuve d'Ascq_AE33_2017- 2019.xlsx
51	PAR_SUB	PM1	44.4	01/01/2014-30/12/2020	0.66	71.4	28.5	0.63	71.1	28.8	Paris_SIRTA_AE33_20 14-2020.xlsx
52	ISP_RB	PM10	69	16/09/2008-31/12/2020	1.78	*	*	1.44	*	*	Ispra_MAAP_2008- 2020.xlsx
53	HYT_RB	PM10	AE33: 34.7 AE31: 49.6 MAAP: 44.5	MAAP: 18/06/2013-09/05/2021 AE33: 15/03/2018-31/12/2021 AE31: 31/05/2006-17/11/2017	MAAP: 0.20 AE33: 0.28 AE31: 0.29	88.9	11	MAAP: 0.19 AE33: 0.28 AE31: 0.17	89.1	10.8	SMEAR II_Hyytiälä_MAAP_2013 -2021.xlsx SMEAR II_Hyytiälä_AE31_2006- 2017.xlsx SMEAR II_Hyytiälä_AE33_2018- 2021.xlsx

*ND: NOT DEFINED

*Link: link to the dataset files in RI-URBANS intranet

3.2 eBC Guidelines/Methods

3.2.1 MAAP

This instrument is currently discontinued. ACTRIS In Situ Aerosol: Guidelines for Manual QC of MAAP (Multiangle Absorption Photometer) data

https://www.actris-ecac.eu/pluginAppObj/pluginAppObj_225_191/2020-08-20_ACTRIS_MAAP_v0.pdf

3.2.2 AE33

ACTRIS In Situ Aerosol: Guidelines for Manual QC of AE33 absorption photometer data

https://www.actris-ecac.eu/pluginAppObj/pluginAppObj_225_189/2021-09-14_ACTRIS_AE33_v1.pdf

Specifications for instruments measuring the particle light absorption coefficients are given for filter-based absorption photometers. We would like to refer to the existing GAW recommendation which is available at <https://www.gaw-wdca.org/Publications>. Filter-based absorption photometers are simple in their technical construction. Therefore, the list of hardware requirements is rather short. In addition, however, there are requirements concerning the data recording and data evaluation that must be considered in sampling sites for measurements as mentioned below:

- The sample flow through the filter must be measured. Since an uncontrolled flow decreases when loading a filter, it is recommended to control the sample flow.
- The attenuation or transmission of light must be recorded.
- When exceeding an instrument-specific maximum attenuation, the filter must be changed either automatically or manually. The station user must estimate how long the device can operate unattended.
- The sample spot size must be regularly checked. Diffuse edges indicate a problem with the closing mechanism.
- The filter type must have been calibrated for use in that instrument. Calibration factors are needed for data evaluation.
- Instruments often report the equivalent BC concentration. The conversion formulas of measurement quantities in optical units to equivalent black carbon must be known.
- The instrument must record the temperature, pressure, and relative humidity.
- The instrument must record housekeeping numbers measured raw intensities.

Related publication:

Muller et al. AMT, 2011

[amt-4-245-2011.pdf \(copernicus.org\)](https://amt.copernicus.org/amt-4-245-2011.pdf)

Petzold et al. ACP, 2013

[ACP - Recommendations for reporting "black carbon" measurements \(copernicus.org\)](https://acp.copernicus.org/ACP-Recommendations-for-reporting-black-carbon-measurements)

Drinovec et al. ACP, 2015

[amt-8-1965-2015.pdf \(copernicus.org\)](https://amt.copernicus.org/amt-8-1965-2015.pdf)

3.2.3 RI-URBANS recommendations

A reliable assessment of atmospheric black carbon depends on the light absorbed by BC measured from BC mass concentrations using the mass absorption cross-section (MAC). Since BC concentrations determined indirectly by

optical and thermo-optical instruments (Bond *et al.*, 2013), equivalent Black Carbon used instead of BC from optical absorption methods (Petzold *et al.*, 2013). Measuring the light absorption coefficient correctly is challenging for filter-based methods (Zanatta *et al.*, 2016). There is no satisfactory solution to determine site-independent equivalent BC (eBC) concentrations (Kalbermatter *et al.*, 2022). Aerosol light absorption and BC mass are the parameters required to accurately calculate mass absorption cross section (MAC_{BC}) values. It is crucial to develop the guidelines to measure these parameters correctly to investigate and compare MAC_{BC} values measured across different urban sites to evaluate the performance of different instruments. To estimate the absorption correctly, a harmonization factor is needed. However, it should be considered that, this harmonization factor can change depending on the properties of particles and can also be λ ly published study (Yus-Díez *et al.*, 2021), It is indicated that the multiple-scattering correction factor (C), which depends on the optical properties of the collected particles, is the parameter with the greatest impact on the absorption coefficients derived from the AE33 measurements.

It has been observed that the C factor can increase noticeably under single scattering albedo, which is common at regional and remote sites. In Barcelona, as an urban site, one of the cities involved in RI-URBANS, on average, it was not observed a change of C, since single scattering albedo is not as high as a remote site. And the C is wavelength-dependent. However, we observed the statistically significant change with wavelengths only in remote stations. From the ACTRIS (Aerosols, Clouds, and Trace gases Research InfraStructure; <http://www.actris.eu>), the harmonization factor was applied to correct systematic differences between instruments. Thus, in this case, everywhere in RI-URBANS, we could reasonably assume that harmonization factor is acceptable. Indeed, it could be interesting to repeat this analysis at all sites in RI-URBANS. To perform this experiment, we would need simultaneous MAAP and AETH data. In addition, we will need Nephelometer data.

In this sense, the MAC is a distinguishing feature of BC. Mass absorption cross-section (MAC) coefficients are required to transform optical absorption observations to eBC mass (Magee Scientific, 2016). The instrument manufacturers use fixed MAC values to calculate BC mass, but any given MAC value will change depending on the PM source (Zotter *et al.*, 2017). Considering that MAC values can vary from site to site depending on the aerosol mixing state, size, and morphology (Bond and Bergstrom, 2006), using a fixed MAC value without considering its spatial-temporal variability to calculate eBC can lead to misleading the estimation of eBC results.

For this reason, we aimed to define MAC values for RI-URBANS urban sites where EC concentration data are available. BC measurement method is associated with biases and uncertainties. To reduce the uncertainties related to eBC estimation from a filter-based photometer, we started collecting RI-URBANS *elemental carbon (EC) concentration* data to calculate an average mass absorption cross-section (MAC) to convert absorption to eBC using collocated elemental carbon (EC) observations. For this, we collected the following information/data:

- Size cut-off used for the eBC data already provided (PM1, PM2.5, PM10...).
- EC concentration data measured (if possible) with the same size cut-off as for eBC data. However, different cut-off inlets for EC and eBC were acceptable.
- EC and eBC data should be co-located as much as possible (i.e., collected in the same measuring station, if possible).
- The longer the period with EC/eBC measurements available. However, if EC data covered a short period (e.g., few weeks/months campaign), this was also acceptable.

To harmonize eBC measurements, we used EC observations as available in 13 sites to determine the optimum value of MAC to reveal how much the choice of the MAC affects the eBC concentrations. Usually, nominal MAC values are used, calculated from the parameters furnished by the Aethalometer/MAAP manufacturer. For MAAP, nominal MAC is $6.6 \text{ m}^2\text{g}^{-1}$ which is low considering the estimated average value in regional background sites in Europe, which is 10 (Zanatta *et al.*, 2016). Moreover, MAC is time-dependent and changes with the chemical composition of

particles (Zanatta *et al.*, 2016; Ciupek *et al.*, 2021; Srivastava *et al.*, 2022). The approach proposed in other studies is the rolling MAC, which is probably the best way to harmonize eBC measurements (K Grange *et al.*, 2020).

To investigate this assumption if applying Rolling correction using EC data is the best way to harmonize eBC data in RI-URBANS, this method applied to compiled RI-URBANS BC datasets. This step has been done once we obtained EC data from several sites. Therefore, we will have the possibility to show the difference between raw eBC and EC-normalized eBC at all available urban sites in RI-URBANS. This will also allow providing an average “urban” MAC. In this case, we can provide possible explanations of the observed trend in MAC values over time with the Theil–Sen slope estimator. The MAC values for absorption at the 880nm and 637nm wavelength were calculated for the trend analysis reported here. The two BC from MAAP and AE33 are comparable. In addition, rolling mean logic was implemented with the zoo R package (Zeileis and Grothendieck, 2005) between absorption and the mass of EC. The time window was 14 days with the right alignment to show the variability, which is also applied in previous studies (K Grange *et al.*, 2020).

Using RI-URBANS absorption and EC data, a median experimental MAC of $10.57 \pm 4.05 \text{ m}^2\text{g}^{-1}$ (MAC=Absorption/EC) is calculated for MAAP and AETH. Since we considered the absorption coefficients measured by the MAAP (637nm) as a basis for calculating the experimental MAC, as shown in Figure. 3.4. A median MAC of 10.57 for urban sites is very close to the median value recently suggested in ACTRIS ($10 \text{ m}^2\text{g}^{-1}$) using data from RB stations operating MAAP and Aethalometer. However, using a constant MAC is not always good. We already observed that the mass absorption cross-section of RI-URBANS is far from being constant.

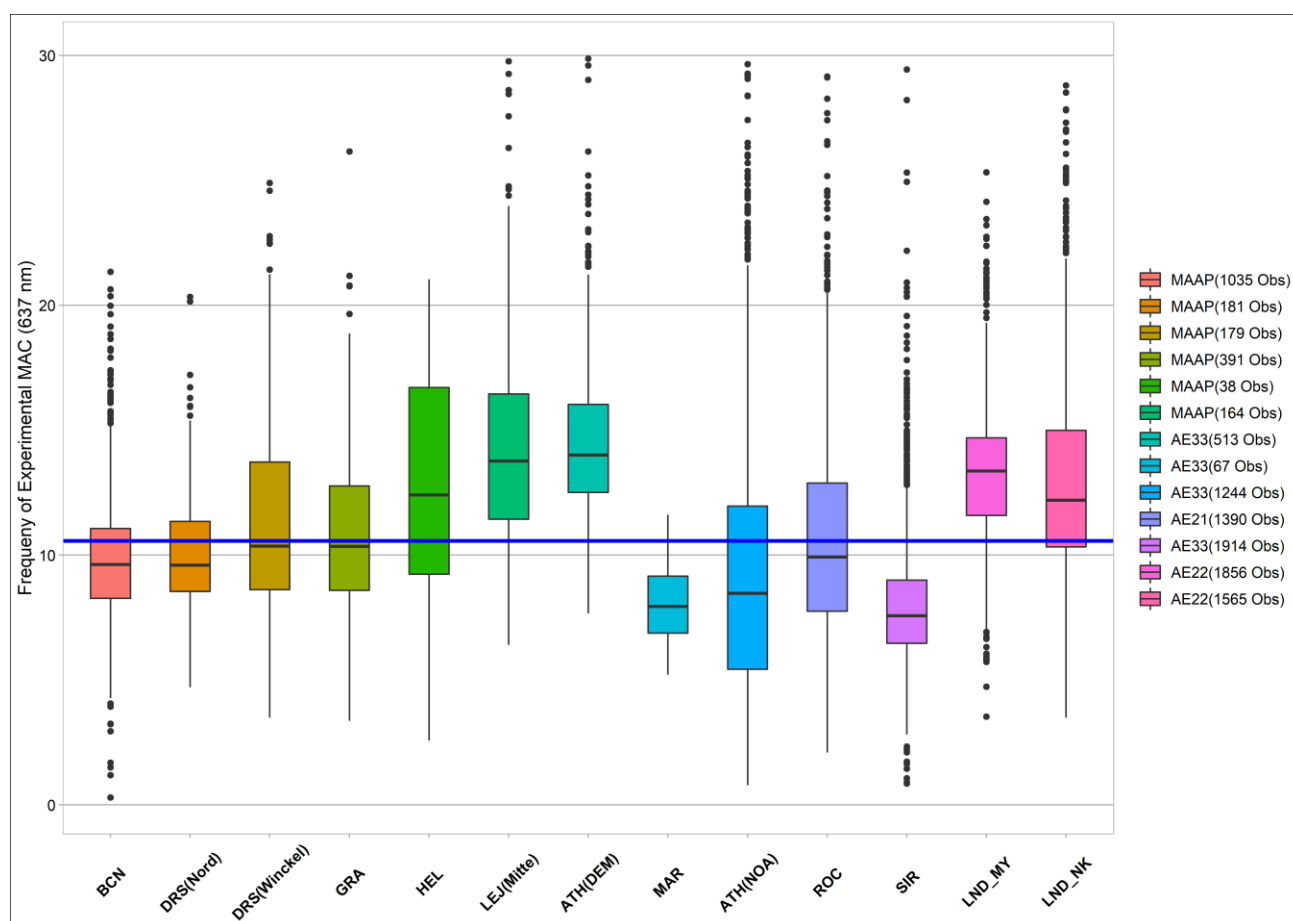


Figure 3.4. Average MAC from RI-URBANS cities

A big difference has been observed using the median value between the raw eBC considering the constant MAC and experimental MAC. In this case, it is essential to provide a different MAC value for all these sites in RI-URBANS. The MAC changes from one measurement site to another and consequently has a strong seasonal cycle (see Figure. 3.5). Therefore, looking at this long-term data, MAC represents a considerable variation. The frequency distribution of MAC depends on the sources, which can change in summer and winter. In addition, it depends on the material available for coating, which can be higher in summer because of changes in chemical and physical properties of eBC. Empirically derived MAC values also depend on the limitations of the measurement techniques used to determine b_{abs} (Zotter *et al.*, 2017). Experimental data can change with time, and MAC can also have a seasonal cycle as a function of changes in SOA/EC or SO₂ ratio. However, MAC values are not only site or seasonally dependent, they might also change over longer periods.

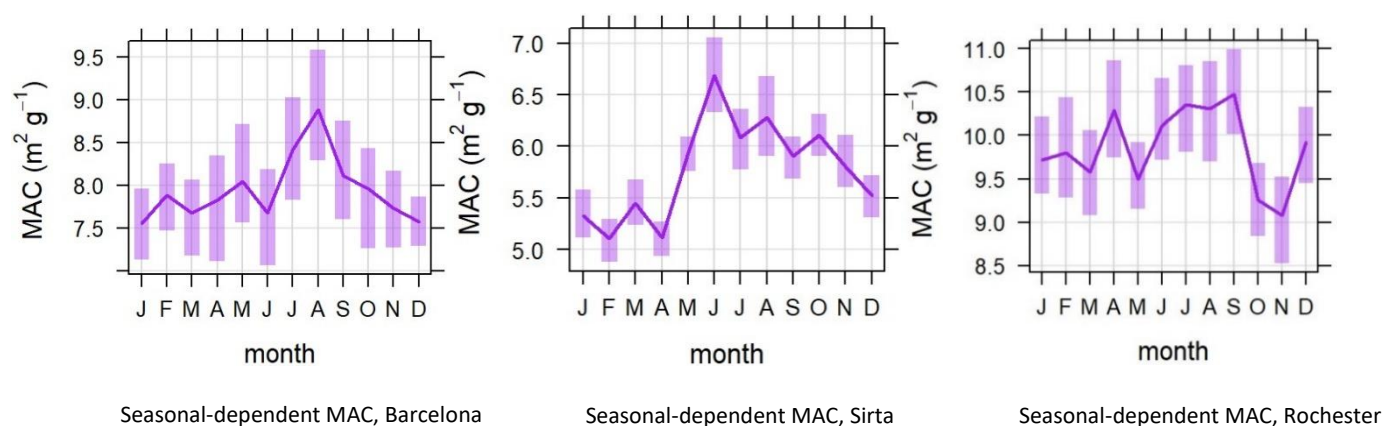


Figure 3.5. MAC seasonal cycle

On the other hand, changes in sources of BC and meteorological conditions, and relative humidity can considerably affect the MAC's trend. The difference in MAC is not constant during all the months. Therefore, it is essential to use varying site-specific (Local) MAC values that change with emission sources, mixing states, and meteorological conditions, including wind and humidity. Local MAC was calculated for 13 sites due to the availability of EC data (see Figure. 3.6). Thus, using a constant MAC value for different months can cause misleading the results (see Figure. 3.7). The trend of MAC is important; when MAC has no trend, the trend of eBC with all types of measurement is consistent. However, if eBC is calculated using a rolling MAC from experimentally calculated MAC values, then the eBC has no trend. This is because the MAC decreased with time.

Finally, the median value proposed by ACTRIS is 10 m²g⁻¹; the median value proposed by RI-URBANS is 10.57 m²g⁻¹. It is essential to note that we cannot use the constant value of 6.6. This work also highlights that the use of site-specific MAC leads to a great improvement in the equivalence of carbon mass quantified from thermal and optical methods and the necessity of using a site-specific, temporally, and spectrally varying MAC. The results of this experiments agree with previous studies that have investigated the implications of site-specific MAC to eBC observations (K Grange *et al.*, 2020; Ciupek *et al.*, 2021; Srivastava *et al.*, 2022).

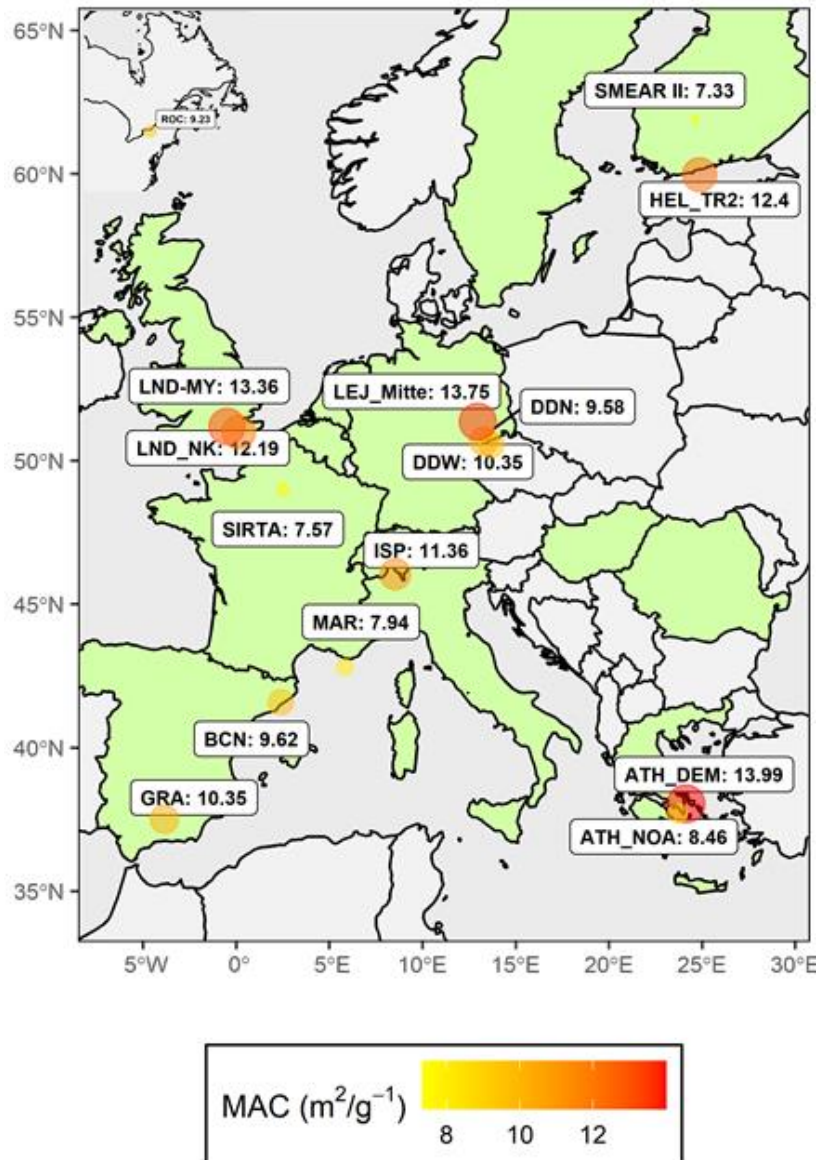


Figure 3.6. Median Local MAC for RI-URBANS cities

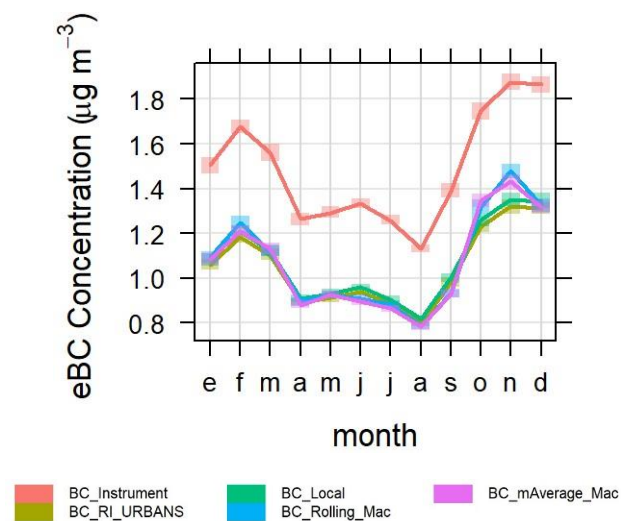


Figure 3.7 Impact of MAC on eBC estimates

This guideline proposes the eBC calibration through EC measurements (MAC determination) in RI-URBANS (site-dependent MAC, etc.). This lends credibility to the fact that the use of site-specific MAC leads to an improvement in the estimates of eBC. The importance of determining site-specific MAC values is highlighted to improve the comparability of eBC results obtained from different instruments. It should be noted that a substantial portion of MAC variability can also be attributed to experimental uncertainties, i.e., systematic biases of the methods applied to determine the MAC (Zanatta *et al.*, 2016). The observed MAC values have distinct seasonal patterns at individual sites and almost all locations. Thus, we believe that a site-dependent MAC should be calculated and used to estimate eBC concentrations properly. We propose continuous parallel measurements of eBC and EC to determine the correct eBC observations as GRIMM and gravimetry.

Further steps are correcting all eBC data properly and applying source apportionment methods to improve eBC results from those obtained using the manufacturer's fixed MAC value. We are performing a sensitivity study for MAC to explore the reason for trends in some locations. We will also study Delta C and Brown Carbon. Finally, Sandradewi should be applied to corrected eBC with RI-URBANS MAC. The MAC values provided here can be further examined for long-term variations over the sites and can be considered for future reporting of eBC measurements. However, EC observations are required for the calculation of MACs. Therefore, the expansion of monitoring networks to include regular EC samples is recommended for better exploitation of aethalometer and MAAP absorption data.

3.3 Annex / Files Datasets

The eBC and EC (if available) datasets are fully available at RI-URBANS intranet ([eBC_EC Final Data](#)). The data is presented in an excel file for each site, organized in three excel sheets:

Sheet 1: metadata

Sheet 2: Absorption 7 wavelengths; BC nominal MAC; BC Average MAC; BCff/BCwb % SD

Sheet 3: 24h EC / Experimental MAC

3.4 References

- Bond, T. C. *et al.* (2013) 'Bounding the role of black carbon in the climate system: A scientific assessment', *Journal of Geophysical Research Atmospheres*, 118(11), pp. 5380–5552. doi: 10.1002/jgrd.50171.
- Bond, T. C. and Bergstrom, R. W. (2006) 'Light absorption by carbonaceous particles: An investigative review', *Aerosol Science and Technology*, 40(1), pp. 27–67. doi: 10.1080/02786820500421521.
- Carslaw, D. C. and Ropkins, K. (2012) 'Openair - An r package for air quality data analysis', *Environmental Modelling and Software*, 27–28, pp. 52–61. doi: 10.1016/j.envsoft.2011.09.008.
- Ciupek, K. *et al.* (2021) 'Challenges and policy implications of long-term changes in mass absorption cross-section derived from equivalent black carbon and elemental carbon measurements in London and south-east England in 2014-2019', *Environmental Science: Processes and Impacts*, 23(12), pp. 1949–1960. doi: 10.1039/d1em00200g.
- Drinovec, L. *et al.* (2015) 'The "dual-spot" Aethalometer: An improved measurement of aerosol black carbon with real-time loading compensation', *Atmospheric Measurement Techniques*, 8(5), pp. 1965–1979. doi: 10.5194/amt-8-1965-2015.
- Helin, A. *et al.* (2018) 'Characteristics and source apportionment of black carbon in the Helsinki metropolitan area, Finland', *Atmospheric Environment*, 190, pp. 87–98. doi: 10.1016/j.atmosenv.2018.07.022.

- <https://www.actris-ecac.eu/measurement-guidelines.html> (no date) *Recommendations, guidelines, standard operating procedures and scientific articles for aerosol in-situ measurements*. Available at: <https://www.actris-ecac.eu/measurement-guidelines.html> (Accessed: 31 August 2022).
- K Grange, S. *et al.* (2020) 'Evaluation of equivalent black carbon source apportionment using observations from Switzerland between 2008 and 2018', *Atmospheric Measurement Techniques*, 13(4), pp. 1867–1885. doi: 10.5194/amt-13-1867-2020.
- Kalbermatter, D. M. *et al.* (2022) 'Comparing black-carbon-and aerosol-absorption-measuring instruments-A new system using lab-generated soot coated with controlled amounts of secondary organic matter', *Atmospheric Measurement Techniques*, 15(2), pp. 561–572. doi: 10.5194/amt-15-561-2022.
- Müller, T. *et al.* (2011) 'Characterization and intercomparison of aerosol absorption photometers: Result of two intercomparison workshops', *Atmospheric Measurement Techniques*, 4(2), pp. 245–268. doi: 10.5194/amt-4-245-2011.
- Petzold, A. *et al.* (2013) 'Recommendations for reporting black carbon measurements', *Atmospheric Chemistry and Physics*, 13(16), pp. 8365–8379. doi: 10.5194/acp-13-8365-2013.
- Sandradewi, J. *et al.* (2008) 'Using aerosol light absorption measurements for the quantitative determination of wood burning and traffic emission contribution to particulate matter', *Environmental Science and Technology*, 42(9), pp. 3316–3323. doi: 10.1021/es702253m.
- Srivastava, P. *et al.* (2022) 'Implications of Site-specific Mass Absorption Cross-section (MAC) to Black Carbon Observations at a High-altitude Site in the Central Himalaya', *Asia-Pacific Journal of Atmospheric Sciences*, 58(1), pp. 83–96. doi: 10.1007/s13143-021-00241-6.
- Tuch, T. and Wiedensohler, A. (2018a) 'ACTRIS In Situ Aerosol: Guidelines for Manual QC of AE33 absorption photometer data'.
- Tuch, T. and Wiedensohler, A. (2018b) 'ACTRIS In Situ Aerosol: Guidelines for Manual QC of MAAP (Multiangle Absorption Photometer) data'.
- Yus-Díez, J. *et al.* (2021) 'Determination of the multiple-scattering correction factor and its cross-sensitivity to scattering and wavelength dependence for different AE33 Aethalometer filter tapes: A multi-instrumental approach', *Atmospheric Measurement Techniques Discussions*, 29, pp. 1–30. doi: 10.5194/amt-2021-46.
- Zanatta, M. *et al.* (2016) 'A European aerosol phenomenology-5: Climatology of black carbon optical properties at 9 regional background sites across Europe', *Atmospheric Environment*, 145, pp. 346–364. doi: 10.1016/j.atmosenv.2016.09.035.
- Zeileis, A. and Grothendieck, G. (2005) 'Zoo: S3 infrastructure for regular and irregular time series', *Journal of Statistical Software*, 14. doi: 10.18637/jss.v014.i06.
- Zotter, P. *et al.* (2017) 'Evaluation of the absorption Ångström exponents for traffic and wood burning in the Aethalometer-based source apportionment using radiocarbon measurements of ambient aerosol', *Atmospheric Chemistry and Physics*, 17(6), pp. 4229–4249. doi: 10.5194/acp-17-4229-2017.

4 Offline PM chemical composition

The term particulate matter (PM) refers to a complex mixture of solid and liquid particles suspended in air. The size, chemical composition, and other physical properties of PM vary with location and time. This variability derives from differences in emission sources that can be of natural origin such as the oceans and deserts or anthropogenic activities including industries and combustion processes. Regarding the formation mechanisms, PM can be directly emitted into the atmosphere (primary particles) or be generated by chemical reactions (secondary particles). These chemical reactions consist of the interactions between precursor gases in the atmosphere to form a new particle by condensation, or between a gas and an atmospheric particle to form a new aerosol by adsorption or coagulation. Major components of PM include crustal elements (metal oxides), organic compounds, elemental carbon, sulphates, nitrates, and ammonium.

Although PM shows significant spatial variation, epidemiological studies in diverse locations have reported statistically significant associations between increases in daily mortality and morbidity with increases in the mass concentrations of PM₁₀ and PM_{2.5} (WHO, 2013). Because the composition of PM is very complex, there has long been a question as to whether some components of the PM mixture are of greater public health concern than others. Obtaining this information would help focus efforts to reduce human exposure by enabling the control of those sources that contribute most to the toxic components of the PM mixture. Thus, some studies such as the WHO REVIHAAP project (WHO, 2013), summarised by Cassee et al. 2013, suggested that metrics related to PM chemical composition could be of higher interest than PM mass concentrations for evaluating health effects. It is, therefore, of great interest to know the impact on health of the different PM components.

To apportion PM sources and to implement efficient abatement measures it is necessary to perform a comprehensive characterisation of PM. To this end, a variety of analytical methods should be deployed to determine PM complete chemical composition followed by the application of receptor models such as Positive Matrix Factorization (PMF).

EU Air Quality Directive 2008/50/EC obliges member states to report on annual values of Pb, As, Cd, and Ni. Other components of PM (i.e EC and OC) are routinely monitored at some monitoring networks (ACTRIS). However, these datasets cannot be used for source apportionment purposes as being incomplete. There is a number of research studies carried out in the framework of different scientific and air quality programs that determine several PM components that can be further exploit for source apportionment. These studies are mostly developed at sites of interest (polluted areas) during relatively short periods (≤ 1 yr) and produce datasets with different PM components.

This section provides information on the offline PM chemical measurements previously conducted in order to establish a beneficial guideline, to produce an accurate offline PM chemical measurement, a good interpretation and treatment of the data and a correct analysis of the different source apportionment contributions. The file or web link where all the dataset information is stored is as follows: https://riurbans-my.sharepoint.com/personal/csic_riurbans_onmicrosoft_com/_layouts/15/onedrive.aspx?ga=1&id=%2Fpersonal%2Fcsic%5Friurbans%5Fonmicrosoft%5Fcom%2FDocuments%2FCSIC%20Scientific%20Data%2FChemistry

4.1 Datasets

In this study, we have considered only data sets from traffic, urban, peri-urban and sub-urban sites with a minimum of one-year data coverage (at least 90 24h samples) in the period 2013-2020, where a number of variables were analysed including at least: OC, EC, metals, ions, and when available specific organic tracers. Although the representation of the different offline chemistry PM stations selected over the surface of Europe is considered acceptable, the process of obtaining offline chemistry data was difficult due to the complexity of the selection criteria. Most of these stations must cover long data periods from 2013 to 2021, must also be located close to urban areas and should also cover different seasons. This kind of requirements have significantly reduced the selected offline PM chemical composition datasets.

Table 4.1 shows the selection of the forty stations available from different European countries, sixteen from France, one from Greece, six from Italy, three from Portugal, nine from Spain and five from Switzerland. Data coverage, and variables measured are presented in Table 4.2. The type of station is well distributed around the countries, as is illustrated in Figure 4.1, and as is explained following:

- One Peri Urban Background (PUB) station was selected from the Nord of France.
- One Peri Urban Background Valley (PUBV) station was selected from the French Alps.
- Two SubUrban Background (SUB) stations were selected, one located in North-Central Italy, and the other in the south of Europe, Greece.
- Eight Traffic (TR) stations were selected covering West-Central-Nord Europe, one was in Switzerland, another in Spain, two were in Portugal and four in France.
- Twenty-two Urban Background (UB) stations were selected covering a large surface in Europe, where one of them was located in Portugal, four in Switzerland, five in Italy, five in Spain and seven in France.
- Five Urban Industrial (UI) stations were selected, two located in the Nord and South of France and three located in the East, Nord-West and South of Spain.
- One Urban Valley (UV) station, located in the west of France, in the Alps zone.

Most data from France has been already published in a number of papers such as Borlaza et al., 2021 or Weber et al., 2019 and 2021, among others. Data from Switzerland has been published by Grange et al., 2021. Data from Greece, Portugal, Italy and Barcelona obtained during AIRUSE project was published by Amato et al., 2016. Recent data from Barcelona has been published in 't Veld et al., 2022.

Table 4.1. List of air quality sites supplying Offline PM Chemistry datasets. PM size, City, station, type of station, coordinates, and data provider.

City (Country)	PM size	Station	ABR	Type	Coordinates (Alt. m asl)	Data provider
Chamonix (FR)	PM10	Chamonix	CHAM_UV	UV	45.923; 6.87 (1038)	IGE
Dunkerke-Gran Synthe (FR)	PM10	Grande Synthe	DKI_UI	UI	51.025; 2.303 (10)	IGE
Grenoble (FR)	PM10	GRE-cb	GRE-cb_UB	UB	45.183; 5.725 (212)	IGE
Grenoble (FR)	PM10	Frenes	GRE-fr_UB	UB	45.162; 5.736 (214)	IGE
Grenoble-VIF (FR)	PM10	VIF	VIF_UB	UB	45.058; 5.677 (310)	IGE
Lens (FR)	PM10	Lens	LEN_UB	UB	50.437; 2.827 (47)	IGE
Marnaz (FR)	PM10	Marnaz	MNZ_PUBV	PUBV	46.058; 6.533 (504)	IGE
Marseille (FR)	PM10/PM1	Marseille-5av	MAR_UB	UB	43.306; 5.396 (64)	IGE
Aix-en-Provence (FR)	PM10	Aix-en-provence	AIX_UB	UB	43.53; 5.441 (188)	IGE
Port de Bouc (FR)	PM10	PdB	PdB_UI	UI	43.402; 4.982 (1)	IGE
Nice (FR)	PM10	Nice	NIC_TR	TR	43.702; 7.286 (1)	IGE
Nogent sur Oise (FR)	PM10	Nogent	NGT_PUB	PUB	49.276; 2.482 (28)	IGE
Poitiers (FR)	PM10	Poitiers	POI_UB	UB	46.584; 0.346 (106)	IGE
Roubaix (FR)	PM10	Roubaix	RBX_TR	TR	50.707; 3.181 (10)	IGE
Rouen (FR)	PM10	Rouen	ROU_TR	TR	49.441; 1.083 (6)	IGE
Strasbourg (FR)	PM10	Strasbourg	STG_TR	TR	48.59; 7.745 (139)	IGE
Athens (GR)	PM10/PM2.5	Demokritos	ATH_SUB	SUB	37.99; 23.82 (270)	AIRUSE
Florence (IT)	PM10/PM2.5	Florence AIRUSE	FLO_UB	UB	43.786; 11.287 (50)	AIRUSE/INFN
Florence (IT)	PM10	Calenzano	CAL_UB	UB	43.852; 11.176 (50)	INFN
Florence (IT)	PM10	Montale	MON_SUB	SUB	43.915; 11.006 (50)	INFN
Florence (IT)	PM10	Capannori (Lucca)	CA_UB	UB	43.84; 10.573 (20)	INFN
Milano (IT)	10;2.5	Pascal	MIL_UB	UB	45.479; 9.235 (120)	ARPA/AIRUSE
Milano (IT)	PM10	Senato	MILSEN_TR	UB	45.470; 9.197 (121)	ARPA
Milano (IT)	PM10/PM2.5	Shivinoglia	MILSHI_TR	UB	45.017; 11.076 (11)	ARPA
Turin (IT)	PM10	Turin	TUR_UB	UB	45.074; 7.676	IGE
Coimbra (PT)	PM10	Coimbra	COIM_UB	UB	40.207; -8.425 (140)	U. Aveiro
Coimbra (PT)	PM10	Coimbra	COIM_TR	TR	40.207; -8.437 (17)	U. Aveiro
Porto (PT)	PM10/PM2.5	Porto	PORT_TR	TR	41.20; -8.55 (140)	U. Aveiro
Bailen (ES)	PM10	Bailén	BAI_UI	UI	38.093; -3.784 (368)	IDAIA / UHU
Barcelona (ES)	PM10/PM2.5	Barcelona	BCN_UB	UB	41.387; 2.115 (80)	IDAIA
Gijon/Aviles (ES)	PM10	Gijón	GIJ_UI	UI	43.547; -5.704 (704)	IDAIA
Granada (ES)	PM10	Granada	GRA_UB	UB	37.164; -3.605 (680)	UGR
Madrid E. Vallecas (ES)	PM10	Madrid	MAD-EV_UB	UB	40.373; -3.612 (629)	IDAIA
Madrid Esc. Aguirre (ES)	PM10	Madrid	MAD-EA_TR	TR	40.422; -3.682 (672)	IDAIA
Manlleu (ES)	PM10/PM2.5	Manlleu	MAN_UB	UB	42.003; 2.287 (460)	IDAIA
Villanueva Arz. V (ES)	PM10;PM2.5	Villanueva	VIL_UB	UB	38.174; -3.005 (692)	IDAIA/CIEMAT
Basel (CH)	PM10/PM2.5	Basel	BAS_UB	UB	47.541; 7.583 (316)	EMPA
Bern (CH)	PM10/PM2.5	Bern	BER_TR	TR	46.951; 7.441 (536)	EMPA
Magadino (CH)	PM10/PM2.5	Magadino	MAG_UB	UB	46.16; 8.934 (203)	EMPA
Payerne (CH)	PM10/PM2.5	Payerne	PAY_UB	UB	46.813; 6.944 (489)	EMPA
Zurich (CH)	PM10/PM2.5	Zurich	ZUR_UB	UB	47.378; 8.53 (409)	EMPA

UV, Urban Valley; UI, Urban Industrial; UB, Urban Background; PUBV, Peri Urban Background Valley; PUB, Peri Urban Background; TR, Traffic; SUB, Suburban Background.

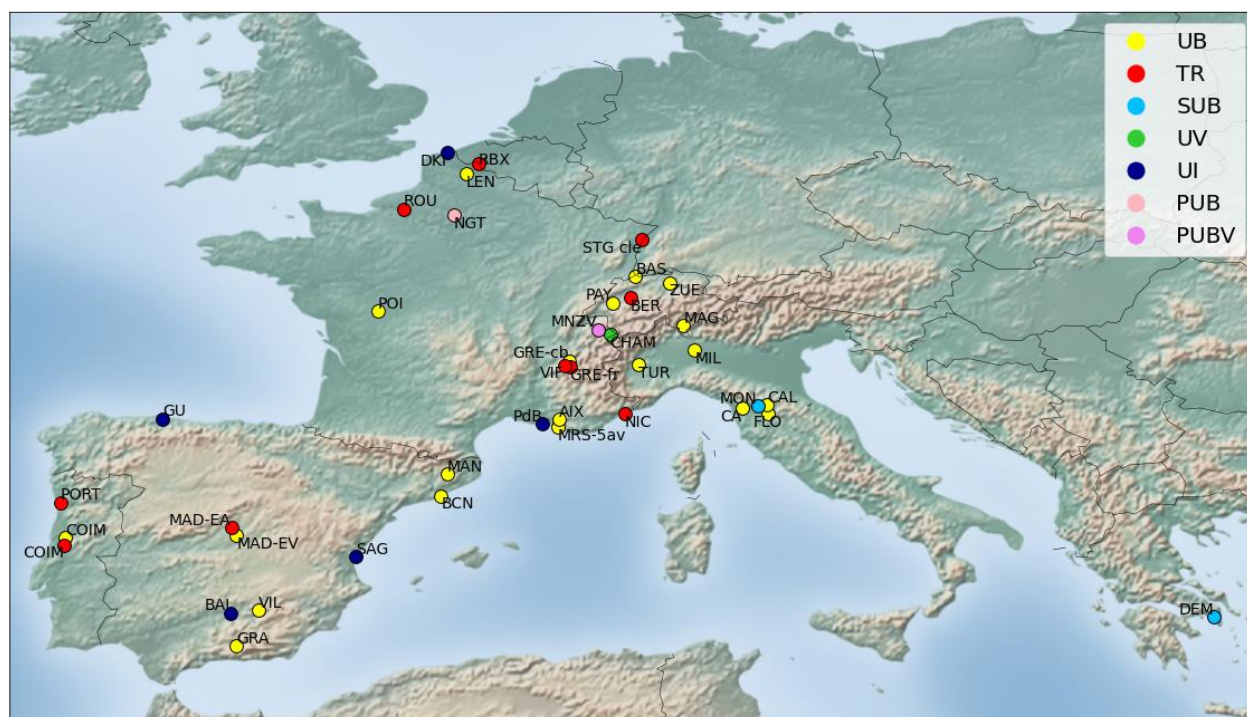


Figure 4.1. Map with sites and type of station. UV, Urban Valley; UI, Urban Industrial; UB, Urban Background; PUBV, Peri Urban Background Valley; PUB, Peri Urban Background; TR, Traffic; SUB, Suburban Background.

4.1.1 Data treatment

Mass concentration data of PM components were averaged by monthly and by annual periods, covering the period 2013-2021. PM components determined have been grouped into: organic matter (OM) derived from OC, elemental carbon (EC), secondary inorganic aerosols (SIA) including SO_4^{2-} , NO_3^- and NH_4^+ , mineral dust and sea-salt, as is shown in Table 4.2.

The methodology for estimating the sea-salt and mineral dust fraction is the one proposed by Alastuey et al., 2016. Some elements such as Na, Mg, Ca and K are associated with both mineral dust and sea-salt aerosol. The sea-salt contribution was estimated for each element before estimating the mineral load. The concentrations of these elements in seawater are well known and therefore it is possible to estimate the marine contribution to PM mass once we know the concentration of one of these elements. Due to the potential volatilization of Cl by the interaction between NaCl with acidic species, the sea salt fraction of each specie was estimated concerning the concentration of marine Na. Thus, given that Na can be partially related to mineral dust, first, we calculated the mineral fraction of Na from the content of Al by using the ratio determined by Moreno et al. (2006) for soils and dust in North Africa. Thus, the mineral sodium (non-sea-salt sodium, Na_{dust}) was obtained by multiplying Al concentration by 0.12, and the sea-salt fraction of Na (Na_{ss}) can be estimated by subtracting Na_{dust} from the total Na.

The sea-salt fraction of calcium, magnesium, potassium and sulphate was estimated by using their seawater ratios concerning Na_{ss} (Nozaki, 1997). Finally, the total sea-salt load was determined by the sum of Cl^- , Na_{ss} , Ca_{ss} , Mg_{ss} , K_{ss} and SO_4^{2-} . The non-sea-salt (nss) fractions of Ca, Mg, Mn, Na, K and SO_4^{2-} were obtained by subtracting the previously calculated sea-salt fraction from their bulk concentration. In addition to the sea salt fraction, K can be related to mineral (K_{dust}) and biomass burning (K_{bb}). The mineral fraction is estimated from Al ($\text{K}_{\text{dust}} = 0.31 * \text{Al}$, Moreno et al., 2006), and the biomass fraction by the difference: $\text{K}_{\text{bb}} = \text{K} - \text{K}_{\text{ss}} - \text{K}_{\text{dust}}$.

Finally, the total mineral dust concentration was determined by addition of the concentrations of all mineral related elements expressed as oxides, such as Al_2O_3 , SiO_2 , Fe_2O_3 , TiO_2 , P_2O_5 , CaO_{dust} , MgO_{dust} , $\text{Na}_2\text{O}_{\text{dust}}$, and $\text{K}_2\text{O}_{\text{dust}}$. Assuming the major presence of CaO_{dust} as CaCO_3 , the CO was estimated from CaO_{dust} by multiplying by 1.274.

This methodology can be only applied when the bulk concentrations of major elements (Al, Si, Ca, Mg, Fe, Na, K) is determined. In the case of most France stations, it was only determined the soluble fraction of Mg, Na, Ca, and K, therefore an underestimation of the crustal load is expected.

Elemental concentration in most samples was determined from acidic digestion by ICP methods or from water leachate by ICP and/or IC. In these cases, Si was not determined and we estimated it from Al content by multiplying Al content by 3 (Alastuey et al., 2016). Only in the samples from Italy and those analysed in the framework of the AIRUSE project, the metal concentration was obtained by PIXE analysis of Teflon filters; this method allows for determining concentrations.

Organic matter (OM) or organic aerosol (OA) has been estimated from organic carbon (OC), applying a factor that can vary according to location and emission sources (Turpin and Huntzicker, 1995). This factor varies from 1.2 in areas very close to emission sources, such as traffic, to 1.7-1.8 in urban areas (Minguillón et al., 2011). In this work, the factor of 1.8 has been applied.

All this methodology was applied in the around ten thousand samples compiled for the offline PM chemistry. All stations were sampled PM10, as well PM2.5 were analysed in twelve stations and PM1 in two stations. The most common device used was the High Volume Sampler, collected in the quartz fibre filters.

Figure 4.2 shows these average measurements of all stations that compiled data during different periods in 2013-2021 in sites from Spain, Italy, France. It is observed a variability of the PM composition depending on location, type of environment and PM fraction sampled. It should be highlighted the higher contribution of dust at Spanish's sites, mainly due to the higher contribution of soil particles.

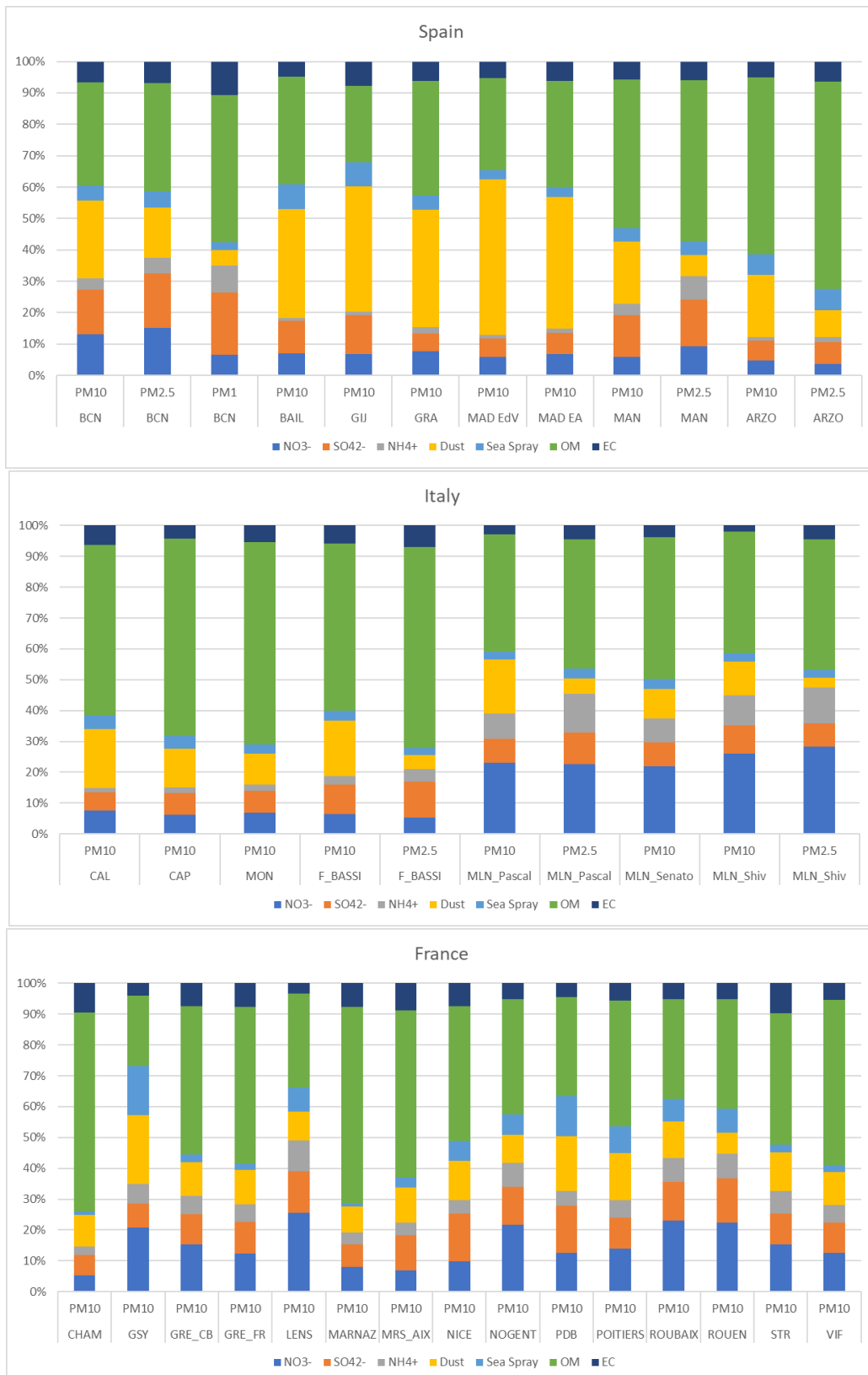


Figure 4.2. Average contribution of NO₃⁻, SO₄²⁻, NH₄⁺, dust, sea spray, organic matter (OM) and elemental carbon (EC) calculated for sites in Spain, Italy and France.

4.2 Guidelines

There are not specific guidelines for a complete chemical characterisation of atmospheric particulate matter. EU Air Quality Directive 2008/50/EC sets limit values for mass concentration of PM₁₀ and PM_{2.5} and PB and objective values for annual concentrations of As, Cd, and Ni. Within the context of the EU Air Quality Directive 2008/50/EC, the European Committee for Standardization (CEN) released procedures for the determination of PM₁₀ and PM_{2.5} (EN12341:2014), OC and EC in PM_{2.5} (EN 16909:2017), of inorganic ions in PM_{2.5} (EN 14902:2005), and of specific metals in PM₁₀ (EN 14902:2005).

ACTRIS provides recommendations for the determination of OCEC in PM_{2.5} and the analysis of metals in PM. However, does not provide any guideline for the analysis of water-soluble ions in PM. The Chemical Co-ordination Centre of EMEP (CCC) produced the “EMEP manual for sampling and chemical analysis (EMEP/CCC-Report 1/95 Revision 1/2001; <https://projects.nilu.no/ccc/manual>) describing the standard recommended methods for sampling and chemical analysis for the EMEP measurement network, including the analysis of chemical components of PM, but focusing on regional background environments.

Following we summarized the existing recommendations for sampling and analysis of specific PM components.

4.2.1 Sampling

Offline determination is based on the collection of a fraction of atmospheric PM on a substrate (usually filters) and the posterior analysis. Frequently, prior to the chemical analyses, the sampled filter is used for the gravimetric determination of the mass concentration of the PM size fraction collected.

The offline analysis of the chemical components of PM is based on the analyses of atmospheric particles collected on specific substrates (mainly filters) by using a pump at a fixed flow during a period of time (usually 24 hours). Samplers are usually equipped with a sampling head, that permits to separate the PM size fraction of interest (i.e. PM₁₀ or PM_{2.5}).

The European Standard EN 12341:2014 for the gravimetric determination of PM₁₀ or PM_{2.5} mass concentrations specifies a 24 h sampling period by using high (i.e. 30 m³ h⁻¹) or low volume samplers (1 – 2.3 m³ h⁻¹ m³). The use of high-volume samplers permits the collection of sufficient PM mass for determining most of PM components from a single filter sample. When low volume samplers are used the collected PM mass might not be sufficient to perform a complete chemical characterisation. In this case, it is usually needed to conduct simultaneous sampling using 2 or more low volume samplers equipped with different kind of filters depending on subsequent chemical analysis.

Selection of the sampling substrate, i.e. filters, is key for the measurements of the different PM components (

Table 4.2). Quartz fibre filters can be used with both high and low volume samplers. These filters are typically used for OC, EC and organic compounds analysis. Can also be used for the determination of ions and elements if blank levels are low in IC and ICP analysis methods. However, these filters are not appropriate for elemental analysis using XRF or PIXE. When quartz fibre filters and high-volume samplers are used, sampled filters are divided in fractions destined to different chemical analysis.

Table 4.2. Comparison of filter types. (Modified from Bergmans et al., 2022)

Filter type	Captor	Hygrosc	Weighing		Chemical characterization			
			El charge	Mass	Elements	OC/EC	Organics	Ions
Glass fiber	HV, LV, VLV	(Low)	Low	High	N	(Y)	Y	Y
Quartz	HV, LV, VLV	Low	Low	High	Y*	Y	Y	Y

Teflon, PTFE	LV, VLV	Low	Low	Variable	Y	N	Y	Y
Polycarbonate	VLV	Low	(High)	Low	Y	N	N	Y
Cellulose esters	LV, VLV	High	(High)	(Low)	Y	N	N	N
PVC	LV, VLV	Low	High	Low	Y	N	N	Y
Nylon	LV, VLV	Low	(High)	Low	Artifacts	N	N	HNO ₃

High (HV), Low (LV), Very-low (VLV) volume samplers; Brackets ¼ Estimate.

*Quartz fibre filters can be used for determination of elements by ICP after bulk dissolution of samples. Not useful for XRF / PIXE analysis.

The other filters are not suitable for High volume sampling and for OC/EC analysis. Teflon filters, used with low-volume samplers are usually employed for subsequent analysis of major and trace elements, and ions. Nylon filters are also recommended for analysis of ions, given the low negative artefact for NO₃⁻. Nevertheless, the nylon filters are usually avoided in many PM field studies, and the ions concentrations are determined in leachates of the Teflon filter after the non-destructive XRF analysis.

4.2.2 Analysis of organic carbon (OC) and elemental carbon (EC)

Concentration of organic carbon (OC) and elemental carbon (EC) in atmospheric particles, collected in quartz fibre filters, are typically measured by using thermal- optical offline analysis of filter samples with transmittance correction (TOT). The most employed thermal protocols for the analysis of OC and EC in PM are the IMPROVE, NIOSH-like protocols, and the EUSAAR2 protocol that reduces the possible positive bias in EC determination due to the incomplete evolution of OC (Cavalli et al., 2010).

The Working Group WG 35 of the European Committee for Standardization (CEN) elaborated a new standard (EN 16909:2017) for the measurement of airborne EC and OC in PM_{2.5} (Karanasiou et al., 2015; Brown et al., 2017). The EUSAAR2 thermal protocol (Cavalli et al., 2010) was adopted as the reference methodology for the determination of EC and OC in ambient PM_{2.5} (EN16909: 2017). The WG35 is currently evaluating the possibility to extend this standard to the determination of EC and OC in ambient PM₁₀ and to automated, (semi) real-time methods used to measure OC and EC such as the Sunset Semi-Continuous OCEC analyzer.

The recommendation for ACTRIS is to follow the CEN standard - EN 16909:2017. ACTRIS guidelines highlighted the following points of EN16909 that are particularly important (<https://www.actris-ecac.eu/actris-gaw-recommendation-documents.html>):

- For off-line analyses: at least one field blank shall be collected every 14 samples.
- Samples should be stored at temperature below 5°C, if not analysed within 28 days from sampling.
- Instruments shall be regularly calibrated or TC (multi-point calibration) at least once every 12 months and after any major maintenance/modifications.
- The calibration should be checked at least every measurement day, e.g. by the analysis of a sucrose spiked filter. Better use a certified sucrose solution for this.
- To verify the instrument long term stability, at least one punch of a large control filter shall be analysed on each measurement day or for each sample batch. Control filters can be obtained from ECAC on request.
- Temperature probe calibration shall be checked at least every 12 months and after any major maintenance/modification.
- Laser signal noise and drift shall be checked during instrument blank analysis on each measurement day or for each sample batch.

On top of EN 16909, ACTRIS recommendations include:

- Field blanks shall be sampled for ca. 30 to 60 s (which is not specified in the EN16909 standard).
- The response of the instrument in the helium and in the helium/oxygen modes shall be checked on each measurement day (or sample batch) by injecting a fixed amount of calibration gas in the two analytical modes and should not differ by more than 5%.

- The laser correction coefficient shall be ≤ 1 but ≥ 0.9 .
- The transit time shall be regularly verified
- The available integration options (such as the initial laser signal value determination, baseline, laser and detector slope corrections) leading to optimal determinations of the peak areas and split point shall be selected. Be sure to record the applied options in your Meta data.

4.2.3 Analysis of ions

The secondary inorganic aerosols (SIA) account for a large fraction of PM. The determination of the concentration of the water-soluble inorganic ions (mainly SO_4^{2-} , NO_3^- and NH_4) in PM is performed by Ion chromatography (IC) analysis of a water leachate of a fraction of filter.

In order to assist EU Member States meeting the requirements of the 2008/50/EC Air Quality Directive, the European Commission issued Mandate M/503 for the development of “standards concerning automated measurements of particle matter in ambient air and the measurement of its chemical composition (OC and EC, inorganic components).” As a result, the European Committee for Standardization (CEN) published a Technical Report for the determination of inorganic ions (SO_4^{2-} , NO_3^- , NH_4 , Cl^- , Na^+ , K^+ , Mg^{2+} and Ca^{2+}) in PM_{2.5} samples (CEN/TR 16269: 2011). The method is based in the analysis of concentrations of ions in a water extraction of a fraction of the filter by IC coupled to a conductivity detector. The cations, except NH_4^+ , can also be analysed by ICP-AES. This procedure was initially devised for rural background sites, but can be also used in other type of environments.

ACTRIS does not provide any guideline for the analysis of water-soluble ions in PM. The EMEP/CCC-Report 2001 provide some recommendations for sampling and analysis of ions in atmospheric particulate matter, mainly focused in background stations.

4.2.4 Analysis of Organic Tracers

The organic component covers a very wide range of compounds of both primary and secondary origin. The characterization of those individual organic PM constituents at the molecular level in highly complex mixtures generally requires chromatographic separation. Classic instrumentation using LC and/or Gas chromatography (GC), with mass spectrometry (MS) or flame ionization detector (FID) detection are commonly used for determination of organic components of PM (see revision by Nozière et al., 2012). GC coupled to MS (GC-MS) has been applied to the identification and quantification of PAHs, phthalates, organophosphate flame retardants, brominated flame retardants, polychlorinated biphenyls (PCBs), chlorinated paraffins, pesticides, alkylphenols, parabens, key organic species as source tracers (e.g., levoglucosan, galactosan, mannosan, squalene, oleic acid, cholesterol, nicotine), and synthetic musk.

For the analysis of organic particulate constituents, no specific recommendations are provided by ACTRIS. For the next years, ACTRIS targets to develop appropriate standard operating procedures (SOPs) enabling an ideal analytical measuring strategy.

The EMEP/CCC-Report 2001 provide some recommendations for sampling and analysis of of persistent organic pollutants (pesticides and PCBs) and polycyclic aromatic hydrocarbons (PAHs) in atmospheric particulate matter, mainly focused in background stations.

4.2.5 Elemental analysis

The analysis of major and trace elements is of high interest for tracing emission sources. Trace elements usually occur at very low concentrations (in the order of ng m^{-3} or lower) requiring robust analytical techniques with low detection limit. The most frequently used techniques can be grouped into three main types: atomic spectrometric techniques, X-ray methods, and activation analysis (Duarte et al., 2021). In recent years, the use of instrumental

neutron activation analysis (INAA) has been considerably reduced, which is why it will not be considered in this section.

The most widely used atomic spectrometry-based techniques for PM chemical characterization are the inductively coupled plasma mass spectrometry (ICP-MS) and ICP - optical emission spectrometry (OES). Combination of ICP-MS and ICP-OES ensures very low detection and quantification limits (LODs and LOQs) in the order of ppb and ppt) and allows to quickly determine the concentration of a wide range of elements, with precision and accuracy. These methods require a complete previous dissolution of the sampled, which involves time-consuming and costly procedures. Generally, the samples are bulk acidic dissolved, with or without the assistance by microwaves. NIOSH and CEN standards recommend microwave acid digestion as a reference method for elemental analysis of atmospheric particulate matter, via ICP-MS or ICP-OES (EN 14902:2005) due to the amount of chemical reagents needed, the faster dissolution and the lower loss of volatile elements. Nevertheless, several methodologies have been proposed in the literature, using different heating programs, digestion time, and acid mixtures (Duarte et al. 2021 and references therein). The acid digestion always carries an associated uncertainty, being the percentage of recovery of the elements always different to 100%. The standard EN 14902:2005 specifies a recovery between 90 to 110% for Pb, Cd and 85 to 115% for As, Ni. The selection of the acid mixture is a key issue since it must perform the complete dissolution of the PM sample, keeping the elements stable in the final solution. Nitric acid (HNO₃) or conventional aqua regia (HNO₃ + HCl) are often used in routine analysis, often in combination with H₂O₂. However, this acidic mixture does not allow complete digestion of silicon-containing compounds for which a combined HF-HNO₃ digestion is necessary. The use of HF is therefore necessary for dissolving silicates, but it can be dangerous and can affect the equipment if it is not completely evaporated and, in addition, it leads to the loss of B and Si during the HF evaporation.

The use of X-ray based techniques increased since the early 2000s. X-ray-based methods such as particle-induced X-ray emission (PIXE) and energy dispersive X-ray fluorescence (EDXRF) are non-destructive techniques that involve minimal sample manipulation. Although PIXE has lower LODs than XRF, it requires more complex instrumentation, making it more expensive and difficult to use.

ACTRIS guidelines provide some recommendations for multielement analysis of PM filters mainly based on XRF/PIXE analysis (<https://www.actris-ecac.eu/pmc-elements.html>): Filters used should have low concentrations of elements of interest. Should be clean, with low contamination, and thin to reduce the background in PIXE spectra and the contribution of residual bulk contaminants. The sampling should produce as much homogeneous aerosol deposit as possible. After the sampling the filters should be stored in Petri slides, in order to avoid that the filter surface with the aerosol deposit on it could get in contact with materials that could results in loss of the aerosol deposit or in contamination. The use of small Ziplock plastic bags or wrapped aluminum foils should be avoided.

XRF techniques can only be applied when PM samples are collected in Teflon filters, which requires the use of low-volume samplers. This technique, unlike ICP-based methods, allows direct determination of Si. However, the detection limits of some tracers of interest to study the contribution of sources, such as As, Cd, Sb, Se, Sn, among others, can be considered high. On the contrary, analysis by ICP-MS and ICP-OES requires acid digestion, are time consuming and more expensive, but LODs are very good for more than 50 elements. A major disadvantage of this method is the impossibility of determining the Si content in quartz filters, of interest in areas with a high crustal contribution.

4.2.6 *Ri-URBANS recommendations*

There is a lack of PM chemical composition data in central and northern Europe. This hampers the study of the spatial and temporal variability of PM levels and sources in Europe. The results obtained in Ri-URBANS, mainly those related to the potential impact on health of PM sources and components, may suggest the convenience of increasing this type of studies in Europe.

We strongly recommend following ACTRIS and CEN standard - EN 16909:2017 for OC and EC determinations in filters. EMEP and ACTRIS guidelines are recommended for analysis of ions, organic tracers and elemental analysis.

Both low and high-volume sampling are suitable for chemical characterization using the adequate filters.

For Ri-URBANS WP4, we suggest using High volume samplers in order to collect enough material for performing the whole analytical strategy devised. Samples are deposited in high purity quartz fibre filters. In this way, all chemical analysis is performed in the same filter sample. To obtain harmonized and comparable data we suggest that each specific analysis will be performed by one centralised laboratory.

4.3 Annex / Files Datasets

All chemical composition data are available at RI-URBANS intranet in the folder “Chemical composition offline” in the link ([Chemical composition offline](#)), where separate folders per country can be found. The data is presented in an excel file for each site, organized in three excel sheets:

Sheet 1: metadata

Sheet 2: Daily (24H) chemical concentrations (when available)

Sheet 3: Monthly/annual averages

4.4 References

ACTRIS guidelines. Preliminary ACTRIS recommendations for aerosol in-situ sampling, measurements, and analyses - by CAIS-ECAC units -Version 3.0 September, 2022. All guidelines for aerosol in-situ measurements can be found under: <https://www.actris-ecac.eu/actris-gaw-recommendation-documents.html>. Last accessed: 19 Sept 2022.

Alastuey, A., Querol, X., Aas, W., Lucarelli, F., Pérez, N., Moreno, T., Cavalli, F., Areskou, H., Balan, V., Catrambone, M., Ceburnis, D., Cerro, J. C., Conil, S., Gevorgyan, L., Hueglin, C., Imre, K., Jaffrezo, J.-L., Leeson, S. R., Mihalopoulos, N., ... Yttri, K. E. (2016). Geochemistry of PM10 over Europe during the EMEP intensive measurement periods in summer 2012 and winter 2013. *Atmospheric Chemistry and Physics*, 16(10), 6107–6129. <https://doi.org/doi:10.5194/acp-16-6107-2016>

Amato, F., Alastuey, A., Karanasiou, A., Lucarelli, F., Nava, S., Calzolari, G., Severi, M., Becagli, S., Gianelle, V. L., Colombi, C., Alves, C., Custódio, D., Nunes, T., Cerqueira, M., Pio, C., Eleftheriadis, K., Diapouli, E., Reche, C., Minguillón, M. C., ... Querol, X. (2016). AIRUSE-LIFE+: a harmonized PM speciation and source apportionment in five southern European cities. *Atmospheric Chemistry and Physics*, 16(5), 3289–3309. <https://doi.org/10.5194/acp-16-3289-2016>

Bergmans, B., Cattaneo, A., Duarte, R. M. B. O., Gomes, J. F. P., Saraga, D., García, M. R., Querol, X., Liotta, L. F., Safell, J., Spinazzé, A., Rovelli, S., Borghi, F., Cavallo, D. M., Villanueva, F., Gilio, A. Di, Maggos, T., Mihucz, V. G., Ao, J., Gomes, F. P., ... Spinazz, A. (2022). Particulate matter indoors: a strategy to sample and monitor size-selective fractions, *Applied Spectroscopy Reviews*, 57:8, 675-704, DOI: 10.1080/05704928.2022.2088554

Borlaza, L. J. S., Weber, S., Uzu, G., Jacob, V., Cañete, T., Micallef, S., Trébuchon, C., Slama, R., Favez, O., & Jaffrezo, J. L. (2021). Disparities in particulate matter (PM10) origins and oxidative potential at a city scale (Grenoble,

- France) - Part 1: Source apportionment at three neighbouring sites. *Atmospheric Chemistry and Physics*, 21(7), 5415–5437. <https://doi.org/10.5194/acp-21-5415-2021>
- Brown, R.J.C., Beccacesi, S., Butterfield, D.M., Quincey, P.G., Harris, P.M., Maggos, T., Panteliadis, P., John, A., Jedynska, A., Kuhlbusch, T.A.J., Putaud, J.-P., Karanasiou, A., 2017. Standardisation of a European measurement method for organic carbon and elemental carbon in ambient air: results of the field trial campaign and the determination of a measurement uncertainty and working range. *Environmental Science: Processes and Impacts* 19, 1249–1259.
- Cassee, F. R.; Héroux, M.-E.; Gerlofs-Nijland, M. E.; Kelly, F. J. Particulate Matter beyond Mass: recent Health Evidence on the Role of Fractions, Chemical Constituents and Sources of Emission. *Inhal. Toxicol.* 2013, 25, 802–812. doi:10.3109/08958378.2013.850127
- Cavalli, F.; Viana, M.; Yttri, K. E.; Genberg, J.; Putaud, J.-P. Toward a Standardised Thermal-Optical Protocol for Measuring Atmospheric Organic and Elemental Carbon: The EUSAAR Protocol. *Atmos. Meas. Tech.* 2010, 3, 79–89. doi:10.5194/amt-3-79-2010
- Duarte, R. M. B. O., Gomes, J. F. P., Querol, X., Cattaneo, A., Bergmans, B., Saraga, D., Maggos, T., Gilio, A. Di, Rovelli, S., Villanueva, F., Ao, J., & Gomes, F. P. (n.d.). Advanced instrumental approaches for chemical characterization of indoor particulate matter, *Applied Spectroscopy Reviews*, 57:8, 705-745, DOI: 10.1080/05704928.2021.2018596
- EMEP/CCC 2001. EMEP manual for sampling and chemical analysis. EMEP/CCC-Report 1/95 Revision 1/2001; <https://projects.nilu.no/ccc/manual>. Last accessed: 16 Sept 2022.
- EN12341:2014. European Committee for Standardization (CEN). Ambient air - Standard gravimetric measurement method for the determination of the PM₁₀ or PM_{2.5} mass concentration of suspended particulate matter, Brussels.
- EN 14902:2005; European Committee for Standardization (CEN). Ambient air quality - Standard method for the measurement of Pb, Cd, As and Ni in the PM₁₀ fraction of suspended particulate matter
- EN 16909:2017. European Committee for Standardisation (CEN). Ambient Air Measurement of Elemental Carbon (EC) and Organic Carbon (OC) Collected on Filters. CEN, Brussels.
- Grange, S. K., Fischer, A., Zellweger, C., Alastuey, A., Querol, X., Jaffrezou, J. L., Weber, S., Uzu, G., & Hueglin, C. (2021). Switzerland's PM₁₀ and PM_{2.5} environmental increments show the importance of non-exhaust emissions. *Atmospheric Environment: X*, 12, 100145. <https://doi.org/10.1016/J.AEAOA.2021.100145>
- in 't Veld, M., Alastuey, A., Pandolfi, M., Amato, F., Pérez, N., Reche, C., Via, M., Minguillón, M.C., Escudero, M., Querol, X. Compositional changes of PM_{2.5} in NE Spain during 2009–2018: A trend analysis of the chemical composition and source apportionment (2021). *Science of the Total Environment*, 795, art. no. 148728, DOI: 10.1016/j.scitotenv.2021.148728.
- Karanasiou, A., Minguillón, M.C., Viana, M., Alastuey, A., Putaud, J.P., Maenhaut, W., Panteliadis, P., Mocnik, G., Favez, O., Kuhlbusch, T.A.J., 2015. Thermal-optical analysis for the measurement of elemental carbon (EC) and organic carbon (OC) in ambient air a literature review. *Atmos. Meas. Tech. Discuss.* 8, 9649–9712. <https://doi.org/10.5194/amtd-8-9649-2015>.
- Minguillón, M. C., Perron, N., Querol, X., Szidat, S., Fahrni, S. M., Alastuey, A., Jimenez, J. L., Mohr, C., Ortega, A. M., Day, D. A., Lanz, V. A., Wacker, L., Reche, C., Cusack, M., Amato, F., Kiss, G., Hoffer, A., Decesari, S., Moretti, F., Hillamo, R., Teinilä, K., Seco, R., Peñuelas, J., Metzger, A., Schallhart, S., Müller, M., Hansel, A., Burkhardt, J. F., Baltensperger, U., and Prévôt, A. S. H. 2011. Fossil versus contemporary sources of fine elemental and

- organic carbonaceous particulate matter during the DAURE campaign in Northeast Spain, *Atmos. Chem. Phys.*, 11, 12067–12084, doi:10.5194/acp-11-12067-2011.
- Moreno, T., Querol, X., Castillo, S., Alastuey, A., Cuevas, E., Herrmann, L., et al. (2006). Geochemical variations in aeolian mineral particles from the Sahara–Sahel Dust Corridor. *Chemosphere*, 65(2), 261–270. <https://doi.org/10.1016/j.chemosphere.2006.02.052>
- Nozaki, Y.: A Fresh Look at Element Distribution in the North Pacific, *Eos*, Vol. 78, No. 21, May 27, 1997.
- Nozière, B.; Kalberer, M.; Claeys, M.; Allan, J.; D'Anna, B.; Decesari, S.; Finessi, E.; Glasius, M.; Grgić, I.; Hamilton, J. F.; et al. The Molecular Identification of Organic Compounds in the Atmosphere: State of the Art and Challenges. *Chem. Rev.* 2015, 115, 3919–3983. doi:10.1021/cr5003485
- Turpin, B. J. and Huntzicker, J. J. 1995. Identification of secondary organic aerosol episodes and quantisation of primary and secondary organic aerosol concentrations during SCAQS, *Atmos. Environ.*, 29, 3527–3544.
- WHO Regional Office for Europe. (2013). Review of evidence on health aspects of air pollution – REVIHAAP Project, Technical Report. Copenhagen: WHO Regional Office for Europe. Available from: http://www.euro.who.int/__data/assets/pdf_file/0004/193108/REVIHAAP-Final-technical-report.pdf [Last accessed: 19 Sept 2022.]
- Weber, S., Salameh, D., Albinet, A., Alleman, L. Y., Waked, A., Besombes, J. L., Jacob, V., Guillaud, G., Meshbah, B., Rocq, B., Hulin, A., Dominik-Sègue, M., Chrétien, E., Jaffrezo, J. L., & Favez, O. (2019). Comparison of PM10 sources profiles at 15 french sites using a harmonized constrained positive matrix factorization approach. *Atmosphere*, 10(6), 1–22. <https://doi.org/10.3390/atmos10060310>
- Weber, S., Uzu, G., Favez, O., Borlaza, L. J. S., Calas, A., Salameh, D., Chevrier, F., Allard, J., Besombes, J. L., Albinet, A., Pontet, S., Mesbah, B., Gille, G., Zhang, S., Pallares, C., Leoz-Garziandia, E., & Jaffrezo, J. L. (2021). Source apportionment of atmospheric PM10 oxidative potential: Synthesis of 15 year-round urban datasets in France. *Atmospheric Chemistry and Physics*, 21(14), 11353–11378. <https://doi.org/10.5194/ACP-21-11353-2021>

5 Online PM chemical composition

The online PM chemical composition is measured at certain sites across Europe using a Quadrupole or Time-of-Flight Aerosol Chemical Speciation Monitor (Q- or ToF-ACSM, Aerodyne Research Inc.). This instrument provides the ambient concentration of the following non-refractory species: Organic aerosol (OA), SO_4^{2-} , NO_3^- , NH_4^+ and Cl^- . Sources of organic aerosols are identified by applying the positive matrix factorisation (PMF) receptor model to the organic mass spectra. The time resolution varies depending on instrument and location between 10 and 30 minutes. The size fraction can be PM1 or PM2.5. The instrument samples ambient air at $0.1 \text{ L}\cdot\text{min}^{-1}$ through a critical orifice (100 μm in diameter) towards an aerodynamic lens which transmits particles between 75 and 650 nm for PM1 instruments or above for PM2.5 instruments. Particles are then flash-vaporized at 600°C in high vacuum conditions and ionized by hard-electron impact (70 MeV), and resulting fragments are analysed by a quadrupole or time-of-flight mass spectrometer (Ng et al., 2011; Fröhlich et al., 2013). The instrument is equipped with a filter-valve system, hence concentrations reported are the result of subtraction of particle-free to particle-laden signal. The fragmentation table (Allan et al., 2004), the ion transmission correction and Response Factor (RF) are used to convert the signal spectra into the species concentrations. Data are corrected to account for flow rate changes, response decay and collection efficiency (CE), whether it is using the composition-dependent (Middlebrook et al., 2012) or a different approach.

5.1 Datasets

The focus period is 2017-2022, for which detailed information is provided below.

Nevertheless, this type of data is available for periods of at least one-year long in Europe starting in 2011. Datasets are available for the following sites in different periods between 2011 and 2015: Barcelona (ES), Birkenes (NO), Cabauw (NL), Dunkirk (FR), Corsica (FR), Finokalia (EL), Hohenpeissenberg (DE), Ispra (IT), Jungfraujoch (CH), London (UK), Magadino (CH), Melpitz (DE), Mace Head (IE), Montsec (ES), Montseny (ES), Prague (CZ), SIRTA facility (FR), Hyytiälä (FI), Tartu (EE), Virolahti (FI), Zurich (CH) (Bressi et al., 2021), and Puy de Dome (FR) (Chen et al., 2022). According to their distance from large pollution sources, the 21 sites are: one natural background (or remote) site, fourteen rural or regional background sites (three of which are coastal), five urban background sites and one industrial site.

The stations and periods after 2017 for which online chemical composition is available can be seen in Figure 5.1. Information on the stations, data provider and contacts can be seen in Table 5.1. Scientific publications on the PM chemical composition and organic sources with high time resolution are also indicated for each sampling site when available. Moreover, when the aforementioned data from 2017 onwards are part of an overview publication on organic sources (Chen et al., 2022), it is indicated in the table. For some of the sites, measurements have been done but data have not been fully processed and/or compiled and it is indicated as such in the table.

A summary of the data results can be seen in Figure 5.2 (from Chen et al., 2022).

Table 5.1. List of sites, location, coordinates, type of station and data provider, contact, instrument, and period. Scientific publications on the PM chemical composition and organic sources with high time resolution are also indicated for each sampling site when available.

Location (Country)	Acronym	Latitude (°)	Longitude (°)	Station type	Data provider (institution)	Contact	Publication (site specific)	Publication overview (Chen et al., 2022)	Instrument	Data available	Period
Athens DEM (EL)	athd	37.99	23.82	urban	Demokritos	Kostas Eleftheriadis	Eleftheriadis et al., 2021; Zografou et al., 2022	Yes	ToF-ACSM	Yes	see Fig.5.1
Athens NOA (EL)	athn	38	23.72	urban	NOA	Nikos Mihalopoulos	Stavroulas et al., 2019	Yes	Q-ACSM	Yes	see Fig.5.1
Barcelona (ES)	bar	41.4	2.1	urban	IDAEA-CSIC	MCruz Minguillón	Via et al., 2021	Yes	Q-ACSM	Yes	see Fig.5.1
Birmingham (UK)		52.46	-1.93	urban	Univ Manchester	James Allan	-	No	Q-ACSM	Not compiled	see Fig.5.1
Bucharest (RO)	buc	44.35	26.03	urban	INOE	Jenni Vasilescu	Mărmureanu et al., 2020	Yes	Q-ACSM	Yes	see Fig.5.1
Dublin (IE)	dub	53.31	-6.22	urban	NUIG	Jurgita Ovadnevaite	Lin et al., 2019	Yes	Q-ACSM	Yes	see Fig.5.1
Granada (ES)	gra	37.18	-3.58	urban	Univ Granada	Gloria Titos	-	No	ToF-ACSM	Not compiled	see Fig.5.1
Helsinki (FI)	hel	60.12	24.58	urban	Univ Helsinki	Hilkka Timonen	Barreira et al., 2021	Yes	Q-ACSM	Yes	see Fig.5.1
Kraków (PL)	kra	50.07	19.92	urban	PSI	Kaspar Daellenbach?	Tobler et al., 2021	Yes	Q-ACSM	Yes	see Fig.5.1
Lille (FR)	lil	47.8	11	urban	IMT Douai	Véronique Riffault	-	Yes	Q-ACSM	Yes	see Fig.5.1
London North Kensington (UK)	lon	51.52	-0.21	urban	Imperial College	David Green	-	Yes	Q-ACSM	Yes	see Fig.5.1
Manchester (UK)				urban	Univ Manchester	James Allan	-	No	Q-ACSM	Not compiled	see Fig.5.1
Marseille (FR)	mar	43.31	5.39	urban	Univ Marseille	Benjamin Chazeau	Chazeau et al., 2021, 2022	Yes	ToF-ACSM	Yes	see Fig.5.1
Nicosia (CY)				urban	Cyprus Institute	Michael Pikridas	-	No	Q-ACSM	Not compiled	see Fig.5.1
Paris (FR)	par	48.7	2.2	urban	LSCE	Olivier Favez	Petit et al., 2021; Zhang et al., 2019	Yes	Q-ACSM	Yes	see Fig.5.1

Prague (CZ)		50.1	14.4	urban	ICPF	Jaroslav Schwarz	-	No	cToF-AMS	Not compiled	see Fig.5.1
Tartu (EE)	tar	58.4	26.7	urban	EERC	Marek Maasikmets	-	Yes	Q-ACSM	Yes	see Fig.5.1
Zürich (CH)	zur	47.4	8.5	urban	EMPA / PSI	Kaspar Daellenbach / Christoph Hüglin	Canonaco et al., 2015, 2021	Yes	Q-ACSM	Yes	see Fig.5.1
Birkenes (NO)	bir	58.4	8.3	non-urban	NILU	Stephen Platt	Yttri et al., 2021	Yes	Q-ACSM	Yes	see Fig.5.1
Carnsore Point (IE)	casp	52.19	-6.34	non-urban	NUIG	Jurgita Ovadnevaite	Lin et al., 2019	Yes	Q-ACSM	Yes	see Fig.5.1
Cyprus Atmos. Obs. (CY)	cao			non-urban	Cyprus Institute	Michael Pikridas	-	Yes	Q-ACSM	Yes	see Fig.5.1
Hohenpeissenberg (DE)	hoh	47.8	11	non-urban	DWD	Thomas Elste	-	Yes	Q-ACSM	Yes	see Fig.5.1
Hyytiälä (FI)	hyy	61.8	24.3	non-urban	Univ Helsinki	Mikael Ehn	Heikkinen et al., 2020	Yes	Q-ACSM	Yes	see Fig.5.1
Košetice (CZ)	kos			non-urban	ICPF	Jaroslav Schwarz	-	Yes	cToF-AMS	Yes	see Fig.5.1
Magadino (CH)	mag			non-urban	EMPA	Christoph Hüglin	-	Not after 2017	Q-ACSM		
Melpitz (DE)	mel	51.5	12.9	non-urban	TROPOS	Laurent Poulain	Poulain et al., 2020	Yes	Q-ACSM	Yes	see Fig.5.1
Puy de Dôme (FR)	puy			non-urban	Univ Clermont Auvergne-CNRS	Evelyn Freney	Farah et al., 2021	Yes	ToF-ACSM	Yes	see Fig.5.1

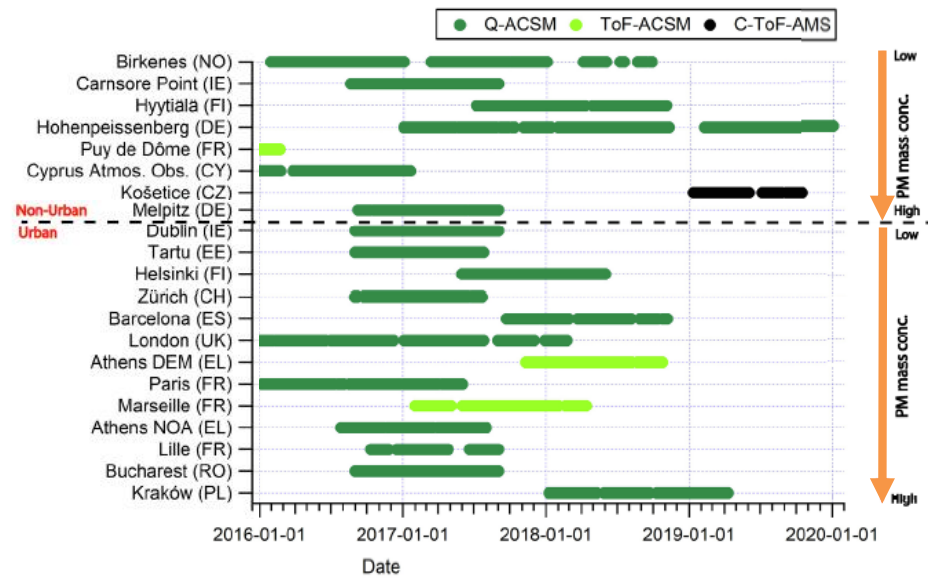


Figure 5.1. Data availability for online chemical composition. Modified from Chen et al., 2022.

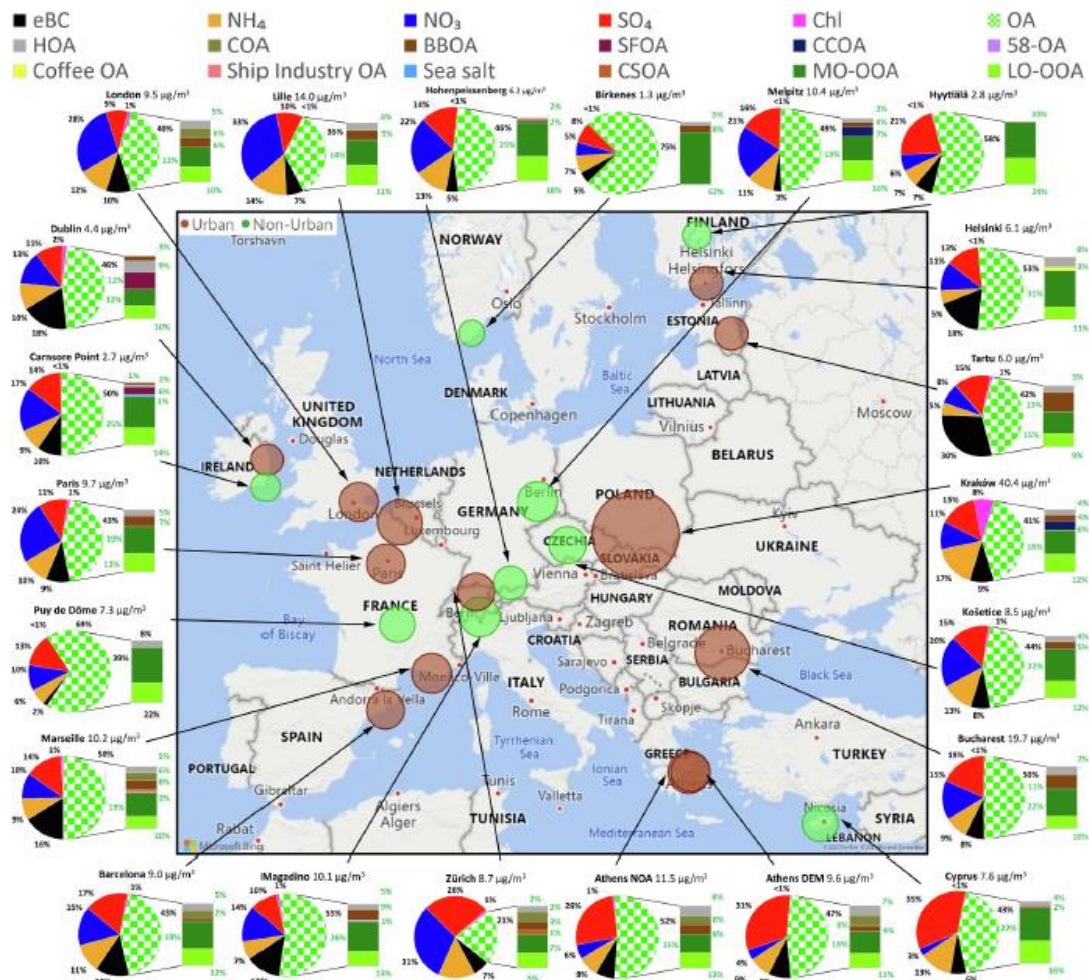


Figure 5.2. Submicron particulate matter (PM₁) mass concentration (in $\mu\text{g}/\text{m}^3$) and composition. Size of the markers: PM₁ mass concentration. Brown markers: urban sites, green markers: non-urban sites. Checkered green/white shading of the pie charts: organic aerosol (OA). Bar charts: OA factors contribution. (Chen et al., 2022). Note that the data for Magadino in this figure corresponds to a period before 2017.

5.2 Guidelines

The Guidelines for this type of measurements are detailed in the following documents:

Quadrupole Aerosol Chemical Speciation Monitor (Q-ACSM) Standard Operating Procedure [WWW Document]. URL <http://www.actris-ecac.eu/pmc-non-refractory-organics-and-inorganics.html> (accessed 27.09.22).

TOF- ACSM Standard Operating Procedures [WWW Document]. URL <http://www.actris-ecac.eu/pmc-non-refractory-organics-and-inorganics.html> (accessed 27.09.22).

The Guidelines for the source apportionment of organic aerosol using organic mass spectra are defined in Chen et al., 2022. Note that there are two different approaches: i) the so-call seasonal approach, the most widely-used approach, which is carried out separating the datasets into different subsets depending on the atmospheric conditions and performing the source apportionment separately for each subset of data; and ii) the rolling approach, consisting in applying the source apportionment at subsets of data with a moving window and integrating the results. The publication of Chen et al.2022 uses the second approach. A deep assessment of the advantages and disadvantages of the two different approaches for the organic aerosol source apportionment is explained in Via et al., 2022.

There are also guidelines to compare the concentrations measured using aerosol mass spectrometry with concentrations of the same species measured by different techniques. The document can be found here:

COLOSSAL, 2021. Guidelines for comparison of ACSM measurements with co-located external data [WWW Document]. URL <http://www.actris-ecac.eu/pmc-non-refractory-organics-and-inorganics.html> (accessed 27.09.22).

5.3 Annex / Files Datasets

The ACSM datasets (chemical species and PMF outputs) already collected and obtained within COLOSSAL Cost Action are fully available at RI-URBANS intranet ([Chemical composition offline](#)) and at the following weblink:

<https://zenodo.org/record/6522811#.Yx2GnRzKGUk>

Results are organized in three folders:

1. External data: containing specific files for each site with information on daily average concentrations, in $\mu\text{g}/\text{m}^3$, of black carbon (BC), organic aerosol (Org), sulfate (SO_4), nitrate (NO_3), ammonium (NH_4), chloride (Cl).
2. PMF results: containing specific files for each site with information on daily average concentrations, in $\mu\text{g}/\text{m}^3$, of OA factors: hydrocarbon-like OA (HOA), biomass burning OA (BBOA), cooking-like OA (COA), coal combustion OA (CCOA), special local factors (if applicable), more oxidized-oxygenated OA (MO-OOA), and less oxidized-oxygenated OA (LO-OOA).
3. Read_me_files: containing specific files for each site with metadata information.

5.4 References

- Allan, J. D., Delia, A. E., Coe, H., Bower, K. N., Alfarra, M. R., Jimenez, J. L., Middlebrook, A. M., Drewnick, F., Onasch, T. B., Canagaratna, M. R., Jayne, J. T., and Worsnop, D. R.: A generalised method for the extraction of chemically resolved mass spectra from Aerodyne aerosol mass spectrometer data, *J. Aerosol Sci.*, 35, 909–922, <https://doi.org/10.1016/j.jaerosci.2004.02.007>, 2004.
- Barreira, L.M.F., Ylisirniö, A., Pullinen, I., Buchholz, A., Li, Z., Lipp, H., Junninen, H., Hörrak, U., Noe, S.M., Krasnova, A., Krasnov, D., Kask, K., Talts, E., Niinemets, Ü., Ruiz-Jimenez, J., Schobesberger, S., 2021. The importance of sesquiterpene oxidation products for secondary organic aerosol formation in a springtime hemiboreal forest. *Atmos. Chem. Phys.* 21, 11781–11800. <https://doi.org/10.5194/acp-21-11781-2021>.
- Canonaco, F., Slowik, J.G., Baltensperger, U., Prévôt, A.S.H., 2015. Seasonal differences in oxygenated organic aerosol composition: implications for emissions sources and factor analysis. *Atmos. Chem. Phys.* 15, 6993–7002. <https://doi.org/10.5194/acp-15-6993-2015>.
- Canonaco, F., Tobler, A., Chen, G., Sosedova, Y., Slowik, J.G., Bozzetti, C., Daellenbach, K.R., El Haddad, I., Crippa, M., Huang, R.-J., Furger, M., Baltensperger, U., Prévôt, A.S.H., 2021a. A new method for long-term source apportionment with time-dependent factor profiles and uncertainty assessment using SoFi Pro: application to 1 year of organic aerosol data. *Atmos. Meas. Tech.* 14, 923–943. <https://doi.org/10.5194/amt-14-923-2021>.
- Chazeau, B., El Haddad, I., Canonaco, F., Temime-Roussel, B., D’Anna, B., Gille, G., Mesbah, B., Prévôt, A.S.H., Wortham, H., Marchand, N., 2022. Organic aerosol source apportionment by using rolling positive matrix factorization: Application to a Mediterranean coastal city. *Atmos. Environ.* X 100176. <https://doi.org/10.1016/j.aeaoa.2022.100176>.
- Chazeau, B., Temime-Roussel, B., Gille, G., Mesbah, B., D’Anna, B., Wortham, H., Marchand, N., 2021. Measurement report: Fourteen months of real-time characterisation of the submicronic aerosol and its atmospheric dynamics at the Marseille–Longchamp supersite. *Atmos. Chem. Phys.* 21, 7293–7319. <https://doi.org/10.5194/acp-21-7293-2021>.
- Bressi, M, Cavalli, F, Putaud, J.P, Fröhlich, R, Petit, J.-E, Aas, W, Äijälä, M, Alastuey, A, Allan, J.D, Aurela, M, Berico, M, Bougiatioti, A, Bukowiecki, N, Canonaco, F, Crenn, V, Dusanter, S, Ehn, M, Elsassner, M, Flentje, H, Graf, P, Green, D.C, Heikkinen, L, Hermann, H, Holzinger, R, Hueglin, C, Keernik, H, Kiendler-Scharr, A, Kubelová, L, Lunder, C, Maasikmets, M, Makeš, O, Malaguti, A, Mihalopoulos, N, Nicolas, J.B, O’Dowd, C, Ovadnevaite, J, Petralia, E, Poulain, L, Priestman, M, Riffault, V, Ripoll, A, Schlag, P, Schwarz, J, Sciare, J, Slowik, J, Sosedova, Y, Stavroulas, I, Teinmaa, E, Via, M, Vodička, P, Williams, P.I, Wiedensohler, A, Young, D.E, Zhang, S, Favez, O, Minguillón, M.C, Prévôt, A.S.H., 2021. A European aerosol phenomenology - 7: high-time resolution chemical characteristics of submicron particulate matter across Europe *Atmospheric Environment: X*, 10, 100108. <https://doi.org/10.1016/j.aeaoa.2021.100108>.
- Chen G., Canonaco F., Tobler A., Aas W., Alastuey A., Allan J., Atabakhsh S., Aurela M., Baltensperger U., Bougiatioti A., De Brito J.F., Ceburnis D., Chazeau B., Chebaicheb H., Daellenbach K.R., Ehn M., El Haddad I., Eleftheriadis K., Favez O., Flentje H., Font A., Fossum K., Freney E., Gini M., Green D.C., Heikkinen L., Herrmann H., Kalogridis A.-C., Keernik H., Lhotka R., Lin C., Lunder C., Maasikmets M., Manousakas M.I., Marchand N., Marin C., Marmureanu L., Mihalopoulos N., Močnik G., Nećki J., O’Dowd C., Ovadnevaite J., Peter T., Petit J.-E., Pikridas M., Platt S.M., Pokorná P., Poulain L., Priestman M., Riffault V., Rinaldi M., Róžański K., Schwarz J., Sciare J., Simon L., Skiba A., Slowik J.G., Sosedova Y., Stavroulas I., Styszko K., Teinmaa E., Timonen H., Tremper A., Vasilescu J., Via M., Vodička P., Wiedensohler A., Zografou O., and Minguillón M.C., Prévôt A.S.H., 2022.

- European aerosol phenomenology – 8: Harmonised source apportionment of organic aerosol using 22 Year-long ACSM/AMS datasets. *Environment International*, 166, 107325, <https://doi.org/10.1016/j.envint.2022.107325>.
- Eleftheriadis, K., Gini, M.I., Diapouli, E., Vratolis, S., Vasilatou, V., Fetfatzis, P., Manousakas, M.I., 2021. Author Correction: Aerosol microphysics and chemistry reveal the COVID19 lockdown impact on urban air quality (*Scientific Reports*, (2021), 11, 1, (14477), 10.1038/s41598-021-93650-6). *Sci. Rep.* 11, 99947. <https://doi.org/10.1038/s41598-021-99947-w>.
- Farah, A., Freney, E., Canonaco, F., Prévôt, A.S.H., Pichon, J., Abboud, M., Farah, W., Sellegri, K., 2021. Altitude Aerosol Measurements in Central France: Seasonality, Sources and Free-Troposphere/Boundary Layer Segregation. *Earth Sp. Sci.* 8. <https://doi.org/10.1029/2019EA001018>.
- Fröhlich, R., Cubison, M. J., Slowik, J. G., Bukowiecki, N., Prévôt, A. S. H., Baltensperger, U., Schneider, J., Kimmel, J. R., Gonin, M., Rohner, U., Worsnop, D. R., and Jayne, J. T.: The ToF-ACSM: a portable aerosol chemical speciation monitor with TOFMS detection, *Atmos. Meas. Tech.*, 6, 3225–3241, <https://doi.org/10.5194/amt-6-3225-2013>, 2013.
- Heikkinen, L., Äijälä, M., Riva, M., Luoma, K., Dällenbach, K., Aalto, J., Aalto, P., Aliaga, D., Aurela, M., Keskinen, H., Makkonen, U., Rantala, P., Kulmala, M., Petäjä, T., Worsnop, D., Ehn, M., 2020. Long-term sub-micrometer aerosol chemical composition in the boreal forest: inter- and intra-annual variability. *Atmos. Chem. Phys.* 20, 3151–3180. <https://doi.org/10.5194/acp-20-3151-2020>.
- Lin, C., Ceburnis, D., Huang, R.-J., Xu, W., Spohn, T., Martin, D., Buckley, P., Wenger, J., Hellebust, S., Rinaldi, M., Facchini, M.C., O’Dowd, C., Ovadnevaite, J., 2019. Wintertime aerosol dominated by solid-fuel-burning emissions across Ireland: insight into the spatial and chemical variation in submicron aerosol. *Atmos. Chem. Phys.* 19, 14091–14106. <https://doi.org/10.5194/acp-19-14091-2019>.
- Mărmureanu, L., Vasilescu, J., Slowik, J., Prévôt, A.S.H., Marin, C.A., Antonescu, B., Vlachou, A., Nemuc, A., Dandocsi, A., Szidat, S., 2020. Online chemical characterization and source identification of summer and winter aerosols in Magurele, Romania. *Atmosphere (Basel)*. 11. <https://doi.org/10.3390/ATMOS11040385>.
- Middlebrook, A. M., Bahreini, R., Jimenez, J. L., and Canagaratna, M. R.: Evaluation of composition-dependent collection efficiencies for the Aerodyne aerosol mass spectrometer using field data, *Aerosol Sci. Technol.*, 46, 258–271, <https://doi.org/10.1080/02786826.2011.620041>, 2012.
- Ng, N. L., Herndon, S. C., Trimborn, A., Canagaratna, M. R., Croteau, P. L., Onasch, T. B., Sueper, D., Worsnop, D. R., Zhang, Q., Sun, Y. L. and Jayne, J. T.: An Aerosol Chemical Speciation Monitor (ACSM) for routine monitoring of the composition and mass concentrations of ambient aerosol, *Aerosol Sci. Technol.*, 45(7), 770–784, doi:10.1080/02786826.2011.560211, 2011.
- Petit, J.-E., Dupont, J.-C., Favez, O., Gros, V., Zhang, Y., Sciare, J., Simon, L., Truong, F., Bonnaire, N., Amodeo, T., Vautard, R., Haeffelin, M., 2021. Response of atmospheric composition to COVID-19 lockdown measures during spring in the Paris region (France). *Atmos. Chem. Phys.* 21, 17167–17183. <https://doi.org/10.5194/acp-21-17167-2021>.
- Poulain, L., Spindler, G., Grüner, A., Tuch, T., Stieger, B., van Pinxteren, D., Petit, J.-E., Favez, O., Herrmann, H., Wiedensohler, A., Pinxteren, D. van, Herrmann, H., Wiedensohler, A., 2020. Multi-year ACSM measurements at the central European research station Melpitz (Germany) – Part 1: Instrument robustness, quality assurance,

- and impact of upper size cutoff diameter. *Atmos. Meas. Tech.* 13, 4973–4994. <https://doi.org/10.5194/amt-13-4973-2020>.
- Stavroulas, I., Bougiatioti, A., Grivas, G., Paraskevopoulou, D., Tsagkaraki, M., Zampas, P., Liakakou, E., Gerasopoulos, E., Mihalopoulos, N., 2019. Sources and processes that control the submicron organic aerosol composition in an urban Mediterranean environment (Athens): A high temporal-resolution chemical composition measurement study. *Atmos. Chem. Phys.* 19, 901–919. <https://doi.org/10.5194/acp-19-901-2019>.
- Tobler, A.K., Skiba, A., Canonaco, F., Močnik, G., Rai, P., Chen, G., Bartyzel, J., Zimnoch, M., Styszko, K., Nęcki, J., Furger, M., Róžański, K., Baltensperger, U., Slowik, J.G., Prevot, A.S.H., 2021. Characterization of non-refractory (NR) PM1 and source apportionment of organic aerosol in Kraków. *Atmos. Chem. Phys.* 21, 14893–14906. <https://doi.org/10.5194/acp-21-14893-2021>.
- Via, M., Chen, G., Canonaco, F., Daellenbach, K. R., Chazeau, B., Chebaicheb, H., Jiang, J., Keernik, H., Lin, C., Marchand, N., Marin, C., O'Dowd, C., Ovadnevaite, J., Petit, J.-E., Pikridas, M., Riffault, V., Sciare, J., Slowik, J. G., Simon, L., Vasilescu, J., Zhang, Y., Favez, O., Prévôt, A. S. H., Alastuey, A., and Minguillón, M.C.: Rolling vs. seasonal PMF: real-world multi-site and synthetic dataset comparison, *Atmos. Meas. Tech.*, 15, 5479–5495, <https://doi.org/10.5194/amt-15-5479-2022>, 2022.
- Via, M., Minguillón, M.C., Reche, C., Querol, X., Alastuey, A., 2021. Increase in secondary organic aerosol in an urban environment. *Atmos. Chem. Phys.* 21, 8323–8339. <https://doi.org/10.5194/acp-21-8323-2021>.
- Yttri, K.E., Canonaco, F., Eckhardt, S., Evangeliou, N., Fiebig, M., Gundersen, H., Hjellbrekke, A.-G., Lund Myhre, C., Platt, S.M., Prévôt, A.S.H., Simpson, D., Solberg, S., Surratt, J., Tørseth, K., Uggerud, H., Vadset, M., Wan, X., Aas, W., 2021. Trends, composition, and sources of carbonaceous aerosol at the Birkenes Observatory, northern Europe, 2001–2018. *Atmos. Chem. Phys.* 21, 7149–7170. <https://doi.org/10.5194/acp-21-7149-2021>.
- Zhang, Y., Favez, O., Petit, J.-E., Canonaco, F., Truong, F., Bonnaire, N., Crenn, V., Amodeo, T., Prévôt, A.S.H., Sciare, J., Gros, V., Albinet, A., 2019. Six-year source apportionment of submicron organic aerosols from near-continuous highly time-resolved measurements at SIRTA (Paris area, France). *Atmos. Chem. Phys.* 19, 14755–14776. <https://doi.org/10.5194/acp-19-14755-2019>.
- Zografou, O., Gini, M., Manousakas, M.I., Chen, G., Kalogridis, A.C., 2022. Combined organic and inorganic source apportionment on yearlong ToF-ACSM dataset at a suburban station in Athens. <https://doi.org/10.5194/amt-2022-38>.

6 Volatile Organic compounds (VOCs)

The measurement of VOCs is of great interest for monitoring air quality since they are precursors of PM, nanoparticles and O₃. However, at present, VOC measurements in urban environments are scarce. In addition, there is no reference methodology, except for specific compounds, which makes it difficult to compare existing measurements.

6.1 Datasets

A total of 21 European sites of different typology mainly urban (16 sites) and 5 sites of other typology (traffic, industrial, suburban...) have been assessed within this project. The measurements have been conducted with different types of instruments mainly by gas chromatography systems as reported in the tables.



Figure 6-1: Map with sites and types of stations providing data sets for atmospheric VOC concentrations.

Table 6-1: List of air quality sites providing VOC datasets, location, type of environment and data provider

No	Country	City	Station name	Station type	Acronym	Coordinates	Data provider
1	France	Marseille	Longchamp	Urban	MAR_UB	43.31 N, 5.39 E; (71)	Direct sending by a Ri-Urbans partner
2	France	Strasbourg	Strasbourg-Ouest	Urban	STB_UB	48.36 N, 7.42 E	Direct sending by a Ri-Urbans partner
3	France	Paris	Châtelet	Urban	PAR_UB	48.51 N, 2.20 E	Direct sending by a Ri-Urbans partner
4	France	Grenoble	Les frênes	Urban	GRE_UB	45.16 N, 5.74 E	Direct sending by a Ri-Urbans partner
5	Belgium	Charleroi-Mayence	Charleroi-Mayence	Urban	CHM_UB	50.41 N, 4.45 E (140)	Direct sending by a Ri-Urbans partner
6	Belgium	Lodelinsart	Lodelinsart	Urban	LDS_UB	50.43 N, 4.46 E (133)	Direct sending by a Ri-Urbans partner
7	Belgium	Angleur	Angleur	Urban	ANG_UB	50.61 N, 5.61 E (68)	Direct sending by a Ri-Urbans partner
8	Belgium	Herstal	Herstal	Urban	HET_UB	50.66 N, 5.63 E (61)	Direct sending by a Ri-Urbans partner
9	Belgium	Namur	Namur	Urban	NAM_UB	50.46 N, 4.87 E (107)	Direct sending by a Ri-Urbans partner
10	Belgium	Mons	Mons	Urban	MON_UB	50.47 N, 3.94 E (36)	Direct sending by a Ri-Urbans partner
11	Switzerland	Zurich	Zurich	Urban	ZUR_UB	47.38 N, 8.53 E (409)	Direct sending by a Ri-Urbans partner
12	Switzerland	Zurich	Zurich	Urban	ZUR_UB	47.38 N, 8.53 E (409)	Direct sending by a Ri-Urbans partner
13	Finland	Helsinki	SMEAR III	Urban	HEL2_UB	60.12 N, 24.58 E (26)	Direct sending by a Ri-Urbans partner
14	UK	London	Eltham	Urban	LND3_UB	51.45 N, 0.07 E	Direct sending by a Ri-Urbans partner
15	Belgium	Mouscron	Mouscron	Industrial	MSR_IND	50.75 N, 3.24 E (43)	Direct sending by a Ri-Urbans partner
16	France	Paris	SIRTA	Suburban	PAR_SUB	48.71N, 2.21 E (156)	Direct sending by a Ri-Urbans partner
17	France	Lyon	Feyzin-stade	Industrial	LYO_IND	45.66 N, 4.85 E	Direct sending by a Ri-Urbans partner
18	France	Lyon	Vernaison	Industrial	LYO2_IND	45.65 N, 4.82 E	Direct sending by a Ri-Urbans partner
19	Greece	Athens	Piraeus port	Urban costal	PIR_UC	37.57 N, 23.37 E	Direct sending by a Ri-Urbans partner
20	UK	London	Marylebone road	Traffic	LND_TR	51.52 N, 0.15 W	Direct sending by a Ri-Urbans partner
21	Finland	Helsinki	MÄkelankatu street	Street Canyon	HEL_CAN	60.20 N, 24.95 E (29)	Direct sending by a Ri-Urbans partner

Table 6-2: Instruments used to measure VOC, VOC measured, period and time resolution of data, % of data available and range of LoD and uncertainty

No	Site	Instrument	VOC measured	Period	Time resolution	% of data	LoD range	Uncertainty range
1	MAR_UB	TD-GC-2FID (C2 – C9 NMHC) + TD-GC-FID (C6 – C16 NMHC)	C2 – C16 NMHC	21/03/2019 – 31/08/2020	Hourly	81% & 84 %	5 – 100 ppt	4 – 40 % for abundant compounds
2	STB_UB	TD-GC-FID	C2 – C9 NMHC	08/07/2002 – ongoing	Hourly	63.5%	3 – 400 ppt	/
3	PAR_UB	TD-GC-FID	C2 – C9 NMHC	2009->31/12/2021	Hourly		3 – 400 ppt	/
4	GRE_UB	TD-GC-FID	C2 – C9 NMHC	ongoing	Hourly		3 – 400 ppt	/
5	CHM_UB	Passive sampler	C4 – C9 NMHC + chloroethanes and chloroethenes	02/10/2001 – Ongoing	24h one day out of two	<50%	0.09 µg/m3	Around 30 %
6	LDS_UB	Passive sampler	C4 – C9 NMHC + chloroethanes and chloroethenes	02/01/2018 – Ongoing	24h one day out of two	<50%	0.09 µg/m3	Around 30 %
7	ANG_UB	Passive sampler	C4 – C9 NMHC + chloroethanes and chloroethenes	01/01/2018 – Ongoing	24h one day out of two	<50%	0.09 µg/m3	Around 30 %
8	HET_UB	Passive sampler	C4 – C9 NMHC + chloroethanes and chloroethenes	01/01/2013 – Ongoing	24h one day out of two	<50%	0.09 µg/m3	Around 30 %
9	NAM_UB	Passive sampler	C4 – C9 NMHC + chloroethanes and chloroethenes	01/01/2018 – Ongoing	24h one day out of two	<50%	0.09 µg/m3	Around 30 %
10	MON_UB	Passive sampler	C4 – C9 NMHC + chloroethanes and chloroethenes	02/10/2001 – Ongoing	24h one day out of two	<50%	0.09 µg/m3	Around 30 %
11	ZUR_UB	TD-GC-FID	C2 – C9 NMHC	01/01/2001 – 31/12/2013	Hourly	85 %	2 – 25 ppt	10 %
12	ZUR_UB	TD-GC-2FID	OVOCs	01/01/2014 – 31/12/2017	Hourly	85 %	2 – 25 ppt	10 %
13	HEL2_UB	TD-GC-MS + Canister (TD-GC-FID)	C7 – C10 NMHC + C5 – C10 biogenic VOC (TD-GC-MS) & C2 – C9 NMHC (TD-GC-FID)	10/01-18/11/2011 29/01-29/02/2016 – (only 29/01/2016 – 26/02/2016 for C2 – C9 NMHC)	Hourly (online) and Daily (offline)	38% & 45 %	Online: 0.1 to 89 ng/m3 Offline: 30 – 150 ppt	6 – 44 %
14	LND3_UB	TD-GC-FID	C2 – C9 NMHC	01/01/1997 – ongoing	Hourly	81 %	10 – 100 ppt	TBC
15	MSR_IND	Passive sampler	C4 – C9 NMHC chloroethanes and chloroethenes	07/03/2007 – Ongoing	24h one day out of two	<50%	0.09 µg/m3	Around 30 %
16	LYO_IND							
17	LYO2_IND							
18	PAR_SUB	PTR-Quad-MS	C5 – C9 NMHC + OVOC	18/01/2020 – 31/12/2021	Hourly	61 %	Work in progress	Work in progress
19	PIR_UC	TD-GC-FID	C6 – C12 NMHC	01/2019 – 12/2019	Each 30 min	79 to 85 %	0.2 to 0.3 µg/m3	10 – 49 %
20	LND_TR	TD-GC-FID	C2 – C9 NMHC	01/01/1993 – ongoing	Hourly	83 %	10 – 100 ppt	TBC
21	HEL_CAN	TD-GC-MS	C6 – C9 aromatics + C5	21/08/2019 – 11/09/2019	Hourly	47 %	0.1 – 5 ng/m3	14 – 46 %

			– C15 biogenic VOC				
--	--	--	-----------------------	--	--	--	--

Table 6-3: EBAS code and name of dataset file in RI-Urbans Intranet ([VOC](#))

No	Site	EBAS Code	Link in RI-Urbans
1	MAR_UB		MAR_UB.xlsx
2	STB_UB		STB_UB.xlsx
3	PAR_UB		
4	GRE_UB		
5	CHM_UB		CHM_UB.xlsx
6	LDS_UB		LDS_UB.xlsx
7	ANG_UB		ANG_UB.xlsx
8	HET_UB		HET_UB.xlsx
9	NAM_UB		NAM_UB.xlsx
10	MON_UB		MON_UB.xlsx
11	ZUR_UB		ZUR_UB.xlsx
12	ZUR_UB		ZUR_UB.xlsx
13	HEL2_UB		HEL2_UB.xlsx
14	LND3_UB		LND_UB.xlsx
15	MSR_IND		MSR_IND.xlsx
16	LYO_IND		
17	LYO2_IND		
18	PAR_SUB	FR0020R	PAR_SUB.xlsx
19	PIR_UC		PIR_UC.xlsx
20	LND_TR		LND2_TR.xlsx
21	HEL_CAN		HEL_CAN.xlsx

6.2 Guidelines

The measurements have been conducted with different types of instruments, offline and online, mainly by gas chromatography (GC) systems as reported in the tables, but following different sampling and analysis procedures. The measurement of NMHCs by GC is generally performed in a series of steps with (1) intake manifold and sampling line, (2) traps to remove water, ozone and possibly CO₂, (3) sample pre-concentration, (4) gas chromatographic separation, (5) analysis in detector, and (6) data processing and data delivery. A sample of atmospheric VOCs can be introduced to the analytical system directly from ambient air (on-line), or via a canister or an adsorptive sampling tube (off-line). As reported in the tables below, the majority of VOCs datasets cover NMHCs measurements.

The ACTRIS topical centre for reactive trace gases in-situ measurement has developed a guideline for the measurement of NMHC ([ACTRIS guideline](#)) with the objectives of harmonizing methodologies, QA/QC procedures, uncertainties calculation, considering the specificities of the different types of instruments used. In respect to the quality assurance, the MG provides an update of the WMO report and is considered as the basis of a future WMO guideline which is in progress, with members of the ACTRIS VOC community being among the drivers of this global effort. As for monoterpenes and oxygenated VOCs (OVOCs) as well as other VOC analysis techniques (e.g. PTR-MS) separate measurement guidelines will be published” within ACTRIS.

Furthermore, the European Standardization Body, CEN-WG12, has published five norms related to benzene measurements as listed here:

- EN 14662-1:2005 (in review) : «Ambient air quality - Standard method for measurement of benzene concentrations - Part 1: Pumped sampling followed by thermal desorption and gas chromatography »
- EN 14662-2 :2005 : « Ambient air quality - Standard method for measurement of benzene concentrations - Part 2: Pumped sampling followed by solvent desorption and gas chromatography »

- EN 14662-3 :2015 : « Ambient air — Standard method for the measurement of benzene concentrations — Part 3: Automated pumped sampling with in situ gas chromatography »
- EN 14662-4 :2005 : « Ambient air quality Standard method for measurement of benzene concentrations - Part 4: Diffusive sampling followed by thermal desorption and gas chromatography »
- EN 14662-5 :2005 : « Ambient air quality Standard method for measurement of benzene concentrations - Part 5: Diffusive sampling followed by solvent desorption and gas chromatography »

More specifically, the “EN 14662-3:2015 - Ambient Air Quality - Standard method for the measurement of benzene concentrations - Part 3: Automated pumped sampling with in situ gas chromatography” specifies a semi-continuous measurement method for the determination of the concentration of benzene present in ambient air based on automated sampling and analysis by gas chromatography. This standard describes the performance characteristics and sets the relevant minimum criteria required to select an appropriate automated gas chromatograph (GC) by means of type approval tests. It also includes the evaluation of the suitability of an analyser for use in a specific fixed site so as to meet the data quality requirements as specified in Annex I of Directive 2008/50/EC and requirements during sampling, calibration and quality assurance for use.

Recently, in 2019, a CEN WG13 has been established, where ACTRIS contributes, with the objectives of developing validated standard measurement methods for the measurement and monitoring of volatile organic ozone precursors in ambient air in order to ensure a harmonized implementation of the Directive. Total non methane hydrocarbons are excluded. The Commission has requested a programme for Standard development for ozone precursors using the following techniques:

- Automatic pumped sampling, pre-concentration and on-line gas chromatography with flame ionisation detector (FID) and/or mass spectrometer detector (MSD);
- Manual or automatic canister sampling followed by off-line gas chromatography with FID and/or MSD;
- Manual or automatic pumped sampling followed by off-line thermal desorption and gas chromatography with FID and/or MSD;
- Diffusive sampling followed by thermal desorption by off-line gas chromatography with FID and/or MSD;
- Manual or automatic pumped sampling of formaldehyde on dinitrophenylhydrazine (DNPH) followed by off-line high-performance liquid chromatography (HPLC) / ultraviolet (UV) detection;
- Diffusive sampling of formaldehyde on DNPH followed by off-line HPLC/UV detection.

Based on the published ACTRIS guideline, we summarize the existing recommendations for off-line and on-line sampling and analysis of NMHCs as follows:

6.2.1 Sampling

- If the online sampling is possible then it should be prioritized to offline sampling and in the case of offline sampling, sorbent tubes, stainless-steel canister or passivated stainless-steel canister (SilcoNert 2000® treated) should be prioritized following the Standard Operation Procedure (SOP) described in the GAW Report No. 204 (WMO, 2012).
- The inlet line connecting the instrument to the manifold should be optimized for minimum surface area and residence time, and it should be flushed prior to sampling for a sufficient time to equilibrate surfaces. The residence time between the manifold and the instrument should not exceed a few seconds. It is recommended to use a high flow inlet manifold to transfer samples with short residence time from the inlet to the laboratory (<1 min). From there, small diameter and short sampling lines go to the sampling devices or directly to the instruments. For NMHCs the manifold and sampling line should preferentially consist of surface passivated steel (e.g. silcosteel® or sulfiner®) or glass.
- An ozone scrubber should be used to remove ozone and avoid artefact formation from the reaction of unsaturated, reactive NMHCs with ozone (O₃).

- A particle filter should be installed to avoid contamination of the system with particles.
- A water removal system is necessary for GC instruments. Water management can be achieved by different methods such as a Nafion® dryer or a cold trap. The use of cold traps is recommended because these systems are less prone to artefacts. For NMHCs measurements a Nafion dryer is usually used despite artefacts for some alkenes (1-butene and isobutene). The Nafion dryer is not adapted to the measurement of OVOCs nevertheless.

6.2.2 Analysis

- A blank or zero air/gas supply, such as dry air or nitrogen, is required for obtaining analytical blanks during the measurements. The presence of interfering compounds in the zero gas shall be lower than 10 % of the lowest mass of any reported compound introduced in the lowest-level calibration standard. During assessment of zero air/gas purity the same volume shall be introduced as the volume of ambient air sampled during routine monitoring. Blanks should be done at least once per month and ideally once per week
- **Reference materials:**

The Central Calibration Laboratory (CCL) maintains the primary standard that defines the calibration scale for GAW sites. For NMHCs, the CCL is the National Physical Laboratory (<http://www.npl.co.uk/>). The calibration scale is transferred to the stations and laboratories through laboratory standards that are prepared by the CCL and that are directly traceable to the primary standard. In case a station does not use a laboratory standard from the CCL, it has to demonstrate that the laboratory standard used is linked to the calibration scale by direct comparisons in time intervals that correspond to the stability of the standard mixture. This standard will have a higher uncertainty than the laboratory standard produced from the CCL as uncertainties increase the further you move down the traceability chain away from the primary standard.

 - A (secondary) laboratory standard which has to be a multi-component standard (synthetic mixture), produced and certified by the CCL (recommended), or at least traceable to the CCL, for ensuring traceability of the measurements to the WMO GAW calibration scale. The recommended frequency is 2/year or at least 1/year for periods without irregularities of the GC system.
 - One or more (tertiary) working standards that cover most (ideally all) components measured and are used for regular calibration of the measurements, regular or high consumption applications like standard addition or dilution series, etc. These working standards can be either other certified or custom-made synthetic mixtures and are calibrated versus the laboratory standard. The recommended frequency is 2/month or at least 1/month for periods without irregularities of the GC system.
 - A target gas which is preferably compressed whole air but could also be a synthetic mixture calibrated by a reference laboratory (CCL or WCC) (recommended) but at least calibrated by the station against the laboratory standard: it is used to check the assigned values of the calibration mixtures and the calibration process itself and is treated as an air sample with unknown mole fraction. Monitoring of the target gas results yields information about the performance of the instrument, drifts of the laboratory standard and potential instrumental problems. The recommended frequency is 1/month.
- A specific method for uncertainties calculation of VOCs from online measurements with GC system is proposed in the ACTRIS Guideline and should be prioritized when calculating uncertainties.

6.3 RI-Urbans recommendations

Firstly, data from urban monitoring sites should be uploaded to the EBAS database. Only one of the twenty-one datasets evaluated in this project is in EBAS at this moment.

Twelve datasets come from online measurements, seven from offline measurements and the information of two industrial French sites is still missing. For the offline measurements database, the % of data available is always less than 50 % because the sampling is 24 hours one day out of two. Concerning the twelve online datasets, six have more than 70 % of data available and only two have less than 50 % of data available. This result shows the importance to prioritize, when possible and depending on the objectives of the measurement strategy, online measurements instead of offline measurements, in order to ensure high temporal resolution and coverage; and the good performance of instruments used for the majority of online measurements.

The majority of VOCs measurement datasets cover only NMHCs. Two datasets have biogenic VOCs (BVOC) measurements and two other ones cover oxygenated VOC (OVOCs) measurements. An effort should be made in the future to implement OVOCs measurements as well as terpenes already identified in the GAW Report No. 171, since these species are important ozone and secondary organic aerosols precursors and tracers of sources and especially new emerging sources, etc. The respective guidelines are under development.

It is worth mentioning that few sites are following the ACTRIS QA/QC procedures for blanks frequency and calibrations for NMHC. If uncertainties have been calculated for the majority of databases, only five of the sites measuring online have used the methodology proposed in the ACTRIS guideline.

The main recommendations from RI-URBANS are:

- (i) Implementation of ACTRIS guidelines recommendations for the measurement of NMHCs in order to harmonize VOCs measurements and QA/QC procedures. A focus is especially needed on uncertainties calculation.
- (ii) The use of online instruments for measuring VOCs is to prioritize when possible
- (iii) Easy access to the datasets (data upload to the EBAS database is recommended)

These available datasets will be assessed using @VOC@ tool from ACTRIS -CiGas.

6.4 **Annex / Files Datasets**

The VOCs datasets are fully available at RI-URBANS intranet ([VOC](#)). The data is presented in an excel file for each site, organized in two excel sheets:

Sheet 1: metadata

Sheet 2: VOC concentrations

6.5 **References:**

ACTRIS -WP4- JRA4, Trace gases networking: Volatile organic carbon and nitrogen oxides Deliverable D4.13: Recommendation on sustainability of QA and SOPs for VOC in Europe, 2015

Directive 2008/50/EC of the European Parliament and of the Council of 21 May 2008 on ambient air quality and cleaner air for Europe, consolidated 18/09/2015

GAW Report No. 171, A WMO/GAW Expert Workshop on Global Long-term Measurements of Volatile Organic Compounds, 2007

Hoerger et al., ACTRIS non-methane hydrocarbon intercomparison experiment in Europe to support WMO GAW and EMEP observation networks, *Atmos. Meas. Tech.*, 8, 2715–2736, 2015

7 Ammonia (NH₃)

Measurements of ambient concentrations of urban ammonia (NH₃) are of high relevance since this gas is precursor of secondary inorganic aerosols (SIA) a major component of particulate matter. Moreover, high emissions of NH₃ over some regions of Europe can have a significant impact on air quality on a regional scale.

However, as in the case of VOCs, NH₃ measurements in urban environments are very scarce and frequently restricted to short campaigns. In addition, there is no reference methodology which makes it difficult to compare the existing measurements.

7.1 Datasets

A total of 6 European sites of different typology urban, suburban and traffic have been assessed within this project. The measurements have been conducted with mainly passive sampling reported in the tables.



Figure 7-1: Map with sites and type of station.

Table 7-1: List of air quality sites providing VOC datasets, location, type of environment and data provider

No	Country	City	Station name	Station type	Acronym	Coordinates	Data provider
1	Spain	Barcelona	Barcelona	Urban	BCN_UB	41.39 N, 2.11 E (64)	Direct sending by a Ri-Urbans partner
2	Finland	Helsinki	SMEAR III	Urban	HEL2_UB	60.12 N, 24.58 E (26)	Direct sending by a Ri-Urbans partner
3	Spain	Valencia	Bulevard S.	Suburban	VLC_SUB	39.97 N, 0.01 E (3)	Direct sending by a Ri-Urbans partner
4	France	Paris	SIRTA	Suburban	PAR_SUB	48.71N, 2.21 E (156)	Direct sending by a Ri-Urbans partner
5	Spain	Barcelona	Barcelona	Traffic	BCN_TR	41.39 N, 2.15 E (70)	Direct sending by a Ri-Urbans partner
6	Spain	Valencia	La marina	Traffic	VLC_TR	39.45 N, 0.40 W	Direct sending by a Ri-Urbans partner

Table 7-2: Instruments used to measure VOC, VOC measured, period and time resolution of data, % of data available and range of LoD and uncertainty

No	Site	Instrument	Period	Time resolution	% of data	LoD	Uncertainties
1	BCN_UB	Passive sampler	14/02/2011 – 07/02/2022	1 – 3 weeks	/	0.01 ppm	6 %
2	HEL2_UB	Marga 2S	01/11/2009 – 25/05/2010	Hourly	89 %	0.05 µg/m3	/
3	VLC_SUB		27/07/2021 – 31/12/2021	Hourly	91 %		
4	PAR_SUB	Airmonia & passive sampler	Airmonia: 12/03/2012 – 18/05/2013 & 22/01/2018 – 17/04/2018 Passive sampler: 22/05/2017 – 21/06/2021	Airmonia: Every 5 min Passive sampler: weekly	/		
5	BCN_TR	Passive sampler	20/11/2013 – 29/06/2018	1 – 3 weeks	/	0.01 ppm	6 %
6	VLC_TR		01/01/2016 – 22/12/2021	Hourly	88 %		

Table 7-3: EBAS code and name of dataset file in RI-Urbans Intranet ([NH3](#))

No	Site	EBAS Code	Link to RI-Urbans
1	BCN_UB		BCN_UB.xlsx
2	HEL2_UB		HEL2_UB.xlsx
3	VLC_SUB		VLC_SUB.xlsx
4	PAR_SUB		PAR_SUB.xlsx
5	BCN_TR		BCN_TR.xlsx
6	VLC_TR		VLC_TR.xlsx

7.2 Guidelines

The European Standardization Body, CEN, has recently published, in 2020, a measurement protocol dedicated to ammonia measurement through CEN Technical Committee 264 Working Group (WG) 11: N 17346:2020 «Ambient air - Standard method for the determination of the concentration of ammonia using diffusive samplers». This norm specifies a method for the sampling and analysis of NH₃ in ambient air using diffusive sampling. It can be used for NH₃ measurements at ambient levels, but the concentration range and exposure time are sampler dependent, and the end user is therefore advised to match the sampler type to the measurement requirement and to follow the operating instructions provided by the manufacturer.

There is also a German norm: VDI 3869-4, Measurement of ammonia in ambient air – Sampling with diffusive samplers – Photometric or ion chromatographic analysis. At French level, the Laboratoire Central de Surveillance de la Qualité de l'Air (LCSQA) provided a guide ([LCSQA](#)) in 2021, for the measurement of NH₃ in ambient air.

Based on these documentation, the following measurement recommendations are for cavity ring-down spectroscopy (CRDS) technique online sampling, and for offline passive sampling.

For online sampling and analysis:

- A SilcoNert 2000® treated (or PTFE or PFA) sampling line of less than 4m length and 1/8-inch diameter must be used.
- The sampling line must be passivated for 24 hours at a flow rate corresponding to the sampling flow rate of the device.
- The part of the sampling line inside the station must be thermally isolated to avoid condensation but sampling lines **must not be heated** for ambient air measurements.
- For CRDS measurements it is recommended to wait one hour for the stabilization of temperature and pressure in the measurement cell.
- It is recommended to do the calibration of the instrument every trimester.

- A blank or zero air/gas supply is required for obtaining analytical blanks during the measurements.
- For the calibration: in the absence of a stable gaseous calibration standard close to ambient levels, the calibration with a permeation system can be a good choice.

For offline passive sampling:

- The sampling duration is comprised between 1 and 14 days for Radiello cartridges and between 1 and 4 weeks for ALPHA badges.
- After their exposition to NH₃, cartridges must be stored at a temperature maintained below 4°C for a maximum of 3 months before the analysis.
- The extraction efficiency when analysing a cartridge must be >95%.
- The linearity deviation of the calibration curve must be less than 2 %.
- The drift between two calibrations must be less than 5 %.
- The weight of ammonium in blanks must be less than 0.2 µg.

7.3 RI-Urbans recommendation

Firstly, data from urban monitoring sites should be uploaded to the EBAS database. None of the six databases evaluated in this project are in EBAS at this moment.

We have been able to collect only six available datasets at urban sites as the majority of NH₃ measurements is in rural areas. Moreover, some new sites like in France, will be equipped with online NH₃ monitors, the more datasets must available in the future.

Among the six datasets, one database is coming from online measurement, two from offline measurements and one from both online and offline measurements. The metadata for three stations (VLC_SUB, VLC_TR and PAR_SUB) is still missing. Globally, the % of data available is more than 80 % showing a good performance of the instruments. The QA/QC measures followed by the sites weren't well informed, thus we recommend to follow the guidelines already mentioned.

7.4 Annex / Files Datasets

The NH₃ datasets are fully available at RI-URBANS intranet ([NH3](#)). The data is presented in an excel file for each site, organized in two excel sheets:

Sheet 1: metadata

Sheet 2: VOC concentrations

8 Data management

Data management (DM) is one of the key tasks in RI-Urbans because of the need for harmonised instrumental and operational protocols. Moreover, data QA/QC, data format, data transfer and data access according to the FAIR principles are key requirements in RI-URBANS.

RI-URBANS will establish the data management framework in the project. To do so, we will develop the modalities by which the data flow is implemented in pilot studies followed by the organization/implementation of the digital platform per se. This activity addresses the most suited organization to ensure that extension ACTRIS services to urban observatories are properly dimensioned and that the conditions for storing, curation and access to data and data services are organized.

The DM Plan will be addressed in WP5, which is responsible for producing the final DMP in M42 of the project. Importantly, the DMP will contain links to the respective relevant data management plans within the participating RIs, and the suggested policies, standards, and sustainability activities related to the created data and service tools. DMP will comply with FAIR principles

At this stage, databases have been collected, checked and processed following the methodology described for each variable. Processed and original databases are archived at RIUrbans intranet and are available for other WP's partners, mainly WP2 and WP3 for health studies and modelling. Guidelines and recommendations are also available for WP4 (Pilot studies).

In next steps, we will use a 3-stage approach for the data collected in RI-URBANS, that has been devised in collaboration with WP5 and ACTRIS Data Centre:

- The complete dataset will be archived as a collection at the ACTRIS secondary dataset repository. It will receive a collection DOI.
- Data from stations that haven't reported to ACTRIS / EBAS before will be independently archived there.
- Stations that have been reporting to ACTRIS, but where quality issues have been discovered, will receive corresponding feedback on ACTRIS QC issue tracker, with a task to improve their data quality.

The data reporting routines for the data are established and go very much along the lines of procedures used in ACTRIS. These are shortly summarized below.

- Nanoparticle PNSD from PNSD:

Established ACTRIS template: <https://ebas-submit.nilu.no/templates/Differential-Scanning-Mobility-Particle-Sizer/lev2>

Stations which haven't been reported before will need station IDs.

- BC:

According to ACTRIS procedures, eBC data are not reported as such, but are converted to the parameter actually measured, which is the absorption coefficient. The data reporting template would be: <https://ebas-submit.nilu.no/templates/Filter-Absorption-Photometer/lev2>

Stations which haven't been reported before will need station IDs.

- Offline PM chemical composition:

This is not an ACTRIS parameter. The templates would be:

<https://ebas-submit.nilu.no/templates/Inorganic-air-aerosol-chemistry-filter-based/lev2>

<https://ebas-submit.nilu.no/templates/Heavy-metals-in-aerosol-particle-phase/lev2>

<https://ebas-submit.nilu.no/templates/Mercury-aerosol/lev2>

Stations which haven't been reported before will need station IDs.

- Online PM chemical composition: ACSM

The guidelines for measurements can be found here:

https://www.actris.eu/sites/default/files/Documents/ACTRIS-2/Deliverables/WP3_D3.3_M16.pdf

The template for data submission can be found here:

<https://ebas-submit.nilu.no/templates/ACSM-regular/lev2>

Stations, which haven't been reported before will need to obtain a station ID.

- VOCs

The ACTRIS template is: <https://ebas-submit.nilu.no/templates/VOC/all>

Stations which haven't been reported before will need station IDs.

- NH₃

No template available for NH₃.